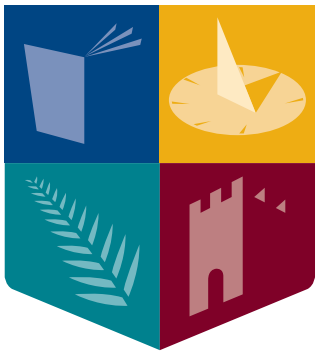

Maynooth University
National University of Ireland Maynooth

STABILITY AND STRING STABILITY ANALYSIS OF FORMATION CONTROL ARCHITECTURES FOR PLATOONING

ANDRÉS ALEJANDRO PETERS RIVAS

A DISSERTATION SUBMITTED FOR THE DEGREE OF
DOCTOR OF PHILOSOPHY

SUPERVISOR: DR. OLIVER MASON
HEAD OF DEPARTMENT: PROF. KEN DUFFY
HAMILTON INSTITUTE
MAYNOOTH UNIVERSITY

OCTOBER 2015

email: andres.peters@nuim.ie, website: http://www.hamilton.ie/apeters/
Hamilton Institute, Maynooth University, Maynooth

ABSTRACT

This thesis presents theoretical results for stability and string stability of formation control architectures for platooning. We consider three important interconnection topologies for vehicles travelling in a straight line as a string: leader following, cyclic and bidirectional.

For the leader following topology we discuss modifications that allow reduced coordination requirements. In the first case we consider the use of the leader velocity as the state to be broadcast to the followers, rather than the standard use of the leader position. This selection yields a formation control architecture that achieves string stability even under time delays in the state broadcast, while reducing typical coordination requirements of leader following architectures. For the second modification we change the way in which the leader position is sent across the string to every follower. This technique keeps some of the good transient properties of the standard leader following architecture but eliminates most of the coordination requirements for the followers. However, we show that this technique does not provide string stability when time delays are present in the communication.

The second topology that we discuss is a cyclic one, where the first member of the platoon is forced to track the last one. We discuss two strategies: one where the inter-vehicle spacings may follow a constant-time headway spacing policy and one where an independent leader broadcasts its position to every member of a cyclic platoon. For both strategies we obtain closed form expressions for the transfer functions from disturbances to inter-vehicle spacings. These expressions allow us to show that if the design parameters are not properly chosen, the vehicle platoon may become unstable when the string size is greater than a critical number. On the contrary, if the design parameters are well chosen, both architectures can be made stable and string stable for any size of the platoon.

The final topology that we consider is bidirectional, where every member of the platoon, with the exception of the first and last, use measurements of the two nearest neighbours to control their position within the string. Although the derivations are more complex than in the two previous unidirectional cases, we obtain closed form ex-

pressions for the dynamics of the platoon. These expressions are in the form of simple transfer functions from disturbances to vehicles. They allow us to obtain stability results for any size of the platoon and understand the behaviour of the least stable pole location as the string size increases.

All of the results obtained are illustrated by numerical examples and ad-hoc simulations.

CONTENTS

LIST OF FIGURES

LIST OF TABLES

1 INTRODUCTION

At the end of the nineteenth century, humanity witnessed the invention of vehicles powered by the internal combustion engine. Prior to this, intercity travel and transport of goods was made almost exclusively by the use of animal traction, railways and ferries. In the years after their emergence, cars evolved into a relatively fast and inexpensive tool for transportation. They have and still provide many benefits to society although not without large financial and non-financial costs.

According to statistics from The World Bank , in 2010, most European countries had around 500 motor vehicles per 1000 inhabitants. In the USA and Australia this figure was around 700. On demand and door-to-door travel, an improvement in the response time of emergency services, on-time food supply and distribution, and a general increase in the effective coverage of many services are some of the benefits that can be credited to the use of vehicles and justify their existence in large quantities.

See http://data.worldbank.org/indicator/IS.VEH.NVEH.P3

On the other hand, use of non-renewable fossil fuels, road congestion, accidental deaths and generation of air and noise pollution are some of the major problems that society has to deal with as a consequence of the intensive use of motor vehicles. Large road networks across the globe have been built in order to provide connectivity between and within urban areas, and nowadays, vehicles have an almost exclusive use of them. In this regard, roads can be seen as a limited resource which must be maintained and used as close to capacity as possible.

Society is aware of these problems. Governments and the scientific community have proposed different mechanisms to decrease the negative impact and improve the benefits of the use of vehicles. One example is the idea of idle reduction, which consists of practices and technological developments that reduce the amount of time that drivers idle their engines. It has been estimated that each year idling of truck and locomotive engines emit over 10 million tons of CO_2, among other polluting gases and particles. Governments in different

See for example http://www1.eere.energy.gov/cleancities/pdfs/2015_strategic_planning_idling_reduction.pdf

countries are reducing idling by implementing fines and promoting the research and development of technologies to deal with the problem. Given the large number of vehicles, even a small improvement in a single aspect such as idling can have a significant impact. It is then clear that the general aspects of vehicular transportation are an important field of study.

One of many other measures that researchers and engineers are taking to decrease the negative impact of vehicles is to model and/or design systems that ensure an optimal use of the existing road networks. These systems could be appended to either vehicles or roads and aim to reduce congestion of the network or improve its throughput.

Another important aspect of vehicular transportation is that of safety. Cars provide a reasonably safe means of transport, even when confronted with unfavourable terrain or weather conditions, but at the same time they must be manoeuvred with caution and skill at every moment. Any improvement in the speed and effectiveness of transportation must be accompanied by an increase in safety measures.

The use of automation is a possible solution to the question of how to achieve an efficient use of roads while maintaining a desired level of safety. The control of vehicle formations consists of the design of a system that forces a desired trajectory for a collection of moving agents, without the need of human drivers. The system must reject disturbances and maintain small or zero error with respect to the desired trajectory. Examples of such systems can be found in the design of unmanned flight squadrons and multi-robot formations among others (Olfati-Saber et al., 2007).

From an engineering point of view, vehicle formation control requires the implementation of sensors and actuators on the collection of vehicles to be controlled. These devices are then interconnected using a certain communication interface, allowing the use of standard control systems. From a mathematical point of view, vehicle formation control requires the study of dynamical systems, and in particular it is usually seen as the interconnection of several simple agents. It can be related to the study of consensus and flocking. In this thesis we focus on the mathematical study of vehicle formation control.

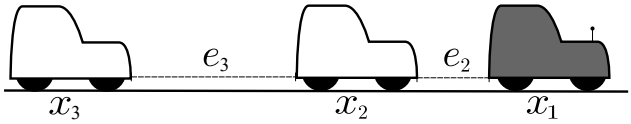

Figure 1: Small vehicle platoon. x_i: position of the i-th vehicle. $e_i = x_{i-1} - x_i$: inter-vehicle spacing between the $(i-1)$-th and i-th vehicles.

1.1 VEHICLE PLATOONS

This work presents mathematical results motivated by problems arising in vehicular platooning, one of the many techniques that have been developed to optimize vehicular transportation through formation control. The simplest example of a vehicle platoon is that of two vehicles travelling in a straight road. The front, or leader, vehicle moves independently, travelling at a constant speed, and the following vehicle aims to maintain a fixed distance to the leader whenever possible. This could be achieved by equipping the follower with a suitable control system. This system will measure the inter-vehicle spacing between the two vehicles and will use it to determine the necessary action on its engine in order to maintain the desired inter-vehicle spacing. A design goal for the control would then be to allow the vehicles to travel close to each other, within reason, at the target speed that the front vehicle dictates. This leads to an increase in the capacity of the road the vehicles use by allowing more vehicles simultaneously in a certain lane. This would also be resilient to disturbances if the control system is designed properly.

It is natural to allow the platoon size to grow. Iterating on the previous strategy, we can increase the size of the platoon by adding another follower vehicle equipped with a similar control system, which in turn is ordered to follow the second member of the original platoon (see Figure 1). This process can be repeated to create a platoon, or vehicle string, of any number of vehicles. It seems reasonable to assume that if the platoon of two vehicles reaches a target speed with a desired inter-vehicle spacing, the platoon with any finite number of vehicles will behave similarly.

1.2 STRING STABILITY

However, with this simple description, there is no way to determine a priori the transient behaviour of the inter-vehicle spacings. For instance, if every vehicle starts from rest and the front vehicle accelerates up to a certain speed, will all the followers take the same relative trajectory? In fact, this would be the optimal desired behaviour of the platoon. To have every follower moving with the same relative trajectory is equivalent to the lane capacity that a train achieves, with inter-wagon spacings that are completely fixed.

In particular, if the vehicles and controllers are modelled by identical linear time invariant (LTI) systems, with two integrators in the vehicle-controller pair, then the answer to the previous question is negative. Moreover, in (Seiler et al., 2004) it was shown that the control strategy described above, with these assumptions for the vehicle-controller pair, will always lead to transients on the inter-vehicle spacings (or errors) with a peak that grows along the string. In simple terms, manoeuvres of the leader or disturbances at any member of the string could lead to collisions if the number of vehicles in the platoon is large enough. This behaviour is referred to as *string instability* (Peppard, 1974; Chu, 1974).

It becomes clear that the original formation control strategy must be modified in order to comply with safety standards and several alternatives have been proposed to deal with *string instability* (or to obtain *string stability*) in recent decades. If safety is a priority when designing a string stable control strategy for platooning, different spacing policies can be used. For example, (Chien and Ioannou, 1992) allow inter-vehicle spacings that depend on the speed of the platoon . Alternatively, the use of more complex interconnections, allowing the controllers of each vehicle to use measurements of the state of two or more other members of the platoon, can give rise to formations that are both tight, or train-like, and string stable. However, this is obtained at the cost of increasing networking requirements (Seiler et al., 2004).

One reason for the study of control strategies such as the one described above, namely, tight formations, where the vehicles keep constant desired inter-vehicle spacings whenever possible, comes from Automated Highway Systems (AHS), (Hedrick et al., 1994), where it is of interest to obtain a high throughput (vehicles/lane/hour). Other

applications aim to reduce wind resistance (drag) in order to obtain fuel savings. This is done by placing the vehicles in certain positions in a longitudinal platoon (Bonnet and Fritz, 2000).

In this work we study a few of the many possible combinations of interconnections and spacing policies that could possibly achieve string stability. These mathematical models possess some interesting properties that could benefit real world implementation or could be used as a starting point for more advanced control designs and/or theoretical results. Although most of the work in this thesis is motivated by vehicular platooning and string stability, the mathematical models associated can also be obtained in the study of other physical or non physical phenomena. In particular, it is of interest to study interconnections of multiple systems (such as collections of robots, coupled fluid tanks, etc.) and the resulting stability of this interconnection.

1.3 ORGANIZATION AND CONTRIBUTIONS OF THIS THESIS

This thesis is organized as follows. In Chapter 2 we present a literature review of vehicular platoons with a focus on string stability and stability of interconnected systems. We discuss the relevance of the kinds of interconnections and spacing policies that we study and how the results obtained here contribute to the state of the art.

In Chapter 3 we discuss string stability results for the leader velocity tracking control architecture. As mentioned before, these architectures are of importance in practical applications for their ability to provide tight formations. In such formations, the vehicles maintain fixed desired inter-vehicle spacings in steady state. This allows to exploit fuel consumption reduction strategies based on aerodynamic properties at close inter-vehicle spacings (see for example Bonnet and Fritz (2000)). We compare our proposed architecture to two different leader position tracking schemes. Additionally, we study the effect of time delays in the broadcast of the leader state on the string stability of all the interconnections. The main motivation of this is that in practical implementations of vehicle to vehicle communication, time delays are considered as a very common disruption. The main benefit of using leader velocity tracking is the possibility of achieving a string stable platoon which is also tight, even under the effect of increasing

time delays. Some remaining topics to be addressed from this chapter are:

- A well defined design technique for the controllers on every vehicle and the parameters associated to the leader velocity tracking scheme.
- Study of robustness of the control architecture to model uncertainty and/or failure.
- Study of the effect of noise in the broadcast along the string.

Chapter 4 contains the results that we have obtained for two different formation control architectures using a cyclic interconnection. The first one consists in a leaderless cyclic formation using a time headway spacing policy and the second one considers a constant spacing policy with the presence of an independent leader that broadcasts its position. The main motivation for the study of such architectures corresponds to transportation systems which are contained in a closed circuit. Examples of such are: circle subway or tram lines, public transport bus lines that connect from point A to point B and return, etc. However, the results we have obtained do not require the vehicles to travel in a closed circuit. The same formation control architecture can be implemented in a one dimensional setting. In this scenario the flow of information is cyclic. The contributions of this chapter are a mathematical description of such interconnection which does not consider particular vehicle models and controllers and corresponding stability and string stability results for both architectures. Some remaining topics to be addressed from this chapter are:

- Study of the effect of time delays and/or noise in the broadcast of the leader state (as in the leader tracking case).
- Study of robustness of the control architecture to model uncertainty and/or failure.
- Consider a heterogeneous setting (varying controllers) and their effect on the time headway parameter that is needed for string stability.

In Chapter 5 we present results obtained for formation control architectures using a bidirectional interconnection. For this particular case the main motivation comes from the intuition of using all the

possible available information to implement a formation control architecture. The simplest bidirectional scheme considers almost every vehicle sensing its distance to the immediate predecessor and immediate follower. The study of this type of interconnection is not straightforward and other researchers have recurred to the use of approximations. We derive closed form formulae for the resulting dynamics, in terms of transfer functions from disturbances to vehicle positions, for a particular type of bidirectional interconnection. We use these expressions to provide some analysis of the stability and resulting dynamical properties of the system when the string size grows, avoiding the use of numerical approximations. Some remaining topics to be addressed from this chapter are:

- Full string stability results for the general case.
- Additional leader and/or different boundary conditions on the last vehicle (we consider only one type).

Chapter 6 contains some miscellaneous results related to vehicular platoons which are complementary to the main results of this work.

Concluding remarks and possible future lines of work are given in Chapter 7.

Some other interesting questions remain open or have been briefly touched by the literature. For example:

- Impact of the use of extra information (other than the closest neighbours) and directionality on the requirements for stability and string stability in architectures using a constant time headway spacing policy.
- Combinations of well known cases (topologies, spacing policies, leader broadcast).
- Many others to be discussed briefly in the main chapters.

1.4 NOTATION

The notation used in this thesis follows much of the standard systems and control literature. Lowercase is used for real scalar signals, $x : \mathbb{R} \to \mathbb{R}$ with specific values of the signal denoted by $x(t)$. Uppercase is used for scalar complex-valued Laplace transforms of signals and transfer functions, $X : \mathbb{C} \to \mathbb{C}$ with specific values denoted by $X(s)$. For the sake of brevity in the notation, where there is no confusion, the argument (s) will be omitted. Vectors will be denoted as $\underline{x}(t) \in \mathbb{R}^n$ and $\underline{X} \in \mathbb{C}^n$, while $\underline{x}(t)^\top$ and $\underline{X}^\top$ denote their transposes. The imaginary unit is denoted by j, with $j^2 = -1$. Boldface will be used for matrices $\mathbf{G} \in \mathbb{C}^{n\times m}$ and the (i,k)-th entry of $\mathbf{G}$ is denoted by $G_{i,k}$. The magnitude of X when $s = j\omega$, $\omega \in \mathbb{R}$, is denoted by $|X|$ and its magnitude peak over all possible values of ω is denoted as $\|X\|_\infty := \sup_\omega |X(j\omega)|$. For $z \in \mathbb{C}$, $\Re(z)$ and $\Im(z)$ denote the real and imaginary parts of z respectively. The derivative of X with respect to s will be noted as

$$\frac{dX(s)}{ds} = X'(s). \tag{1}$$

Finally, the symbol $\square$ will be used for the end of proofs.

1.5 PUBLICATIONS

The following papers have been published/submitted to report the contributions of this thesis:

Andrés A. Peters, Richard H. Middleton.
Leader Velocity Tracking and String Stability in Homogeneous Vehicle Formations With a Constant Spacing Policy.
International Conference on Control & Automation 2011, Santiago, Chile, December 2011.

Andrés A. Peters, Oliver Mason, Richard H. Middleton.
Cyclic interconnection in 1-D vehicle formation control.
European Control Conference 2014, Strasbourg, France, June 2014.

Andrés A. Peters, Richard H. Middleton and Oliver Mason.
Leader tracking in homogeneous vehicle platoons with broadcast delays.
Automatica, Vol. 50, No. 1, pp. 64-74, 2014.

Andrés A. Peters, Oliver Mason and Richard H. Middleton.
Cyclic Interconnection for Formation Control of 1-D Vehicle Strings.
European Journal of Control, Under review.

Andrés A. Peters, Oliver Mason and Richard H. Middleton.
Bidirectional Interconnection for Formation Control of 1-D Vehicle Strings.
In preparation.

1.6 ADDITIONAL MATERIAL

The following weblink contains Matlab® and Simulink® files for simulations contained in this thesis.

`http://tinyurl.com/stringstabilitypeters`

2

LITERATURE REVIEW

In this chapter we present the state of the art in the mathematical study of vehicular platooning. We start with its origins and then we focus on some important aspects and problems that arise in this kind of interconnected system. Specifically, we gather important results on the stability and string stability of vehicle platoons. Finally, we discuss how the work presented in this thesis advances the state of the art.

2.1 ORIGINS OF VEHICULAR PLATOONING

As discussed in the previous chapter, scientists have been searching for techniques to optimize the usage of road networks and at the same time increase the safety of these roads. The work reported in (Levine and Athans, 1966) was one of the first to propose the mathematical study of an automated platoon of vehicles. It presented the design of an optimal linear feedback system to regulate the position and velocity of every vehicle in a densely packed string of N vehicles moving in a straight line (See Figure 2). The specifications of the system originated from safety considerations, capacity requirements, velocity control, passenger comfort, and fuel economy. These translate into forcing desired fixed inter-vehicle spacings and mitigating large deviations from a constant target velocity for the platoon. Another early work, reported in (Melzer and Kuo, 1971) developed a theory for the optimal regulation of linear systems described as a countably infinite collection of agents. The theory is then used in the example of a string of vehicles where the string size is infinite.

One main drawback of the strategies above is that the resulting controllers were centralized, requiring every member of the string to have access to all the state variables of the interconnected system. Vehicle formation control approaches that utilize nearest neighbour measurements were reported in (Bender and Fenton, 1968) and (Peppard and Gourishankar, 1972). However, reducing the number of required measurements produced some undesired behaviours. The

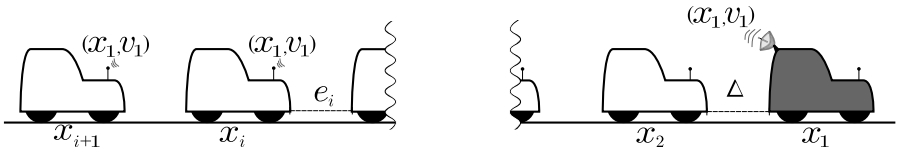

Figure 2: Platoon of vehicles. (x_i, v_i): position-velocity pair of the i-th vehicle. $e_i = x_{i-1} - x_i$: inter-vehicle spacing between the $(i-1)$-th and i-th vehicles. Δ: desired inter-vehicle spacing.

author of (Peppard, 1974) informally defined as *string stability* the property of a vehicle string to attenuate disturbances as they propagate down the string. He also identified that there is a connection between string stability properties and the measurements of other vehicles (looking both forward and backward) used to compute the control action for each member of the string. In particular, the analysis used a frequency domain approach, computing the magnitude of the quotient of the transfer functions of two successive vehicle positions (i. e. $|X_i(j\omega)/X_{i-1}(j\omega)|$). In (Chu, 1974), decentralized optimal control strategies for vehicular strings are discussed, studying six combinations of measurements to be used by the controllers. The author aimed to identify the relative importance of various measurements in the minimization of the cost functional used in the optimal control problem.

Over the following years, besides designing physical implementations of vehicle platoons, the focus of researchers was on studying different mathematical descriptions of vehicle platoons and control architectures. In the following section we cover some of the most important lines of work that have been developed for the general problem before focusing on the specific setting that is of interest to us.

2.2 DESIGN OF VEHICLE FORMATION CONTROL ARCHITECTURES

2.2.1 *Aspects of the Mathematical Problem*

The mathematical modelling of vehicular platoons possesses many aspects. In this subsection we discuss some of the most important of these and related lines of work in the literature.

Heterogeneous vs Homogeneous The works described in the previous section considered a collection of identical vehicles. In particular, (Peppard, 1974) described a platoon of vehicles where every member

is controlled by a local PID controller. These controllers are also assumed to be identical for every vehicle. This kind of vehicle platoon, where the vehicle model and the controller attached to it are identical along the string, is referred to as *homogeneous* and it is the most widely used assumption when studying vehicle formations. However, in optimal control designs, the resulting optimal controller gains are not necessarily identical, even when identical models are used for every vehicle (see for example Levine and Athans (1966)). The alternative assumption, defines a *heterogeneous* string, where the vehicle and/or controller model varies with its position along the string, has also been studied. In (Lestas and Vinnicombe, 2007), the vehicle models are considered to be identical, but the local controllers are allowed to be different. The authors propose the use of symmetrical bidirectional control, where the local controllers of every vehicle use the relative distance to their two nearest neighbours to compute the control signal, in addition to a weak coupling with the leader. They show that this control strategy provides a string stable (the authors use the term *scalable*) platoon when the controllers are identical. Next, the controllers are allowed to vary along the string. The authors exploit the symmetry of the information flow to show that there are local conditions that, if satisfied, ensure a stable interconnection for strings of arbitrary length. The authors of (Shaw and Hedrick, 2007) focus on string stability of a heterogeneous string with both vehicle and controllers varying along the string. The main results state that a heterogeneous string using leader-predecessor following control (i. e. where the controllers use measurements from the leader state and their immediate predecessor simultaneously) can be made string stable. This is shown by computing a transfer function T that depends on the vehicle model and controller, both allowed to vary along the string. In particular, the vehicle model is assumed to belong to a set of parametrized transfer functions. The authors then prove that string stability in the platoon occurs if and only if $\|T\|_\infty < 1$ (where $\|T(\cdot)\|_\infty = \max_\omega |T(j\omega)|$) for every possible vehicle type. More recent work reported in (Yu et al., 2012) studies string stability in a system of heterogeneous coupled oscillators. Although the motivation for the work is the problem of synchronization (i. e. force the oscillators to follow the same oscillating trajectory), the framework is very similar to the one used in the study of vehicular platoons.

The work presented in this thesis will use the assumption of an homogeneous platoon almost exclusively. One reason for this is that it simplifies the analysis in many mathematical descriptions of platoons. Moreover, it has been shown in other works that heterogeneity does not immediately provide a practical improvement in the performance of the string. We will cover the details in a later section.

Linear vs Non-linear

A key distinction in modelling vehicle platoons, as in many applications, is that between linear and non-linear models. Accuracy in the description of vehicle models suggests the use of a non-linear approach, given the inherent non-linearities present in real cars. Additionally, non-linear control techniques are also an option. In (Sheikholeslam and Desoer, 1992), a first approach to a fully non-linear description of the platoon problem is presented. Non-linear adaptive control schemes for platooning of heavy duty vehicles were presented in (Yanakiev and Kanellakopoulos, 1998). Here, the authors designed two non-linear spacing policies with the aim of alleviating string instability issues in the formation control of heavy duty vehicles. Sliding mode control was used in (Hedrick et al., 1991; Lee and Kim, 2002), motivated by the ability of such schemes to provide a robust control action in the presence of model uncertainties. In (Swaroop and Hedrick, 1996) the authors introduced the concept of string stability for a class of non-linear interconnected systems. An application of the theoretical approach described by the authors was given in the case of a type of non-linear vehicular platoon (referred to as a *vehicle-following system*).

On the other hand, linear approaches provide easy access to many control design tools and can reflect reality accurately enough for some purposes. In particular, linear time invariant models (LTI) allow the use of frequency domain techniques which are in some cases tractable and powerful enough to provide many interesting results and insights. In particular, frequency domain techniques have been important in understanding the causes of platooning problems such as string instability. The work in (Bender and Fenton, 1968) was one of the first descriptions in the frequency domain of a vehicular platoon. From that point, several extensions and studies were done. However, the work presented in (Seiler et al., 2004) is one that deserves greater attention. In particular, the authors show, using frequency domain techniques, that string instability in vehicle platoons can be an un-

avoidable issue if some conditions are met. The main theoretical result used to conclude this was reported earlier in (Middleton, 1991), and it states that a certain closed loop transfer function will always have a magnitude peak greater than one when the open loop contains two integrators. It is reasonable to assume that the LTI model of a vehicle possesses at least one integrator (or a pole at the origin in its transfer function). Additionally, the natural platooning goals of constant speed and constant inter-vehicle spacings, even with the presence of disturbances, motivate the use of integration in the controller. Earlier, string instability was known to occur when vehicles use only relative spacing information to control the spacing that they keep with predecessors (Peppard, 1974; Chu, 1974). However, it was only in (Seiler et al., 2004) where it was noted that this was due to the dynamical restriction on the vehicle and controller pair of possessing two integrators. On top of providing this theoretical result, the authors show that if every member of the string uses also the position of the leader (by averaging it with the relative position with respect to its predecessor), string stability can be achieved. This last result motivates many questions and also motivates some of the work presented in this thesis.

Distributed parameter

Although, a collection of vehicles is discrete in space, distributed parameter approaches have been used to study vehicle platoons. For example, in (Bamieh et al., 2002) the authors discuss the distributed control of *spatially invariant systems*, of which vehicular formations can be seen as a particular case. The authors of (Barooah et al., 2009) consider a partial differential equation (PDE) method to study the stability margins of a bidirectional vehicular platoon. In particular, it is shown that, if a homogeneous platoon of N vehicles modelled by double integrators is controlled with a nearest neighbour symmetric bidirectional strategy, the least stable closed loop eigenvalue of the resulting interconnected system approaches the origin as $O(1/N^2)$. This result is obtained by studying the continuous approximation of the platoon dynamics via a PDE. The authors also discuss a way to improve the asymptotic behaviour to $O(1/N)$ by using small amounts of *mistuning*. In this thesis we present an alternative method to obtain similar results to the ones discussed above, using a more direct approach to compute the eigenvalues of the interconnected system (without recourse to the continuous PDE approximation).

Optimal control approaches

Optimal control provides a reasonable framework for the study of many issues related to the control of vehicular systems. The goals of vehicular platoons are in many cases to optimize the usage of road networks while increasing safety and reducing energy consumption (among many others). The definition of performance measures, energy costs, and relative errors or spacings in platoons are well suited for the use of optimal control approaches. As mentioned before, some of the earlier results in vehicle platoons considered an optimal control scheme. An interesting finding reported in (Jovanovic and Bamieh, 2005) states that some optimal control problems for vehicular platoons studied in earlier papers (Levine and Athans, 1966; Melzer and Kuo, 1971) are *ill-posed*. The authors highlight that studying the infinite size platoon is useful to predict the behaviour of a large-but-finite platoon size. Additionally, they propose alternative optimal control problems that are well-posed by using the insight provided by the study of the infinite size platoon. Model predictive control has been studied in (Yan and Bitmead, 2003; Kianfar et al., 2014). The resulting control architecture that an optimal control strategy yields is usually centralized. This means that to compute the control signal of any member of the string would require the use of the state of every other member. This is a feature that does not suit well for real world implementations of platooning systems. In (Stankovic et al., 2000) the authors presented a decentralized optimal control strategy that is based on decomposing the larger interconnected system into a collection of smaller ones. They also defined conditions to ensure that the resulting interconnection is string stable. In (Lin et al., 2012), the authors formulate a structured optimal control problem for a platoon where the vehicles are modelled by single and double integrators. The control is defined as nearest neighbour bidirectional and for the single integrator case, the optimal control problem to obtain the corresponding gains is shown to be convex. Convexity of the optimization problem implies its tractability and allows the use of modern effective algorithms and toolboxes to obtain its solution. Decentralized receding horizon control was studied in (Dunbar and Caveney, 2012). Finally, linear matrix inequality (LMI) based techniques have been reported in (D'Andrea and Chandra, 2002; Maschuw et al., 2008).

Other mathematical descriptions

Some approaches to vehicular platoons model them as a two dimensional (2-D) system (Hurák and Šebek, 2010; Šebek and Hurák, 2011). The recent work contained in (Knorn, 2013) presented results for both linear and non-linear 2-D systems theory motivated by vehicular platoons. In particular, the two dimensional aspect of the platoon comes from the fact that a string of vehicles possesses a spatially discrete nature. The position of a vehicle can be defined to depend on the time variable (t) and a spatial index (k). In the LTI case, the position can then be studied in the frequency domain by taking a joint Laplace and $\mathcal{Z}$-transform. The resulting mathematical objects of study are quotients of bivariate polynomials. The presence of *nonessential singularities of the second kind* in these objects is of major importance in this approach since it complicates the analysis both for stability and string stability (Bose et al., 2003). This is currently a major disadvantage of the approach.

Given that vehicle platoons are interconnections of dynamical systems, techniques from Graph Theory can be naturally applied. In particular, the structure of the interconnection plays a key role in the dynamical properties of the platoon, and this structure is appropriately modelled by a graph. A framework for the study of vehicle platoons using graph theory is provided in (Fax and Murray, 2004). This work is of great relevance for some of the results presented in this thesis and it will be covered in greater detail in a following section. Other similar results can be found in (Lafferriere et al., 2005).

2.2.2 *Measurements and Networking in Vehicular Platoons*

The focus of this thesis is primarily on the study of decentralized strategies for longitudinal control of vehicle platoons. Longitudinal control means that there is no control of lateral movement of the vehicles; so we disregard overtaking and changes of lane. By a decentralized strategy we refer to the situation where the members of the platoon are equipped with a controller that has reduced knowledge of the states of the full interconnected system. Normally, the control signal for each vehicle is computed using only the states of the same vehicle and local relative measurements of the nearest neighbours. One reason for the study of such strategies is the simplicity of the implementation in real world situations (due to reduced networking

and/or sensing demands). However, as noted in (Peppard, 1974; Chu, 1974) and more recently (Seiler et al., 2004), extremely simplistic control strategies can lead to string instability, compromising the performance and safety of the platoon.

Leader and leaderless schemes

The presence of a *leader* in the platoon is one of the first selections that can be made when discussing the networking aspects of the problem. Let $x_i(t) \in \mathbb{R}$ be the position of the i—th vehicle in the string. If the first vehicle, with position $x_1(t)$ follows a trajectory that is independent of the interconnection, then this vehicle is said to be the leader of the platoon. In other words, the control action on the leader is unconstrained by the motion of the other members of the platoon.

The authors of (Sheikholeslam and Desoer, 1990) discuss a platoon of vehicles where the velocity $\dot{x}_1(t)$ and acceleration $\ddot{x}_1(t)$ of the leader are transmitted to every other follower. For a certain type of vehicle dynamics (linearisation of a non-linear model), the authors define control laws for each follower of the form (normally known as leader-predecessor following)

$$\begin{aligned} c_i(t) := {} & c_p(x_{i-1}(t) - x_i(t) - L) + c_v(\dot{x}_{i-1}(t) - \dot{x}_i(t)) \\ & + c_a(\ddot{x}_{i-1}(t) - \ddot{x}_i(t)) + k_v(\dot{x}_1(t) - \dot{x}_i(t)) + k_a(\ddot{x}_1(t) - \ddot{x}_i(t)), \end{aligned} \tag{2}$$

where L is a constant desired inter-vehicle spacing and the real constants c_p, c_v, c_a, k_a and k_v are design parameters. Then, they obtain the resulting dynamics of the interconnection and show that with an appropriate selection of the parameters, the platoon reaches a steady-state velocity with a tight formation. In simulations they observe that there are no amplifications in the successive inter-vehicle spacings for a leader acceleration manoeuvre. Later, in (Sheikholeslam and Desoer, 1993) the same authors considered a similar setting as in the previous paper but without allowing either the leader velocity or acceleration to be communicated. Although they show that the new control strategy yields a platoon that reaches a tight formation with a constant velocity, the authors note that the transient behaviour of the inter-vehicle spacings is degraded when comparing it to the case with leader information. In particular they observe that the inter-vehicle spacings transient has a peak value that increases along the string, when the leader vehicle performs an acceleration manoeuvre. Both of

these results are in accordance with the findings reported in (Seiler et al., 2004) that we discussed earlier. However it is interesting to note that in this work the information being transmitted to the followers is the instantaneous position of the leader ($x_1(t)$). One of the main contributions in this thesis corresponds to the study of control strategies where the leader information is transmitted to the followers. In particular we restrict this information to just be the instantaneous velocity of the leader ($\dot{x_1}(t)$) and develop some theoretical results that show the possible real world benefits of such a strategy.

An alternative to broadcasting leader information is to use reference or steady state information. In this setting, the control strategy for the platoon relies on giving to every vehicle a certain steady state velocity or time evolving trajectory. Examples of such strategies can be found in (Peppard, 1974).

Spacing policies

In designing a decentralised LTI control strategy for vehicular platoons, we first must decide on an underlying physical policy. Arguably the simplest class of such policies is based on vehicle spacing. Let $e_i(t) = x_{i-1}(t) - x_i(t) - \delta_i(t)$, then we say that $\delta_i(t)$ is a desired inter-vehicle spacing between two adjacent vehicles with positions $x_i(t)$ and $x_{i-1}(t)$. If $\delta_i(t) = c$ for all i, with c a real positive constant, then the spacing policy is said to be constant. This is a very common selection and highly desirable policy since it implies that if the control architecture brings the errors $e_i(t)$ to zero, the formation is tight. If this is the case, the platoon resembles a train and small values of c imply a higher throughput in a road. In (Swaroop et al., 1994), the authors discussed another control architecture for platooning based in a constant *time headway* policy. A headway time, measured in seconds, is the time that the i-th vehicle takes to travel the inter-vehicle spacing that it has with its predecessor, i. e. $x_{i-1}(t) - x_i(t) - c$. For this type of spacing policy we have $\delta_i(t) = c + h\dot{x}_i(t)$, with $h > 0$ being the time headway parameter. In other words, the desired inter-vehicle spacing depends on the speed at which the vehicles are travelling, becoming larger with faster speeds. Although the throughput decreases with the use of this spacing policy, the authors show that it has the potential to achieve string stability in the platoon without the use of leader information. This property is not shared with the constant spacing policy if the leader state is not available to the followers. More recently, the authors of (Klinge and Middleton, 2009) obtained

formulae for a critical value of the time headway constant in order to achieve string stability; for all values of time headway greater than the critical value, the formation is string stable. This was done for a platoon that only uses unidirectional nearest neighbour information (i. e. predecessor information) to compute the control signals. In particular, the critical time headway needed will depend on the vehicle models and local controllers used. More detail on these results will be given in a later section.

Interconnection topologies

In addition to the spacing policy chosen, the topology of the interconnections is a key aspect in analysing the string stability of vehicle platoons. So far in this section we have covered mostly unidirectional strategies, where each vehicle uses its local sensor measurement of distance to a predecessor. This measurement is completely necessary in a control strategy since safety in a vehicular system is an absolute requirement. For tight platooning, if the state of the leader or steady state information is available to every member, it is enough to require every follower to track it, without using the predecessor error. However, this does not account for possible disturbances and/or faults in the followers that would not be compensated by the local controller. For example, in a three vehicle platoon, if the third vehicle only uses the leader information to maintain a desired spacing with respect to it, a sudden stop or braking manoeuvre of the second vehicle will most likely result in a collision. On the other hand, it is possible to add measurements and information to compute the inputs to the local controllers of every follower, on top of the predecessor error (with leader information being the simplest example). The authors of (Seiler et al., 2004; Lestas and Vinnicombe, 2007) and (Barooah et al., 2009) have considered nearest neighbour bidirectional strategies, using simultaneously the front and rear inter-vehicle spacings at every follower. As mentioned before, in this thesis we present some results connected to this selection of network topology.

We also present results when the topology of the interconnection is cyclic. In (Roberson and Stilwell, 2006) the authors present an observer based platooning strategy. It is assumed that the vehicles communicate through a cyclic communication network and every member of the platoon uses the data to estimate the full state of the whole interconnection. The control then is implemented as a state feedback of the observed states. The results reported in (Rogge and Aeyels,

2008) motivate much of the work described here on platoons with simple cyclic interconnections. In this work, the authors consider a simple cyclic interconnection, where there is no leader. It corresponds to a predecessor following strategy with the vehicle of position $x_1(t)$ tracking the position of the last member of the platoon, with position $x_N(t)$. This can correspond to an idealized ring road (where the physical curvature of the road is negligible for the dynamics) but not necessarily limited to this case. A benefit of this, and a main difference with respect to unidirectional approaches, is that a disturbance at any member can be detected by every other follower, possibly allowing to compensate it (if the control scheme is designed properly). The authors chose simple dynamics for the vehicles and design constant gains to implement a simple control using the cyclic interconnection described above. In particular the controller inputs were given by

$$u_i(t) = w_i + K(x_{i-1}(t) - x_i(t) - L_i - h\dot{x}_i(t)), \tag{3}$$

where w_i, K (control gain), L_i (constant spacing) and h (time headway parameter) are real valued parameters to be designed. The cyclic interconnection is made explicit by setting $x_0 = x_N$. Note that the authors obtained the trajectories in the time domain that are solutions to the system of ODEs that define the interconnection. These solutions depend on the parameters and the initial conditions of the vehicles. Stability and string stability of the interconnection were discussed in terms of the parameters and the authors finish with a study of robustness to malfunctioning in a vehicle. In the present thesis, we generalize some of the results given in the last paper by considering general vehicle and controller models. We also consider the use of an independent leader, while maintaining the use of a cyclic interconnection for the rest of the platoon.

The work reported in (Middleton and Braslavsky, 2010) studies a platoon of vehicles where every follower has a limited range of forward and backward communication with other vehicles. They aimed to extend the results presented in (Seiler et al., 2004) for string stability in the constant spacing predecessor following architecture. The assumptions on the interconnection and vehicle model are quite light. The string is considered heterogeneous. The network topology is more general, allowing vehicles to measure the position of vehicles beyond the nearest neighbour (both front and back), although with a limited

range. In that setting, if the platoon size grows, several followers will not have access to the leader information. This restriction is studied mathematically by the use of banded matrices (Golub and Van Loan, 2012). Finally, they consider a constant time headway spacing policy. The main result of this paper gives a lower bound on achievable performance, measured as the worst case disturbance amplification along the string (in the frequency domain), that depends on the characteristics of the platoon mentioned above: limited networking range and spacing policy. The main conclusions can be summarized as follows:

1. System heterogeneity does not necessarily circumvent string instability issues.

2. Extra forward communication range, but with a limit, does not avoid string instability issues. However it reduces the rate of the disturbance amplification.

3. The use of a non rigid spacing policy may permit string stability. (this has been shown to be true in (Klinge and Middleton, 2009)).

4. Bidirectional control seems to improve the string instability issue, but at the cost of long transients as the string size increases.

Some discussion on the last point will be presented in a later chapter of this thesis.

Communication aspects

The final aspect that we will discuss in this section is that of communication. To implement some of the architectures discussed above, vehicles need to obtain measurements from the leader or vehicles that are not in the reach of their local sensors. The use of wireless networking (See for example Willke et al. (2009) for a survey in inter-vehicle communication protocols) introduces issues such as delays and errors in the communication. In (Liu et al., 2001), the effect of communication delays on the string stability of a platoon was studied. The authors consider particular vehicle and controller dynamical structures and analyse the effect of delays in the transmission of the leader information, as well as delays on the measurement of the immediate predecessor errors of any vehicle. In particular, by the use of some numerical examples it was suggested that delays on any measurement can have detrimental effects on the string stability of an oth-

erwise string stable leader-predecessor following platoon. A solution to the problem was proposed which consisted of trying to synchronize every delay of the system to the same value. The authors also estimate the maximum possible delay to retain the string stability. A more recent work presented in (Xiao et al., 2009) discussed a similar approach to the one presented in (Liu et al., 2001). They consider a PD local control for every vehicle in a leader-predecessor following architecture with constant spacing policy. The authors state that this selection does not guarantee string stability under the presence of parasitic time delays and lags (of the type $e^{-\Delta s}/(\tau s + 1)$ in the frequency domain with $\Delta > 0$ the total amount of delay and τ the amount of lag). Then, they propose an alternative sliding mode control with a constant time headway spacing policy. Simulations suggest that this control strategy retains string stability if designed properly, even with delays.

We finalize this section noting that most of the aspects reviewed above can be mixed and used simultaneously in a platoon description or in the design of a control strategy. For example, in the following chapters we present results that combine leader following techniques with the study of time delays. We also consider leaderless cyclic interconnections with constant time headway spacing policies and a cyclic interconnection using an independent leader.

2.3 SAFETY AND PERFORMANCE

In this section we focus our attention on mathematical descriptions of safety and performance regarding vehicular platoons. The main results of this thesis are mostly connected to the topics described below.

2.3.1 *String Stability*

String stability is one of the many aspects that has attracted the attention of researchers in the study of vehicular platoons. This interest stems from the fact that string instability plays a major role when analysing the safety and performance of a platooning control architecture. Since the works reported in (Peppard, 1974) and (Chu, 1974) the concept or mathematical property regarding the propagation of disturbances along the string has been named in a few different ways.

The issue where a vehicle platoon amplifies disturbances as they propagate along the string has been called *slinky effect* in (Chien and Ioannou, 1992). Works such as (Seiler et al., 2004) or (Lestas and Vinnicombe, 2007) refer to this issue as lack of *scalability*. This comes from the fact that, if disturbances are amplified along the string, there is a limit to the number of vehicles that can form the platoon before having issues with possible collisions in braking manoeuvres. If the size of the string is known a priori, it is possible to tolerate a small rate of amplification of disturbances along the string.

Definitions of string stability

Regardless of the name given to the issue, it is desirable for safety, performance and scalability, to design a formation control architecture that achieves a uniformly bounded propagation of disturbances. One of the first attempts to give a formal definition was reported in (Swaroop and Hedrick, 1996). For any general interconnection of non-linear systems, string stability is defined as a boundedness requirement, in time and spatial index, of the states of the whole system whenever the initial condition is bounded (everything measured in l_p norms).

In (Eyre et al., 1998) the authors worked with three definitions of string stability. The vehicle models and controllers were considered to be LTI due to the tractability of such systems. In order to obtain a simplified framework for the study of string stability, the platoon was modelled by a mass-string-damper system, where the vehicles are considered to be the masses, and the controller gains are considered to be the spring and damping constants. The definitions of string stability involve transfer functions $G_i(s)$ from an inter-vehicle spacing error to the next one (of the form $Z_i(s)/Z_{i-1}(s)$ where $Z_i(s)$ is the Laplace transform of the desired distance from the i-th to the $i-1$-th vehicle) and their impulse response $g_i(t)$. The first definition is L_2 string stability, which is equivalent to $\|G_i(s)\|_\infty < 1$ (recalling that $\|G_i(s)\|_\infty = \max_\omega |G_i(j\omega)|$). The second one is L_∞ string stability, equivalent to $\|g_i(t)\|_1 < 1$ (where $\|g_i(t)\|_1 = \int_0^\infty |g_i(t)|dt$). The final one involves both L_∞ string stability and $g_i(t) \geqslant 0$ for all t and is referred to as string stability *without overshoot*. In most situations, these definitions were shown to be equivalent, except the third one that is aimed to design controllers that avoid overshoot in response to vehicle acceleration of the lead vehicle. The authors then analysed several

formation control architectures and studied if they could achieve the conditions for the three kinds of string stability that they defined.

More recently, (Middleton and Braslavsky, 2010) defined the term string stability as the situation where a transfer function of interest, reflecting the scaling (in size) nature of a platoon, possesses a H_∞ norm that is bounded independently of the string length. The transfer function studied was $H_{x_N,d_1}(s)$ which describes the response of the last vehicle, with position $x_N(t)$, to a disturbance $d_1(t)$ at the first vehicle. In the following chapters, we will use a definition of string stability that is inspired by the one given in (Middleton and Braslavsky, 2010). However, we will focus on sequences of transfer functions from disturbances to different possible spacing errors within the platoon, rather than to the actual position of the last vehicle. This makes it possible to extract more information about the performance of the vehicle platoon, particularly when time delays in the communications are considered. In particular, string stability will be defined as the uniform boundedness in the H_∞ norm of a sequence of specific transfer functions resulting from a formation control architecture. More details will be given in Chapter 3.

Factors for string instability

As was discussed in previous sections, string instability is known to occur in predecessor-following schemes with a constant inter-vehicle spacing policy. The authors of (Seiler et al., 2004) were the first to note that one reason behind this issue is a dynamical feature of the vehicle model and controller pair. In particular, they use a result from (Middleton, 1991) for LTI feedback loops in terms of a Bode Integral of the complementary sensitivity function $T(s)$. This result is also key for many of our derivations and we use the following simplified version (Seron et al., 1997)

Lemma I (Simplified Bode Complementary Sensitivity Integral) *Let* $T(s) = L(s)/(1 + L(s))$ *where* $L(s)$ *is a real rational scalar function of the complex variable* s *which is proper and satisfies* $L(0) \neq 0$. *Suppose that* $T(0) = 1$ *and also that* $T(s)$ *is stable (analytic in the closed right half complex plane). Then*

$$\int_0^\infty \ln|T(j\omega)|\frac{d\omega}{\omega^2} \geqslant \frac{\pi}{2}\lim_{s\to 0}\frac{dT(s)}{ds}. \tag{4}$$

Proof: According to part i) of Theorem 3.1.5 in (Seron et al., 1997)

$$\int_0^\infty \ln\left|\frac{T(j\omega)}{T(0)}\right| \frac{d\omega}{\omega^2} = \frac{\pi}{2}\frac{1}{T(0)} \lim_{s\to 0} \frac{dT(s)}{ds} + \pi \sum_{i=1}^{n_q} \frac{1}{q_i}, \tag{5}$$

where q_i for $i = 1, \ldots, n_q$ are the zeros in the open right half plane (i.e. $\Re(q_i) > 0$ for all i) of $L(s)$. Given that $L(s)$ is real, the second term in the right hand side of (5) is greater or equal than zero. Since we consider $T(0) = 1$, the result follows. □

It was assumed that the vehicle and controller pair (which will be denoted by $P(s)$ and $K(s)$ respectively) both possessed a single pole at $s = 0$. This assumption is normally needed to ensure a platoon that reaches a tight formation in steady state even with constant disturbances at any follower. This means that every member of the platoon reaches the same constant speed and the inter-vehicle spacings are constant and equal to the desired ones, after the transient response has faded. The resulting complementary sensitivity transfer function $T(s) = P(s)K(s)/(1 + P(s)K(s))$ will then satisfy $T(0) = 1$ and $T'(0) = 0$. Hence, the previous Lemma implies that $|T(j\omega)| > 1$ for some $\omega > 0$, or equivalently $\|T(s)\|_\infty > 1$. With a simple analysis, it was shown in (Seiler et al., 2004) that the condition $\|T(s)\|_\infty > 1$ is enough to claim string instability of a vehicle formation control architecture that uses a predecessor following approach with a constant inter-vehicle spacing policy. This is regardless of the actual values and extra dynamics of the pair $P(s)$, $K(s)$. In particular, in such an interconnection, the input to the i—th vehicle $U_i(s)$ of the string is assumed to be the inter-vehicle spacing error scaled by the controller gain, i.e. $U_i(s) = (X_{i-1}(s) - X_i(s))K(s)$, where $X_i(s)$ is the Laplace transform of the time signal $x_i(t)$. A simple computation shows that if the leader of the platoon moves independently, the successive inter-vehicle spacings in terms of the trajectory of the leader $X_1(s)$ are

$$E_2(s) = \frac{1}{1 + P(s)K(s)} X_1(s) = (1 - T(s))X_1(s), \tag{6}$$

$$E_i(s) = \frac{P(s)K(s)}{1 + P(s)K(s)} E_{i-1}(s) = T(s)E_{i-1}, \quad i > 2 \tag{7}$$

and therefore, the inter-vehicle spacing at the last vehicle is given by $E_N(s) = (1 - T(s))T(s)^{N-2}X_1(s)$. Since there exists ω_c such that $|T(j\omega_c)| > 1$, the authors conclude that $|1 - T(j\omega_c)||T(j\omega_c)|^N$ grows

without bound as N increases, which implies the presence of string instability in the formation.

Alternatives to achieve string stability

As discussed in the previous section, researchers have studied several control architectures based on the basic approach of predecessor following. One of the main goals of these alternative approaches was to overcome string instability, while maintaining a certain degree of decentralization. The authors of (Seiler et al., 2004) show that by allowing every follower of a predecessor following scheme to use the instantaneous position of the leader ($x_1(t)$) to compute their controller input, string stability can be achieved. In particular, the new predecessor-leader following architecture uses the inputs $U_i(s) = K_p(s)(X_{i-1} - X_i) + K_l(s)(X_1(s) - X_i(s))$ (we omit the initial conditions for simplicity). Using the same method as before, the authors compute the successive inter-vehicle spacings in terms of the trajectory of the leader $X_1(s)$:

$$E_2(s) = \frac{1}{1 + P(s)(K_p(s) + K_l(s))} X_1(s) = S_{lp}(s) X_1(s), \tag{8}$$

$$E_i(s) = \frac{P(s)K_p(s)}{1 + P(s)(K_p(s) + K_l(s))} E_{i-1}(s) = T_{lp}(s) E_{i-1}, \quad i > 2. \tag{9}$$

The main difference when comparing these expressions to (6) and (7) is that $T_{lp}(s)$ can be designed such that $\|T_{lp}(s)\|_\infty < 1$ by using the extra degree of freedom that the controllers $K_p(s)$ and $K_l(s)$ add. It is also worth noting that setting $K_l(s) = 0$ for all s yields the same expressions as in (6) and (7) with $K(s) = K_p(s)$. One drawback of this scheme is the need for increasing networking requirements as the string grows. In this thesis we look at modifications to this architecture and also study the effects of time delays in the broadcasting of the leader state along the string. Similar extensions to the use of the leader state include the use of the back inter-vehicle spacing, which in this setting would be $X_i(s) - X_{i+1}(s)$. This scheme, usually named bidirectional control, shows potential benefits for alleviating string instability, although slow transients are to be expected with its use (Barooah et al., 2009; Middleton and Braslavsky, 2010).

Another alternative to achieve string stability is to modify the spacing policy (Swaroop, 1997; Eyre et al., 1998). In (Klinge and Middleton, 2009), it was shown that there exists a critical value of the time headway parameter h_c such that for every $h > h_c$ the predecessor

following interconnection can be made string stable (for $h \leqslant h_c$ the interconnection is shown to be string unstable). In particular, if the spacing policy is such that the inter-vehicle spacings are written as $E_i(s) = X_{i-1}(s) - X_i(s) - hsX_i(s)$, the transfer function that dictates the disturbance amplification along the string is

$$\Gamma(s) = \frac{1}{1+hs}\frac{P(s)C(s)}{1+P(s)C(s)}, \tag{10}$$

where $C(s) = K(s)Q(s)$. The authors show that if $|\Gamma(j\omega)| < 1$ for all $\omega > 0$ (note that regardless of the value of h, $\Gamma(0) = 1$), the control scheme is string stable. For this to be true, the value of h must be greater than

$$h_c := \sqrt{\max_{\omega}\left(\frac{\left|\frac{P(j\omega)C(j\omega)}{1+P(j\omega)C(j\omega)}\right|^2 - 1}{\omega^2}\right)}. \tag{11}$$

The main drawback of this control strategy is the increase in the inter-vehicle spacings with the velocity of the platoon, which reduces the throughput of the system. On the positive side, it requires only local measurements of the immediate predecessor error and velocity for every vehicle, which simplifies its implementation in a real world setting.

Multi-look ahead control has been studied in (Swaroop and Hedrick, 1999) and (Cook, 2007), where the vehicles are capable of measuring their distance from multiple vehicles that are ahead of them. It was shown in (Knorn, 2013) that the use of a communication range of two (i. e. the vehicles are allowed to measure $x_{i-1}(t)$ and $x_{i-2}(t)$ to compute their control signal) reduces the critical time headway for string stability without leader information, and therefore improves the throughput of the system. Further increase of the communication range has been shown to decrease disturbance amplification (Middleton and Braslavsky, 2010), however it is not known if it has an impact on the critical time headway for string stability.

A final alternative that we review is heterogeneous controller tuning. The authors of (Canudas de Wit and Brogliato, 1999) and (Khatir and Davidson, 2004) studied, among others, a control approach where the local controllers of every vehicle varied with its position along the string. However, it has been shown in (Middleton and Braslavsky, 2010) that heterogeneous control does not overcome the issue of string

stability unless the control bandwidths are allowed to diverge as the string size grows.

Similar concepts to string stability

String stability of vehicular platoons is connected to behaviours observed in other phenomena. For example, in supply chains or inventory control systems, where the dynamics are usually modelled in discrete time, a behaviour named as the *Forrester effect* or *bullwhip effect* has been observed (Forrester, 1961).

In the control of irrigation channels, where successive pools are connected through gates, water-level errors are amplified when decentralised feedback control is used (Li et al., 2005). The work presented in this thesis is in its majority of a theoretical nature. Therefore it is possible to use it or extend it to the study of non-vehicular applications such as the examples mentioned above.

In (Bamieh et al., 2012) the concept of *coherence* is studied in large-scale networks. The authors refer to coherence as the ability of a formation (or networked interconnection of systems) to behave in a *macroscopic* scale as close as possible to a solid object. They note that this feature will depend on the dimensionality of the system and whether the control is localized or not. In particular, a 1-D formation can be made string stable with only localized control, and will behave well on a *microscopic scale*, since errors will not be amplified along the string of vehicles. However, with the same control structure, a large formation will exhibit an *accordion* type of motion if it is observed as a unit, with slow and long spatial wavelength modes that are unregulated. This will occur whenever the formation is excited with any amount of distributed stochastic disturbances. The authors remark that this is not a safety issue, since the formation is string stable, but it could affect the throughput performances of a vehicular platoon. In this thesis, we consider one framework for the study of string stability that not only focuses on inter-vehicle spacings, but also on leader-follower spacings. In particular we show that the presence of time delays in a leader-predecessor following scheme affects the formation in a similar way as the one exposed in the study of coherence.

2.3.2 *Stability*

The control of dynamical systems has usually the goal of stabilization, among others. It is normal to assume that in the control of a vehicular platoon, the stability of the resulting interconnected system is needed.

Remark 2.1. *The notion of stability used throughout this thesis is BIBO (bounded input bounded output) stability. For LTI systems this is equivalent to having every transfer function from disturbances to vehicle positions with poles in the open left half plane (Goodwin et al., 2001).*

In a LTI setting, unidirectional strategies always result in a stable interconnection if the local feedback control loops at each vehicle (determined by $P(s)$ and $K(s)$) are stable (Seiler et al., 2004). In a more general interconnection topology this is not necessarily true. The authors of (Fax and Murray, 2004) provide a framework, based on tools from Graph Theory, to study the stability of an interconnected system. In particular, the stability of the interconnection can be related to the study of the eigenvalues of the *Laplacian* matrix associated to the graph that describes the interconnection topology. An adaptation of this result to the study of a bidirectional formation control strategy was provided in (Barooah and Hespanha, 2005) and (Lestas and Vinnicombe, 2007). In particular, the resulting interconnection is stable if certain transfer functions that depend on the local dynamics at every vehicle (the vehicle model $P(s)$ and controller $K(s)$) and the eigenvalues of a Laplacian-like matrix are stable.

For cyclic and bidirectional formation control architectures we provide results that echo the ones mentioned above. In order to study these interconnections we obtain closed form expressions for the dynamics of the systems generated by the resulting inter-vehicle spacings. To do so we use a matrix description of the interconnected system of the form:

$$\underline{X}(s) = (\mathbf{I} - P(s)K(s)\mathbf{G})^{-1}P(s)\underline{D}(s), \tag{12}$$

where $\underline{X}(s) = [X_1(s) \cdots X_N(s)]$ is the vector of Laplace transforms of the vehicle positions, $\underline{D}(s) = [D_1(s) \cdots D_N(s)]$ is the vector of Laplace transforms of the disturbances affecting each vehicle, $\mathbf{I}$ is the $N \times N$ identity matrix and $\mathbf{G}$ is the $N \times N$ interconnection matrix that reflects the measurements from the platoon that each vehicle uses to compute its control signal. While we do not directly apply the results

mentioned in the previous paragraph, our results are closely related to these. However, we have developed our approach with the aim of obtaining insights into more than just the stability of the particular interconnections studied. Our later discussions in Chapter 5 will illustrate this point.

2.4 RELATED TOPICS

In this section we briefly review some research topics that are related to formation control of vehicular platoons.

Consensus

The coordinated movement of a collection of vehicles can be viewed as a consensus problem. The vehicles agree to travel at a certain desired speed, while achieving a certain formation pattern. Some works that acknowledge the connection and provide more details are given in (Fax and Murray, 2004) and (Bamieh et al., 2008).

Flocking

Flocking behaviours in birds have been studied in connection to consensus and formation control problems. For example, the works in (Cucker and Smale, 2007) and more recently (Bongini et al., 2014) have presented mathematical models that give rise to an emergent consensus. They describe N agents that are interconnected in a nonlinear way and follow a trajectory that reaches a consensus velocity. This consensus depends only on the initial conditions of the agents but it can be modified by the use of feedback in order to obtain desired directions and/or formations.

Multi-agent systems

Cooperative control of multi-agent systems is a more general kind of problem. In (Olfati-Saber et al., 2007) the authors discuss the connections of consensus problems in networked dynamics with applications to topics such as synchronization of coupled oscillators, formation control, Markov-processes and gossip-based algorithms, rendezvous in space, and many others.

3

FORMATION CONTROL WITH LEADER TRACKING

3.1 INTRODUCTION

In this chapter we revisit the leader-predecessor following architecture for formation control of vehicles travelling in a straight line. In principle, each follower tracks simultaneously the positions of its immediate predecessor and a leader that follows an arbitrary trajectory. In Section 3.2 we present the notation and corresponding framework, with emphasis on the vehicle dynamics and the important variables to be studied. In Section 3.3 we propose two novel control architectures based on leader-predecessor following: the first one considers a modification of the way the leader position is communicated to the followers; the second one makes the followers track the velocity of the leader instead of its position. We continue our work in Section 3.4 obtaining closed form expressions in the frequency domain for the dynamics of the inter-vehicle spacing that result from the use of these interconnections. The main contributions of this chapter are presented in Section 3.5. We discuss string stability under certain configurations of time delays in the leader state broadcast for all of the architectures presented. Section 3.6 includes numerical examples that illustrate our theoretical results and Section 3.7 gives some final remarks.

Most of the contents of this chapter have been published in (Peters et al., 2014).

3.2 FRAMEWORK AND PROBLEM FORMULATION

3.2.1 *Vehicle model and preliminaries*

We consider a platoon of $n \in \mathbb{N}$ identical vehicles that travel in a straight line, with the aim of maintaining a desired and constant inter-

vehicle spacing $\Delta > 0$. The vehicle dynamics considered are linear and time invariant, namely

$$m\ddot{x}_i(t) = -k_d\dot{x}_i(t) + d_i(t) + f(u_i(t)) \quad \text{for } 1 \leqslant i \leqslant n, \tag{13}$$

where: $x_i(t)$ denotes the position of the i-th vehicle along the string; m is its mass; k_d is the vehicle drag coefficient; f is the force applied by the engine, which is a function of $u_i(t)$, the control signal; and $d_i(t)$ is a disturbance force that acts on the vehicle. Assuming simple dynamics for the engine, i.e. $f(u_i(t)) = u_i(t)$, we can work in the frequency domain. For simplicity we assume that every car starts from rest and is initially positioned in the desired formation, that is $x_i(0) = (1-i)\Delta$ and $\dot{x}_i(0) = 0$ for $i = 1, \ldots, n$ and we define $\tilde{x}_i(t) = x_i(t) + (i-1)\Delta$. Therefore, taking the Laplace transform of (13) we obtain the frequency domain vehicle models

$$\tilde{X}_i = \frac{U_i + D_i}{s(ms + k_d)} = X_i + (i-1)\frac{\Delta}{s} \quad \text{for } 1 \leqslant i \leqslant n. \tag{14}$$

3.2.2 *Formation control objectives*

Now, the control goal is to keep a tight formation, that is, to maintain the errors $e_i^{pre}(t) = x_{i-1}(t) - x_i(t) - \Delta = \tilde{x}_{i-1}(t) - \tilde{x}_i(t)$ as close to zero as possible. This small error performance should be achieved in steady state, under disturbances to any member of the platoon, and for a constant speed of the leader. To achieve this, the control signal for each vehicle $u_i(t)$ is computed using the local measurement of the immediate predecessor position (indirectly through measuring the inter-vehicle spacing) and the information being received from the leader (see Figure 3). The leader-follower errors $e_i^{lea}(t) = x_1(t) - x_i(t) - (i-1)\Delta = \tilde{x}_1(t) - \tilde{x}_i(t)$ will have a steady state response similar to that of $e_i^{pre}(t)$. These error signals can be associated with the performance of the system when considering traffic density issues and throughput. Essentially, smaller errors imply a higher density of vehicles in the road. With this, the Laplace transforms for the errors are given by

$$E_i^{pre} = X_{i-1} - X_i - \frac{\Delta}{s} = \tilde{X}_{i-1} - \tilde{X}_i, \tag{15}$$

$$E_i^{lea} = X_1 - X_i - (i-1)\frac{\Delta}{s} = \tilde{X}_1 - \tilde{X}_i. \tag{16}$$

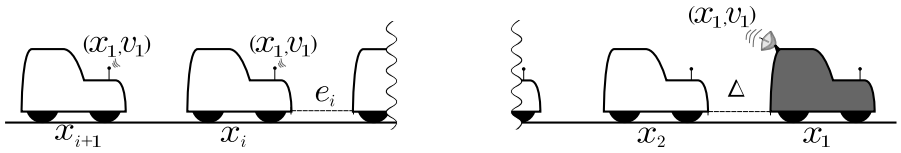

Figure 3: Platoon of vehicles. (x_i, v_i): position-velocity pair of the i-th vehicle. $e_i = x_{i-1} - x_i$: inter-vehicle spacing between the $(i-1)$-th and i-th vehicles. Δ: desired inter-vehicle spacing.

These two errors will be central to our later analysis.

3.3 ARCHITECTURES FOR FORMATION CONTROL

We consider three main approaches to achieve the platoon control objectives.

3.3.1 *Leader-predecessor following*

The leader-predecessor following architecture (Seiler et al., 2004) is implemented by the use of the vehicle inputs

$$U_i = K(\eta E_i^{pre} + (1-\eta)E_i^{lea}) = K(\eta \tilde{X}_{i-1} + (1-\eta)\tilde{X}_1 - \tilde{X}_i), \tag{17}$$

where $\eta \in (0,1)$ and K is a dynamic compensator (in the present case taken to be identical for all vehicles) that stabilizes each vehicle in closed loop. If H denotes the transfer function model for the vehicle, by stabilizing the vehicle in closed loop we refer to having the transfer function

$$T = \frac{KH}{1+KH}, \tag{18}$$

being stable and having no unstable cancellations in the product HK.

Each car takes the weighted average spacing error of its predecessor and leader to regulate its own position. Some drawbacks of the scheme are:

- each follower must be aware of its own position within the string since the leader-follower errors are given by $e_i^{lea}(t) = x_1(t) - x_i(t) - (i-1)\Delta$;
- each vehicle must have a highly accurate absolute position reference to compute $x_1(t) - x_i(t)$;

- each follower must use the same value for Δ, imposing a coordination requirement.

These can be overcome by the schemes described below.

3.3.2 *Leader velocity tracking and predecessor following*

Here we drop the leader position knowledge for each vehicle, exchanging it for measurements of the position of its predecessor and the velocity of the leader. The control signal for each car takes the form

$$U_i = K_p E_i^{pre} + K_v s E_i^{lea} = \tilde{K}\left(\frac{K_p}{\tilde{K}}\tilde{X}_{i-1} + \left(1 - \frac{K_p}{\tilde{K}}\right)\tilde{X}_1 - \tilde{X}_i\right), \quad (19)$$

where K_p, K_v and $\tilde{K} = K_p + sK_v$ are dynamic compensators such that $\tilde{K}$ stabilizes each vehicle in closed loop. By this we refer to having a stable transfer function $T = HK/(1+HK)$ and no unstable cancellations in the product HK (Goodwin et al., 2001).

The selections for U_i aim to keep a tight inter-vehicle spacing and simultaneously track the leader velocity in every follower. One advantage of this architecture is that each follower does not need to be aware of its position along the string. New members can join the rear of the platoon without having to know the number of vehicles that separate them from the leader. Every follower has to listen to $\dot{x}_1(t)$ (see Fig 3) while measuring with local sensors (e.g. radar) its distance to its predecessor.

Remark 3.1. *This scheme has a connection with time headway policies (see for example Klinge and Middleton (2009) and Chapter 2). This can be seen from (19), which can be written as:*

$$U_i = K_p\left(\tilde{X}_{i-1} - \tilde{X}_i - \frac{K_v}{K_p}s\tilde{X}_i\right) + K_v s\tilde{X}_1. \quad (20)$$

Therefore, in terms of the local dynamics, the feedback includes the equivalent of a (possibly dynamic) time headway, K_v/K_p. The use of the leader velocity means that improved dynamic properties may be achieved without increasing the steady state vehicle separation that commonly occurs with time headway policies (Chien and Ioannou, 1992).

3.3.3 *Alternative algorithm: indirect leader state broadcast*

Leader state information need not be sent directly to each member. Alternatively it can be computed indirectly at any follower from local measurements and information being sent by its predecessor. For instance, consider the control signal

$$u_i = k(e_i^{pre} + (1-\eta)\Gamma\varepsilon_{i-1}), \tag{21}$$

where ε_{i-1} is a signal sent by the $(i-1)$-th member, containing an estimate of the state of the leader and Γ is a stable transfer function that can be used to represent communication issues. In the particular case $\varepsilon_{i-1} = e_{i-1}^{leq}$ and $\Gamma = 1$, i. e. the estimation is perfect, the control signals coincide with the first case of leader-predecessor following

$$u_i = k(e_i^{pre} + (1-\eta)e_{i-1}^{leq}) = k(\eta\tilde{x}_{i-1} + (1-\eta)\tilde{x}_1 - \tilde{x}_i), \tag{22}$$

and the resulting dynamics are identical to (17).

In the general case, each member receives $\Gamma\varepsilon_{i-1}$ from its predecessor assuming that it is exactly e_{i-1}^{leq}. This allows any vehicle to estimate their own leader-follower error adding the local measurement e_i^{pre} to the received signal, that is

$$\varepsilon_i = \Gamma\varepsilon_{i-1} + e_i^{pre}, \tag{23}$$

which in turn is sent to the immediate follower. The main benefit of this alternative is that the coordination requirements of the leader-predecessor following are no longer needed.

3.4 CLOSED LOOP DYNAMICS

In this section we derive formulae that will allow us to study the properties of the three architectures defined in Section 3.3. In particular we are interested in studying the effect of time delays in the reception of the leader state and the following derivations prove to be useful in that regard.

3.4.1 *Vehicle string dynamics for direct leader state broadcast schemes*

The two unidirectional control structures introduced in Sections 3.3.1 and 3.3.2 share a similar mathematical description, differing only in the compensator and the weights of the errors. Moreover, they belong to a broader class of MIMO systems. In particular we consider the class of control laws

$$U_i = K(P\tilde{X}_{i-1} + L_i\tilde{X}_1 - \tilde{X}_i), \tag{24}$$

where L_i and P are arbitrary stable transfer functions such that $L_i(0) + P(0) = 1$.

Remark 3.2. *This constraint on the DC gains of* L_i *and* P *is required to ensure bounded control signals* $u_i(t)$ *when the vehicles move at a constant speed.*

Here we allow the leader transfer function L_i to vary, while considering homogeneous predecessor transfer functions P. This will allow us to include a factor that accounts for time delays in the reception. In particular, setting $P = \eta$, $L_i = 1 - \eta$ with $\eta \in [0, 1]$ yields (17). Similarly, setting $P = K_p/\tilde{K}$ and $L_i = 1 - K_p/\tilde{K}$ yields (19).

Remark 3.3. *In some of the following discussions when referring to the leader-predecessor following architecture we will note it by stating* $P = \eta \in (0, 1)$. *Otherwise, a dynamic* P *will be referring to leader velocity tracking.*

We are interested in the response of the string to input disturbances on the vehicles. First, we use the vehicle model transfer function, from (14), given by

$$\tilde{H} = \frac{1}{ms + k_d}, \quad H = \frac{\tilde{H}}{s}, \tag{25}$$

and we let

$$T = HK(1 + HK)^{-1}, \quad S = 1 - T, \tag{26}$$

be the usual closed loop sensitivity functions. Then, if the lead vehicle does not possess a controller and it drives independently, the vehicle dynamics are given by

$$\underline{\tilde{X}} = (\mathbf{I} - HK\mathbf{G})^{-1}H\underline{D}, \tag{27}$$

where

$$\underline{\tilde{X}} = \begin{bmatrix} \tilde{X}_1 & \cdots & \tilde{X}_n \end{bmatrix}^\top, \tag{28}$$

$$\underline{D} = \begin{bmatrix} D_1 & \cdots & D_n \end{bmatrix}^\top, \tag{29}$$

$\mathbf{I}$ is the $n \times n$ identity matrix and $\mathbf{G} \in \mathbb{C}^{n\times n}$ is the interconnection matrix:

$$\mathbf{G} = \begin{bmatrix} 0 & \underline{0}^\top \\ \underline{L} & \mathbf{\Phi} \end{bmatrix}, \tag{30}$$

where $\underline{L} = [L_2\ L_3\ \cdots\ L_n]^\top$, $\underline{0} \in \mathbb{R}^{(n-1)}$ is the zero vector and the matrix $\mathbf{\Phi} \in \mathbb{C}^{(n-1)\times(n-1)}$ is given by $\mathbf{\Phi}_{i,i} = -1$ for $1 \leqslant i \leqslant n-1$, $\mathbf{\Phi}_{i+1,i} = P$ for $1 \leqslant i \leqslant n-2$ and all other entries of $\mathbf{\Phi}$ are zero. Note that the selection $G_{1,1} = 0$ represents freedom of movement for the lead vehicle. In other words, its trajectory will be determined only by $X_1 = HD_1$. Corresponding results to those presented here can be derived for alternative formulations using a fictitious leader or other strategies, but the essential results that follow remain unaltered.

Now, the matrix $(\mathbf{I} - HK\mathbf{G})$ and its inverse have the following structures

$$(\mathbf{I} - HK\mathbf{G})^{-1} = \begin{bmatrix} 1 & \underline{0}^\top \\ -KH\underline{L} & \mathbf{\Theta} \end{bmatrix}^{-1} = \begin{bmatrix} 1 & \underline{0}^\top \\ KH\mathbf{\Theta}^{-1}\underline{L} & \mathbf{\Theta}^{-1} \end{bmatrix}, \tag{31}$$

where $\mathbf{\Theta} \in \mathbb{C}^{(n-1)\times(n-1)}$ satisfies $\Theta_{i,i} = KHT^{-1}$ for $1 \leqslant i \leqslant n-1$, $\Theta_{i+1,i} = -KHP$ for $1 \leqslant i \leqslant n-2$ and all other entries of $\mathbf{\Theta}$ are zero.

Computing $\mathbf{\Theta}^{-1}$ is straightforward since $\mathbf{\Theta}$ is lower triangular

$$\mathbf{\Theta}^{-1} = \frac{T}{KH} \begin{bmatrix} 1 & & & \\ PT & \ddots & & \\ \vdots & \ddots & \ddots & \\ (PT)^{n-2} & \dots & PT & 1 \end{bmatrix}. \tag{32}$$

Under these considerations, disturbances at any member of the string will affect the vector of predecessor errors as

$$\left[E_2^{pre} \cdots E_n^{pre}\right]^\top = \mathbf{F}\underline{D} = \begin{bmatrix} 1 & -1 & & \\ & \ddots & \ddots & \\ & & 1 & -1 \end{bmatrix} (\mathbf{I} - HK\mathbf{G})^{-1} H\underline{D}. \tag{33}$$

3.4.2 *Vehicle string dynamics for indirect leader state broadcast*

The string dynamics for the alternative algorithm from Section 3.3.3 can be determined by first inserting (21) in (14) and taking the difference in position for two successive followers

$$\tilde{X}_{i-1} = HK((1-\eta)\Gamma\mathcal{E}_{i-2} + E_{i-1}^{pre}) + HD_{i-1}, \tag{34}$$

$$\tilde{X}_i = HK((1-\eta)\Gamma\mathcal{E}_{i-1} + E_i^{pre}) + HD_i, \tag{35}$$

$$E_i^{pre} = HK((1-\eta)(1-\Gamma)\mathcal{E}_{i-1} + \eta E_{i-1}^{pre} - E_i^{pre}) + H(D_{i-1} - D_i). \tag{36}$$

Merging the last equation with (23) we can write in matrix form

$$\begin{bmatrix} E_i^{pre} \\ \mathcal{E}_i \end{bmatrix} = \begin{bmatrix} \eta HK & (1-\eta)(1-\Gamma)HK \\ 0 & \Gamma \end{bmatrix} \begin{bmatrix} E_{i-1}^{pre} \\ \mathcal{E}_{i-1} \end{bmatrix} - \begin{bmatrix} HK & 0 \\ -1 & 0 \end{bmatrix} \begin{bmatrix} E_i^{pre} \\ \mathcal{E}_i \end{bmatrix} + H \begin{bmatrix} D_{i-1} - D_i \\ 0 \end{bmatrix}, \tag{37}$$

for $i \geqslant 3$.

For this case we will only focus on disturbances at the leader and set $D_i = 0$ for $i = 2, \ldots, n$. The reason for this will become evident in a following section. For the first follower, i. e. $i = 2$, we have

$$\begin{bmatrix} E_2^{pre} \\ \mathcal{E}_2 \end{bmatrix} = - \begin{bmatrix} HK & 0 \\ -1 & 0 \end{bmatrix} \begin{bmatrix} E_2^{pre} \\ \mathcal{E}_2 \end{bmatrix} + H \begin{bmatrix} D_1 \\ 0 \end{bmatrix}, \tag{38}$$

and hence, $\mathcal{E}_2 = E_2^{pre} = SHD_1$. With these facts we can solve the first order recursion in (37) to obtain the desired dynamics. In particular the solution for

$$\underline{Y}_i = \mathbf{A}\underline{Y}_{i-1} + \mathbf{B}\underline{Y}_i, \tag{39}$$

with initial condition $\underline{Y}_2 = \underline{y}$ is given by (see for example Aström and Wittenmark (2011))

$$\underline{Y}_i = ((\mathbf{I} - \mathbf{B})^{-1}\mathbf{A})^{i-2}\underline{y}, \quad \text{for } i \geqslant 2. \tag{40}$$

In the present case, we have

$$\mathbf{A} = \begin{bmatrix} \eta HK & (1-\eta)(1-\Gamma)HK \\ 0 & \Gamma \end{bmatrix}, \tag{41}$$

$$\mathbf{B} = \begin{bmatrix} HK & 0 \\ -1 & 0 \end{bmatrix}, \tag{42}$$

$$\underline{y} = \begin{bmatrix} 1 \\ 1 \end{bmatrix} SHD_1, \tag{43}$$

which yields

$$\begin{bmatrix} E_i^{pre} \\ \mathcal{E}_i \end{bmatrix} = \begin{bmatrix} \eta T & (1-\eta)(1-\Gamma)T \\ \eta T & (1-\eta)(1-\Gamma)T + \Gamma \end{bmatrix}^{i-2} \begin{bmatrix} 1 \\ 1 \end{bmatrix} SHD_1, \tag{44}$$

for $i \geqslant 2$

3.5 PROPERTIES OF THE INTERCONNECTIONS

In this section we present the main results of this chapter. Our approach to string stability is to show that certain transfer functions from disturbances to errors have a magnitude peak with a bound that is independent of the string length (Middleton and Braslavsky, 2010). We use the following definition.

Definition 3.1. *Let* $\{F_n\}$ *be a sequence of stable transfer functions. The sequence will be called* string stable *if there exists* $c \in \mathbb{R}$*, independent of* $n \in \mathbb{N}$ *such that* $\|F_n\|_\infty \leqslant c$ *for all* $n \in \mathbb{N}$*. It will be called* string unstable *otherwise.*

TRANSFER FUNCTION	POLES AT $s = 0$	NOTES
H	1	$\tilde{H}(0) = 1/k_d$
K	1	-
$T = KH/(1+KH)$	none	$T(0) = 1$, $T'(0) = 0$

Table 1: Assumptions on some transfer functions.

Remark 3.4. *In the following we assume that K has at least one pole at $s = 0$. Since the vehicle model H is assumed to also have a single pole at $s = 0$, having another at the controller is a requirement for the string to achieve zero velocity tracking error for constant velocity trajectories of the leader (i. e. ramp trajectories, see for example Middleton and Braslavsky (2010)). Table 1 collects some of the assumptions made for this chapter.*

The following result is a restatement of Lemma I from Chapter 2 for future referencing. This result implies string instability under the assumptions given above in the leader-predecessor following scheme when there is no leader communication (which is equivalent to set $\eta = 1$).

Lemma 3.1. (Simplified Bode Complementary Sensitivity Integral) *Let $T(s) = H(s)K(s)/(1 + H(s)K(s))$ where $L(s) = H(s)K(s)$ is a real rational scalar function of the complex variable s which is proper and satisfies $L(0) \neq 0$. Suppose that $T(0) = 1$ and also that $T(s)$ is stable (analytic in the closed right half complex plane). Then*

$$\int_0^\infty \ln|T(j\omega)|\frac{d\omega}{\omega^2} \geqslant \frac{\pi}{2}\lim_{s\to 0}\frac{dT(s)}{ds}. \tag{45}$$

In the current case, T is given by (26). The dynamics considered for vehicles and controllers are such that the term HK has two poles at the origin. Given that

$$S = 1 - T = \frac{1}{1+HK}, \tag{46}$$

the internal stability of the loop (see for example Goodwin et al. (2001)) implies that S has two zeros at the origin. Moreover, $T'(s) = -S'(s)$ and therefore it follows that at $s = 0$, $T'(0) = S'(0) = 0$. Lemma 3.1 now implies that $\|T\|_\infty > 1$.

In the leader-predecessor following scheme, it is straightforward from (17) that with no leader communication, i. e. $\eta = 1$, the sequence of predecessor errors for a disturbance D_1 at the leader will be given

by $E_n^{pre} = HST^{n-2}D_1 = F_n D_1$. Since H and K have a finite number of zeros it is possible to choose ω_0 such that $|H(j\omega_0)S(j\omega_0)| \neq 0$ and $|T(j\omega_0)| > 1$ (Seiler et al., 2004). Therefore, we have that the sequence $\{F_n\} = \{HST^{n-2}\}$ is string unstable according to Definition 3.1. The following simple proposition will help in the presentation of the main results.

Proposition 3.1. *Let* PT *be a stable and proper transfer function such that* $\|PT\|_\infty \leqslant 1$. *Also let* W, Q *be transfer functions such that* $\|W\|_\infty, \|Q\|_\infty$ *are well defined and* $W + Q(PT)^n$ *is stable for every* $n \in \mathbb{N}$. *Then, the sequence* $\{W + Q(PT)^n\}$ *is string stable.*

Proof: First, we have from the triangle inequality that $|W + Q(PT)^n| \leqslant |W| + |Q||(PT)^n|$ holds for all $\omega \geqslant 0$, $n \in \mathbb{N}$. Since $\|PT\|_\infty \leqslant 1$ it is also true that $|W| + |Q||(PT)^n| \leqslant |W| + |Q|$. If we let $\|W\|_\infty = a$ and $\|Q\|_\infty = b$ then $|W + Q(PT)^n| \leqslant a + b$ for all $\omega \geqslant 0$, $n \in \mathbb{N}$. Hence, the sequence $\{W + Q(PT)^n\}$ is string stable according to Definition 3.1 with $c = a + b \in \mathbb{R}$. □

3.5.1 *Disturbances at followers: direct leader state broadcast schemes*

A disturbance D_k at the k-th follower, where k is fixed, will affect the last predecessor error E_n^{pre}, $n \geqslant k > 1$, through the entry $F_{n,k}$ of the matrix $\mathbf{F}$ defined in (33). In other words

$$E_n^{pre} = F_{n,k} D_k, \tag{47}$$

with

$$F_{n,k} = \begin{cases} (1 - PT)(PT)^{n-k-1}SH & \text{if } n > k \\ SH & \text{if } n = k \end{cases}. \tag{48}$$

If $\mathcal{F}_{n,k} = \sum_{i=k}^{n} F_{n,k}$, the corresponding leader errors are given by

$$E_n^{lea} = \sum_{i=k}^{n} E_i^{pre} = \mathcal{F}_{n,k} D_k = (2 - (PT)^{n-k})SHD_k, \tag{49}$$

that is, $\mathcal{F}_{n,k}$ is the transfer function from a disturbance at the k-th member to the last leader error.

The selection of L_i (which determines leader information reception) does not affect these responses directly. Moreover, disturbances at the

followers will not affect predecessors (which is obvious from the interconnection). The following result gives a condition for string stability of the sequence $\{\mathcal{F}_{n,k}\}$ and also gives the DC gain of these transfer functions.

Theorem 3.1. (Disturbances at the followers) *Consider the sequences* $\{F_{n,k}\}$ *and* $\{\mathcal{F}_{n,k}\}$ *given by* (48) *and* (49) *respectively. The following statements are true:*
1) $F_{n,k}(0) = \mathcal{F}_{n,k}(0) = 0$ *for all* $n \geqslant k > 1$.
2) If $\|PT\|_\infty \leqslant 1$, *then* $\{F_{n,k}\}$ *and* $\{\mathcal{F}_{n,k}\}$ *are string stable.*

Proof:

1) Since the product KH has exactly two poles at $s = 0$, we can write $S = s^2\tilde{S}$ with $\tilde{S}(0) \neq 0$ (S has two zeros at $s = 0$). The vehicle transfer function is $H = \tilde{H}/s$, $\tilde{H}(0) \neq 0$ as defined in (33). From their definitions P and T are stable and consequently we can rewrite

$$F_{n,k} = s(1 - PT)(PT)^{n-k-1}\tilde{S}\tilde{H}. \tag{50}$$

Evaluating at $s = 0$ yields $F_{n,k}(0) = 0$ for $n \geqslant k > 1$. From its definition

$$\mathcal{F}_{n,k} = \sum_{i=k}^{n} F_{n,k}, \tag{51}$$

and therefore $\mathcal{F}_{n,k}(0) = \sum_{i=k}^{n} F_{n,k}(0) = 0$, for $n \geqslant k > 1$ which is the required result.

2) For $\{F_{n,k}\}$ Proposition 3.1 can be used. In particular we have that $F_{n,k}$ is stable for all $n \in \mathbb{N}$. This is due to the stability of PT and the stability of the product SH. Setting $W = 0$ and $Q = (1 - PT)SH$ implies that $\{F_{n,k}\}$ is string stable. Similarly, if we set $W = 2SH$ and $Q = -SH$ and noting that $\mathcal{F}_{n,k}$ is stable for all $n \in \mathbb{N}$ implies that $\{\mathcal{F}_{n,k}\}$ is also string stable. □

The first part of Theorem 3.1 implies that constant disturbances at the followers will yield zero steady state errors. String stability of $\{F_{n,k}\}$ implies that disturbances at the k—th member are not amplified for the remaining followers ($n > k$), accounting for a *string safety* condition. Moreover, string stability of $\{\mathcal{F}_{n,k}\}$ ensures that disturbances at the k—th follower do not create increasing leader-follower spacings.

On the other hand, suppose there exists $\omega_0 \geqslant 0$ such that we have $P(j\omega_0)T(j\omega_0) = \gamma e^{j\theta}$ with $\gamma > 1$. Since the product SH has no poles at the origin (the pole of H is canceled by one of the zeros of S) and

is stable, we have $|S(j\omega_0)H(j\omega_0)| = \alpha < \infty$. Moreover, PT is stable which implies $|1 - P(j\omega_0)T(j\omega_0)| = \beta < \infty$ and therefore

$$|F_{n,k}(j\omega_0)| = \alpha\beta\gamma^{n-k+1}, \tag{52}$$

$$|\mathcal{F}_{n,k}(j\omega_0)| = \alpha|2 - \gamma^{n-k+1}e^{j(n-k+1)\theta}|, \tag{53}$$

for all $n \geqslant k > 1$. Therefore, in this case the disturbance amplification will grow unbounded with the string length, i. e. we will have string instability in (48).

Remark 3.5. *Our assumptions on the vehicle and controller dynamics* H *and* K *imply that* $\|T\|_\infty > 1$. *Therefore the design of* P *through the leader state communication must be aimed to achieve at least* $\|PT\|_\infty \leqslant 1$. *For the leader-following approach* $P = \eta \in (0, 1)$ *and it suffices to have* $\eta \leqslant \|T\|_\infty^{-1}$. *However, for the leader velocity tracking approach* $K = K_p + sK_v$ *and* $P = K_p/(K_p + sK_v)$ *where* K_p *and* K_v *are stable transfer functions. This means that*

$$PT = \frac{K_p H}{1 + H(K_p + sK_v)} = K_p HS, \tag{54}$$

and K_p, K_v *must be designed in order to satisfy at least* $\|PT\|_\infty \leqslant 1$. *Whether it is possible to satisfy this condition for any* H *with marginally stable (for integration)* K_p *and* K_v *is the subject of ongoing research (although it can be seen that* $K = K_p + sK_v$ *can be fixed to achieve closed loop stability and* K_p *can be designed to achieve the bound, the question is whether the resulting* $K_v = (K - K_p)/s$ *remains stable). In the following we will be interested in transfer functions* P *such that* $P(0) = 1$ *and* $\|PT\|_\infty \leqslant 1$. *We will provide some numerical examples that show the feasibility of satisfying this condition.*

3.5.2 *Disturbances at the lead vehicle: direct leader state broadcast schemes*

Now we focus our attention on the effect of disturbances to the lead vehicle. From (33), the inter-vehicle spacing transfer function for the last member of the string when a disturbance in the leader occurs is given by

$$F_{n,1} = \left[(1 - PT)\sum_{i=2}^{n-1} L_i(PT)^{n-i-1} - L_n\right] TH. \tag{55}$$

The transfer function that describes the effect of D_1 on the leader error for the last member, that is E_n^{lea}, is given by

$$\mathcal{F}_{n,1} = \sum_{i=2}^{n} F_{i,1}. \tag{56}$$

In general $L_2 = 1$ since the second member of the platoon just follows the leader using its predecessor error $E_2^{pre} = \tilde{X}_1 - \tilde{X}_2$. The elements L_i for $i \geqslant 3$ can be used to describe the reception of the leader information along the string. We are mainly interested in the effect of time delays on the resulting DC gains and string stability conditions for the transfer functions mentioned above. Three cases are studied.

a) *Perfect communication*

The case of perfect reception of the leader information can be studied when $L_i = 1 - P$ for $i = 3, \ldots, n$. In this case (55) and (56) yield

$$F_{n,1} = SH(PT)^{n-2}, \tag{57}$$

$$\mathcal{F}_{n,1} = SH \sum_{i=2}^{n} (PT)^{i-2} = SH \frac{1 - (PT)^{n-1}}{1 - PT}. \tag{58}$$

We have the following result.

Theorem 3.2. (Disturbances at the leader: perfect communication) *Consider the sequences* $\{F_{n,k}\}$ *and* $\{\mathcal{F}_{n,k}\}$ *given by* (57) *and* (58) *respectively. The following statements are true:*
1) $F_{n,k}(0) = \mathcal{F}_{n,k}(0) = 0$ *for all* $n \geqslant k > 1$.
2) If $\|PT\|_\infty \leqslant 1$, $\{F_{n,1}\}$ *is string stable.*
3) If $\|PT\|_\infty \leqslant 1$ *and* $PT \neq 1$ *for* $s = j\omega$, $\omega > 0$, *then* $\{\mathcal{F}_{n,1}\}$ *is string stable.*

Proof: 1) The proof is analogous to part 1) of Theorem 3.1.

2) Proposition 3.1 applies with $W = 0$ and $Q = SH$, which implies string stability of the sequence $\{F_{n,1}\}$.

3) If $\|PT\| \leqslant 1$, $PT \neq 1$ for $s = j\omega$, $\omega > 0$, then the magnitudes $|W| = |SH/(1 - PT)|$ and $|Q| = |SH/(PT - 1)|$ are well defined for $\omega > 0$. If $P = \eta \in (0, 1)$ or $P(0) \neq 1$, evaluating $|W(j\omega)|$ and $|Q(j\omega)|$

at $\omega = 0$ yields $W(0) = Q(0) = 0$. For dynamic P such that $P(0) = 1$ (and therefore $P(0)T(0) = 1$) it is easy to compute

$$\lim_{s\to 0} \frac{SH}{1-PT} = \lim_{s\to 0} \frac{s\tilde{S}\tilde{H}}{1-PT} = -\frac{\tilde{S}(0)\tilde{H}(0)}{P'(0)}, \tag{59}$$

which implies that $\|W\|_\infty$ and $\|Q\|_\infty$ are well defined for any P satisfying the conditions. Hence, Proposition 3.1 shows that the sequence $\{\mathcal{F}_{n,1}\}$ is string stable. □

If there is perfect reception of the leader state, and disturbances occur at the lead vehicle, Theorem 3.2 shows that the two architectures with direct leader state broadcast, namely leader-predecessor following and leader velocity tracking, achieve a tight formation. Also, both architectures are string stable for the error signals of interest, for appropriately designed P, differing only in the resulting dynamics.

It can be noted that there is an extra condition for the string stability of $\{\mathcal{F}_{n,1}\}$, when compared to Theorem 3.1. Let $PT = e^{j\theta}$ at some $\omega = \omega_0$, then, if $\theta = 2k\pi$ $k \in \mathbb{Z}$, that is $PT = 1$ at $s = j\omega_0$, we have

$$\lim_{\omega\to\omega_0} \frac{1-(PT)^{n-1}}{1-PT} = \lim_{\theta\to 2k\pi} \frac{1-e^{j\theta(n-1)}}{1-e^{j\theta}} = n-1, \tag{60}$$

and consequently, $|\mathcal{F}_{n,1}(j\omega_0)| = |S(j\omega_0)H(j\omega_0)|(n-1)$. This means that the disturbance amplification grows linearly with the size of the platoon and we have string instability.

b) *One-step string relay communications*

Here we study the effects of a single occurrence of time delay on the architectures. Choose some n_r with $3 \leqslant n_r < n$ and setting $L_i = 1 - P$ for $i = 3, \ldots, n_r$ and $L_i = (1-P)e^{-\tau s}$, $\tau > 0$ for $i = n_r + 1, \ldots, n$. This corresponds to one rebroadcast of the leader state with a delay τ, by the n_r-th member of the string. The formula for $F_{n,1}$ in (55), when $n > n_r$, is given by

$$\begin{aligned} F_{n,1} = TH\Bigg[&(1-PT)(PT)^{n-3} + (1-PT)(1-P)\sum_{i=3}^{n_r}(PT)^{n-i-1} \\ &+ (1-PT)(1-P)e^{-\tau s}\sum_{i=n_r+1}^{n-1}(PT)^{n-1-i} - L_n\Bigg] \\ = TH&\left[(PT)^{n-3}PS + (1-e^{-\tau s})(1-P)(PT)^{n-n_r-1}\right]. \end{aligned} \tag{61}$$

To compute (56) first we note that

$$\mathcal{F}_{n,1} = \sum_{i=2}^{n} F_{i,1} = \sum_{i=2}^{n_r} F_{i,1} + \sum_{i=n_r+1}^{n} F_{i,1}, \tag{62}$$

where we separate terms for vehicles without time delay, from those with delay. Inserting the formulae obtained before in (61) and (57) for $F_{i,1}$ with and without delay we obtain

$$\mathcal{F}_{n,1} = SH\frac{1-(PT)^{n-1}}{1-PT} + (1-e^{-\tau s})(1-P)TH\frac{1-(PT)^{n-n_r}}{1-PT}. \tag{63}$$

Substituting $\tau = 0$ yields the same expressions as in the perfect communication case.

Theorem 3.3. (Disturbances at the leader: one-step string relay communication) *Consider the sequences* $\{F_{n,k}\}$ *and* $\{\mathcal{F}_{n,k}\}$ *given by* (61) *and* (63) *respectively. If* $\tau > 0$, $3 \leqslant n_r < n$, *then the following holds:*
1) If $P = \eta \in (0,1)$ *then* $F_{n,1}(0) = \tau\tilde{H}(0)(1-\eta)\eta^{n-n_r-1}$ *and* $\mathcal{F}_{n,1}(0) = \tau\tilde{H}(0)(1-\eta^{n-n_r})$. *If* P *is dynamic with* $P(0) = 1$ *then* $F_{n,1}(0) = \mathcal{F}_{n,1}(0) = 0$.
2) If $\|PT\|_\infty \leqslant 1$, $\{F_{n,1}\}$ *is string stable.*
3) If $\|PT\|_\infty \leqslant 1$ *and* $PT \neq 1$ *for* $s = j\omega$, $\omega > 0$, *then* $\{\mathcal{F}_{n,1}\}$ *is string stable.*

Proof: See Section A.1 where a complete proof is given.

The previous result states that both architectures using direct leader state communication (leader following and leader velocity tracking) are affected in different ways if there is a time delay in the reception of the leader state – in particular, time delays after a certain position along the string. We see that the tight formation is lost when $\tau > 0$ for the leader-predecessor following scheme, whereas leader velocity tracking still provides 0 DC gain on both transfer function errors $F_{n,1}$ and $\mathcal{F}_{n,1}$. Both architectures remain string stable for both sequences $\{F_{n,1}\}$ and $\{\mathcal{F}_{n,1}\}$, when the leader state reception is delayed τ seconds for vehicles behind the n_r-th member.

c) Multi-step string relay communications

An increasing time delay along the string can be seen as a worst case of communication constraints where multiple re-broadcasting along the string is required. This corresponds to the selections $L_i =$

$(1-P)e^{-(i-2)\tau s}$ for $i = 3, \dots, n$. Now, the predecessor error transfer function is given as

$$F_{n,1} = TH\Big[(1-PT)(PT)^{n-3} - (1-P)e^{-(n-2)\tau s} + (1-PT)(1-P)\sum_{i=3}^{n-1} e^{-(i-2)\tau s}(PT)^{n-1-i}\Big]. \tag{64}$$

With some more manipulations we obtain

$$F_{n,1} = TH\Big[(1-PT)(PT)^{n-3} - (1-P)e^{-(n-2)\tau s} + (1-PT)(1-P)e^{-\tau s}\frac{((PT)^{n-3} - e^{-(n-3)\tau s})}{PT - e^{-\tau s}}\Big]. \tag{65}$$

Now, to compute $\mathcal{F}_{n,1} = \sum_{i=2}^{n} F_{i,1}$ we apply the formula for the sum of the geometric series to the three terms inside the brackets in (65). Simplifying we obtain

$$\mathcal{F}_{n,1} = H\left[\frac{(1-(PT)^{n-1})(e^{-\tau s} - T)}{e^{-\tau s} - PT} + \frac{(1-P)(1-e^{-(n-1)\tau s})T}{e^{-\tau s} - PT}\right]. \tag{66}$$

Once more, setting $\tau = 0$ results in the expression for the perfect communications case in (57).

Theorem 3.4. (Disturbances at the leader: multi-step string relay communication) *Consider the sequences* $\{F_{n,k}\}$ *and* $\{\mathcal{F}_{n,k}\}$ *with elements defined in* (65) *and* (66) *respectively. If* $\tau > 0$, *then the following holds:*
1) If $P = \eta \in (0,1)$ *then*

$$F_{n,1}(0) = \tau\tilde{H}(0)(1-\eta^{n-2}), \tag{67}$$

$$\mathcal{F}_{n,1}(0) = \tau\tilde{H}(0)\left(n-1-\frac{1-\eta^{n-1}}{1-\eta}\right). \tag{68}$$

If P *is dynamic with* $P(0) = 1$ *then* $F_{n,1}(0) = \mathcal{F}_{n,1}(0) = 0$.
2) Let $\|PT\|_\infty \leqslant 1$, *and* $PT - e^{-\tau s} \neq 0$ *for* $s = j\omega$, $\omega > 0$. *If* $\tau \neq -P'(0)$ *the sequence* $\{F_{n,1}\}$ *is string stable.*
3) The sequence $\{\mathcal{F}_{n,1}\}$ *is string unstable for any selection of* P.

Proof: See Section A.2 where a complete proof is given.

If the magnitude of time delay for the reception of the leader state increases at every member, Theorem 3.4 states that neither architecture can provide string stability for $\{\mathcal{F}_{n,1}\}$. This means that the leader

error $E_n^{lea} = \tilde{X}_1 - \tilde{X}_n$ will grow unbounded with the platoon size. This can be interpreted as a degradation of the performance of the string. On the other hand, both architectures achieve string stability on the predecessor errors, provided that P is designed properly. This ensures a degree of safety, even when the time delay increases progressively along the string. The key difference between the two architectures is the values of the DC gains $F_{n,1}(0)$ and $\mathcal{F}_{n,1}(0)$. When the platoon travels at a constant speed the leader velocity tracking scheme provides a tight formation under the communication constraint, whereas the leader-predecessor following scheme will have spacings that differ from the desired formation with an offset that increases with the magnitude of time delay as seen from (67) and (68).

Remark 3.6. *It is interesting to compare the previous discussion to the concept of coherence of an interconnection of systems, defined and studied in (Bamieh et al., 2012) (and discussed in Chapter 2). In that work, the authors refer to a particular behaviour of a platoon of vehicles in a macroscopic sense, i. e. when observing the string as a whole. This behaviour resembles the movement of an* accordion*, with some slow and long spatial movements. This can occur even if the platoon is string stable in the inter-vehicle spacings.*

In the present case with increasing time delays, the vehicles remain string stable in the inter-vehicle spacings (locally), which is measured by the boundedness of $\|F_{n,1}\|_\infty$, but not in the leader error (which can be seen as a macro view of the string), given by the growth of $\|\mathcal{F}_{n,1}\|_\infty$ with n.

Remark 3.7. *Part 2) of Theorem 3.4 shows that a condition for string stability is that $\tau \neq -P'(0)$, which is only relevant for dynamic P, that is, for the leader velocity tracking case. This critical value for the time delay yields string instability in the predecessor errors (see A.2 for details). However, for time delays larger or smaller than this critical value, which depends on the design of P, the leader velocity tracking architecture remains string stable in $\{F_{n,1}\}$.*

3.5.3 *Disturbances at lead vehicle: indirect leader state broadcast schemes*

We study the string stability properties of the dynamics obtained from the use of the alternative algorithm defined in (21). Only time delay on the communications will be studied, that is $\Gamma = e^{-\tau s}$.

The last predecessor error is affected by a disturbance on the leader as $E_n^{pre} = F_{n,1} D_1$ which can be computed from (44) by expanding the powers of the matrix

$$\begin{bmatrix} \eta T & (1-\eta)(1-e^{-\tau s})T \\ \eta T & (1-\eta)(1-e^{-\tau s})T + e^{-\tau s} \end{bmatrix} = e^{-\tau s}\mathfrak{M}(s)$$
$$= e^{-\tau s} \begin{bmatrix} 1 & 0 \\ 1 & 1 \end{bmatrix} \begin{bmatrix} \eta e^{\tau s} T & (1-\eta)(e^{\tau s}-1)T \\ 0 & 1 \end{bmatrix}. \tag{69}$$

We will prove that for any selection of the parameters H, K or η, the existence of time delay in the estimation of the leader error, i. e. $\Gamma = e^{-\tau s}$, with $\tau > 0$ will yield string instability. The following lemma will aid us in that regard.

Lemma 3.2. *Let T be any stable rational transfer function, and consider the real parameters $\eta \in (0, \|T\|_\infty^{-1}]$ and $\tau > 0$. Then, the spectral radius of the matrix*

$$\mathfrak{M}(s) = \begin{bmatrix} \eta T & (1-\eta)(e^{\tau s}-1)T \\ \eta T & (1-\eta)(e^{\tau s}-1)T + 1 \end{bmatrix}, \tag{70}$$

satisfies $|\rho(\mathfrak{M}(j\omega))| > 1$ at some $\omega \in \mathbb{R}$.

Proof:

If $\tau > 0$, we note that for values $s = j\omega_k$ with $\omega_k = 2k\pi/\tau$, $k \in \mathbb{Z}$, the factor $e^{\tau s} - 1$ vanishes, $\mathfrak{M}(j\omega_k)$ becomes lower triangular and therefore the eigenvalues satisfy $\lambda_1(j\omega_k) = \eta T(j\omega_k)$ and $\lambda_2(j\omega_k) = 1$ at these frequencies. Since the equality $\eta T(j\omega_k) = 1$ can only hold at a finite number of these ω_k (given that T is real rational), we have that the eigenvalues $\lambda_1(j\omega_k), \lambda_2(j\omega_k)$ are algebraically simple for infinitely many ω_k. Now, for algebraically simple eigenvalues, Theorem 6.3.12 of (Horn and Johnson, 1999) can be applied to $\mathfrak{M}(j\omega_k)$ yielding the derivative of $\lambda_2(j\omega)$ with respect to ω at $\omega = \omega_k$ as

$$\lambda_2'(j\omega_k) = \frac{\underline{y}^* \mathfrak{M}'(j\omega_k)\underline{x}}{\underline{y}^* \underline{x}}, \tag{71}$$

where $\underline{x}, \underline{y}$ are the right and left eigenvectors of $\mathfrak{M}(j\omega_k)$ corresponding to $\lambda_2(j\omega_k)$ respectively and $(\cdot)^*$ denotes conjugate transpose. In particular, as

$$\mathfrak{M}(j\omega_k) = \begin{bmatrix} \eta T(j\omega_k) & 0 \\ \eta T(j\omega_k) & 1 \end{bmatrix}, \tag{72}$$

the right and left eigenvectors $\underline{x}, \underline{y}$ corresponding to $\lambda_2(j\omega_k)$ are given by

$$\underline{x} = \begin{bmatrix} 0 \\ 1 \end{bmatrix}, \quad \underline{y}^* = \begin{bmatrix} \dfrac{\eta T(j\omega_k)}{1-\eta T(j\omega_k)} & 1 \end{bmatrix}. \tag{73}$$

The derivative $\mathfrak{M}'(j\omega_k)$ takes the form

$$\mathfrak{M}'(j\omega_k) = \begin{bmatrix} \eta T'(j\omega_k) & j(1-\eta)\tau T(j\omega_k) \\ \eta T'(j\omega_k) & j(1-\eta)\tau T(j\omega_k) \end{bmatrix}, \tag{74}$$

and substituting these expressions in (71) results in

$$\lambda_2'(j\omega_k) = \frac{j(1-\eta)\tau T(j\omega_k)}{1-\eta T(j\omega_k)}. \tag{75}$$

If we consider the derivative of $|\lambda_2(j\omega)|^2$ with respect to ω at $\omega = \omega_k$ we have

$$(\lambda_2^*(j\omega)\lambda_2(j\omega))'\big|_{\omega=\omega_k} = (\lambda_2'(j\omega_k))^* + \lambda_2'(j\omega_k), \tag{76}$$

since $\lambda_2(j\omega_k) = 1$ and therefore $|\lambda_2(j\omega)| > 1$ either at $\omega > \omega_k$ or $\omega < \omega_k$ if and only if $\Re\{\lambda_2'(j\omega_k)\} \neq 0$. Now, from (71) $\Re\{\lambda_2'(j\omega_k)\} = 0$ if and only if $\Im\{T(j\omega_k)/(1-\eta T(j\omega_k))\} = 0$, however, recalling that T is a rational function this can at most be true at a finite number of frequencies. Consequently, since there are infinitely many ω_k, $\Im\{T(j\omega_k)/(1-\eta T(j\omega_k))\} \neq 0$ and $|\lambda_2(j\omega)| > |\lambda_2(\omega_k)| = 1$ holds for some $\omega \neq \omega_k$. □

Theorem 3.5. *Let* $E_n^{pre} = F_{n,1}D_1$ *where* $F_{n,1}$ *is computed from* (44). *Then, if* $\tau > 0$ *and* $\|\eta T\|_\infty \leqslant 1$ *the sequence* $\{F_{n,1}\}$ *is string unstable.*

Proof: Lemma 3.2 states that there exists ω_c such that the spectral radius of $\mathfrak{M}(j\omega_c)$ satisfies $\rho(\mathfrak{M}(j\omega_c)) > 1$, then $\lambda_1(j\omega_c) \neq \lambda_2(j\omega_c)$

since $|\det \mathfrak{M}(j\omega)| = |\eta T| \leqslant 1$ for all $\omega \geqslant 0$. Now, the following decomposition holds at all ω such that $\rho(\mathfrak{M}(j\omega)) > 1$

$$\mathfrak{M}(j\omega)^{i-2} \begin{bmatrix} 1 \\ 1 \end{bmatrix} = c_1 \lambda_1 (j\omega)^{i-2} \underline{v}_1(j\omega) + c_2 \lambda_2 (j\omega)^{i-2} \underline{v}_2(j\omega), \tag{77}$$

where $\underline{v}_1(j\omega), \underline{v}_2(j\omega)$ are the respective eigenvectors and $c_1, c_2 \in \mathbb{C}$ are constants such that in (44) we can write

$$c_1 \underline{v}_1(j\omega) + c_2 \underline{v}_2(j\omega) = \begin{bmatrix} 1 \\ 1 \end{bmatrix}, \tag{78}$$

at the particular value ω. Furthermore, if we take the products

$$\mathfrak{M}(s) \begin{bmatrix} 1 \\ 1 \end{bmatrix} = \begin{bmatrix} \eta e^{\tau s} T + (1-\eta)(e^{\tau s} - 1)T \\ \eta e^{\tau s} T + (1-\eta)(e^{\tau s} - 1)T + 1 \end{bmatrix}, \tag{79}$$

$$\mathfrak{M}(s) \begin{bmatrix} 0 \\ 1 \end{bmatrix} = \begin{bmatrix} (1-\eta)(e^{\tau s} - 1)T \\ (1-\eta)(e^{\tau s} - 1)T + 1 \end{bmatrix}, \tag{80}$$

we see that $[1 \;\; 1]^\top$ cannot be an eigenvector for any ω and therefore the constants c_1 and c_2 in (78) belong to $\mathbb{C} \setminus \{0\}$. Similarly, the vector $[0 \;\; 1]^\top$ can only be an eigenvector if $e^{j\tau\omega} - 1 = 0$ which shows that $v_{1,1}(j\omega)$ and $v_{2,1}(j\omega)$, the first components of the vectors $\underline{v}_1(j\omega)$ and $\underline{v}_2(j\omega)$ respectively, are not 0 at the frequencies considered. The result is that both eigenvalues in (77) will be contained in the expression for $F_{n,1}$ whenever $e^{j\tau\omega} - 1 \neq 0$. In other words, at frequencies such that $\rho(\mathfrak{M}(j\omega)) > 1$

$$|F_{n,1}| = |SH| |c_1 v_{1,1} \lambda_1^{n-2} v_1 + c_2 v_{2,1} \lambda_2^{n-2} v_2|, \tag{81}$$

and recalling that at these frequencies $|\lambda_1|^{n-2} \to 0$ and $|\lambda_2|^{n-2} \to \infty$ as $n \to \infty$ we can state that there is no $c \in \mathbb{R}$ such that $\|F_{n,1}\|_\infty \leqslant c$ for all $n \in \mathbb{N}$. □

The previous result does not require $\|T\|_\infty > 1$ nor does it depend on the value η. We can see that this particular method for providing the followers with the leader state (alternative algorithm) leads to unavoidable string instability when there is time delay in the broadcast.

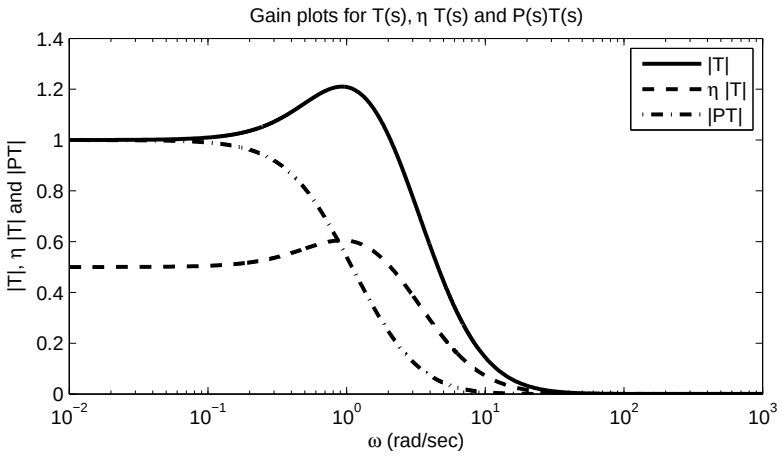

Figure 4: Magnitude plots of T, ηT and PT for the selected parameter values.

3.6 EXAMPLES AND SIMULATIONS

For all the examples we use

$$H = \frac{1}{s(0.1s+1)}, \quad K = \frac{2s+1}{s(0.05s+1)}, \quad K_p = \frac{1}{s(0.05s+1)},$$
$$K_v = \frac{2}{s(0.05s+1)}, \quad P = \frac{1}{2s+1}, \quad \eta = 0.5.$$

The transfer functions H and K are taken from examples in (Seiler et al., 2004) and will be used for most of the examples throughout the thesis.

In Figure 4 we can view the magnitude plots of T, ηT and PT associated with the selected parameters above. The reader can note that K_p and K_v are marginally stable and that $\|PT\|_\infty \leqslant 1$ with $P(0) = 1$ (See Remark 3.5).

3.6.1 *Leader-predecessor following*

Simulations for the leader-predecessor following scheme illustrate the results stated in the previous sections. Under the absence of time delays in the communications it can be seen in Figure 5 that the response of a step disturbance of magnitude 10 on the leader yields inter-vehicle errors that decrease along the string. Moreover, the steady state errors are 0, which is consistent with our derivations. It is of no surprise to see that the leader-follower errors are also bounded even when the string size increases.

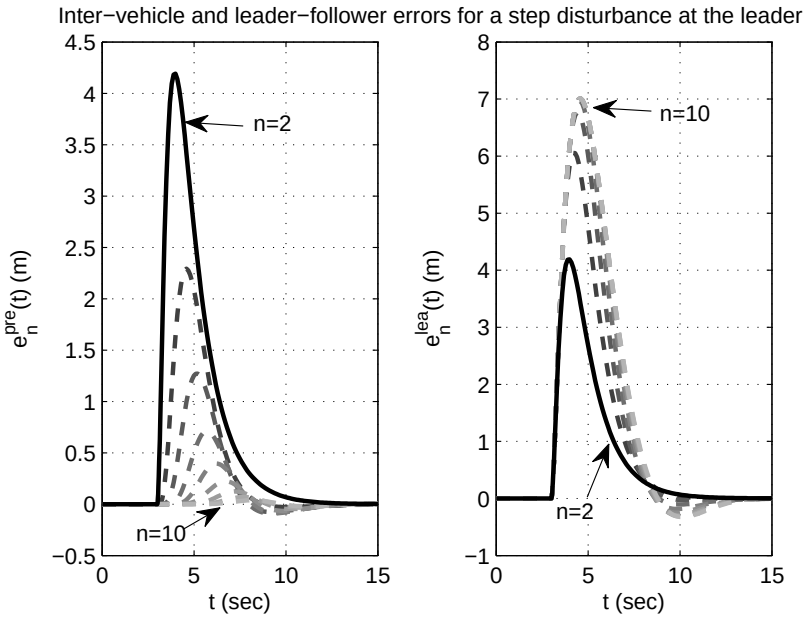

Figure 5: Inter-vehicle and leader-follower errors for the leader-predecessor following scheme for a step disturbance of magnitude 10 at the leader. No time delay.

Next, we consider multi-step string relay communications. For a time delay of $\tau = 0.6(sec)$ we see in Figure 6 that the 0 DC gain of the inter-vehicle spacing error transfer functions is lost, as predicted by Theorem 3.3, which in this case yields

$$F_{n,1}(0) = \tau\tilde{H}(0)(1-\eta^{n-2}) = 0.6(1-0.5^{n-2}), \tag{82}$$

which tends to 0.6 as $n \to \infty$. Additionally we see the leader-follower errors growing along the string, as predicted by Theorem 3.4.

3.6.2 *Leader velocity tracking*

For the velocity tracking scheme we compute some magnitude plots of $F_{n,1}$ in the multi-step string relay communications. The first and third plots of Figure 7 show that values of time delay different from the critical value (which in this case is $\tau = -P'(0) = 2(sec)$), yield string stability for the predecessor error transfer functions. This is suggested by the fact $\|F_{1000,1}\|_\infty \leqslant \|F_{100,1}\|_\infty$ in both plots. On the contrary, for the critical time delay, the second plot of Figure 7 shows a clear increase of $\|F_{n,1}\|_\infty$ as n grows. Finally it can be seen that the bound on the magnitude peak increases with the value of τ.

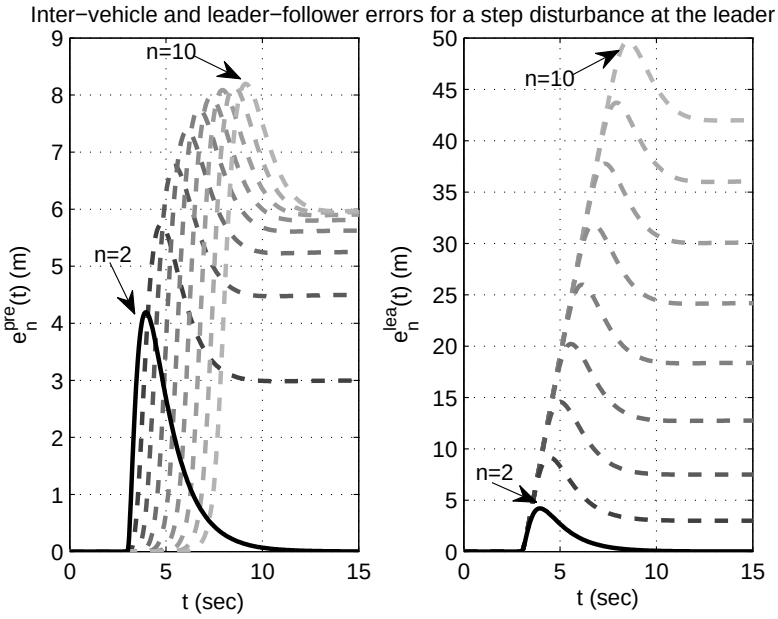

Figure 6: Inter-vehicle and leader-follower errors for the leader-predecessor following scheme for a step disturbance of magnitude 10 at the leader. Multi-step string relay communications with $\tau = 0.6(sec)$.

3.6.3 *Alternative algorithm: indirect leader state broadcast*

Finally we consider the alternative algorithm for leader state broadcast. In Figure 8 the step response of the predecessor errors is plotted for a time delay of $\tau = 0.6(sec)$. It provides 0 DC gain for the predecessor errors; however, string stability is lost under the presence of time delay. This is reflected by the increase on the peak response of the predecessor errors as the string length grows.

The magnitudes of the eigenvalues of the matrix $\mathfrak{M}(j\omega)$ are plotted in Figure 12 with the time delay as a varying parameter. It is clear that $|\lambda_2(j\omega)|$ takes values greater than 1 for $\tau > 0$ as predicted by Lemma 3.2.

3.6.4 *Effect of the time delay on the magnitude peaks*

We will study how the magnitude peaks of $F_{n,1}$ and $\mathcal{F}_{n,1}$ behave for single and multi step string relay communications with different values of time delay, for a fixed number of vehicles ($n = 10$).

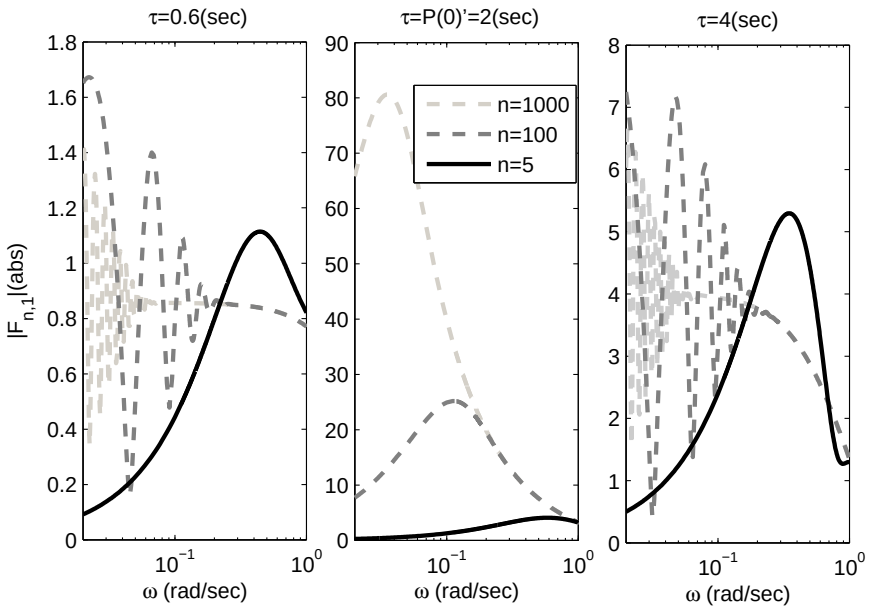

Figure 7: Magnitude plots of $F_{n,1}$ for $n = \{5, 100, 1000\}$ for the leader velocity tracking scheme. Multi-step string relay communications with $\tau = 0.6(sec)$ (string stable), $\tau = -P'(0) = 2(sec)$ (string unstable) and $\tau = 4(sec)$ (string stable).

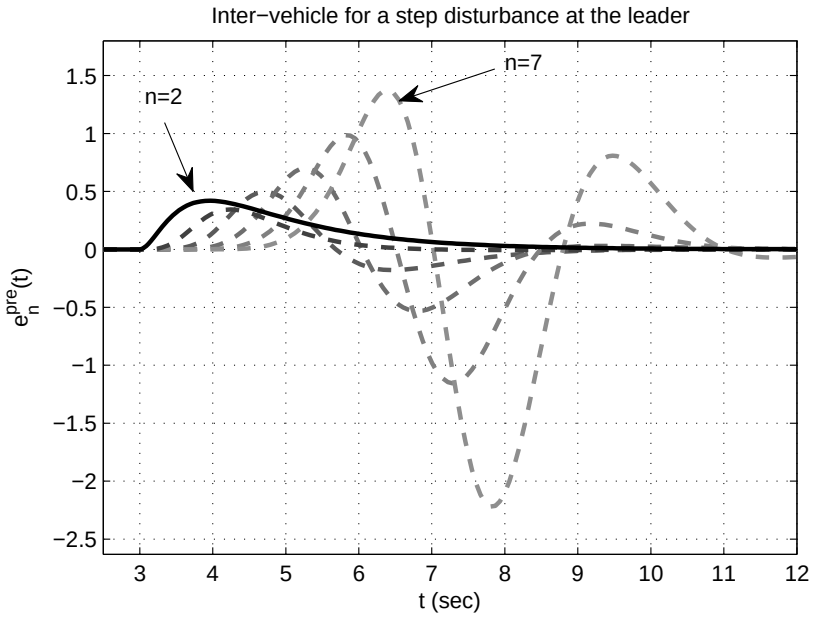

Figure 8: Inter-vehicle errors of the alternative leader-predecessor algorithm for a step disturbance of magnitude 10 at the leader. Communications with $\tau = 0.6(sec)$.

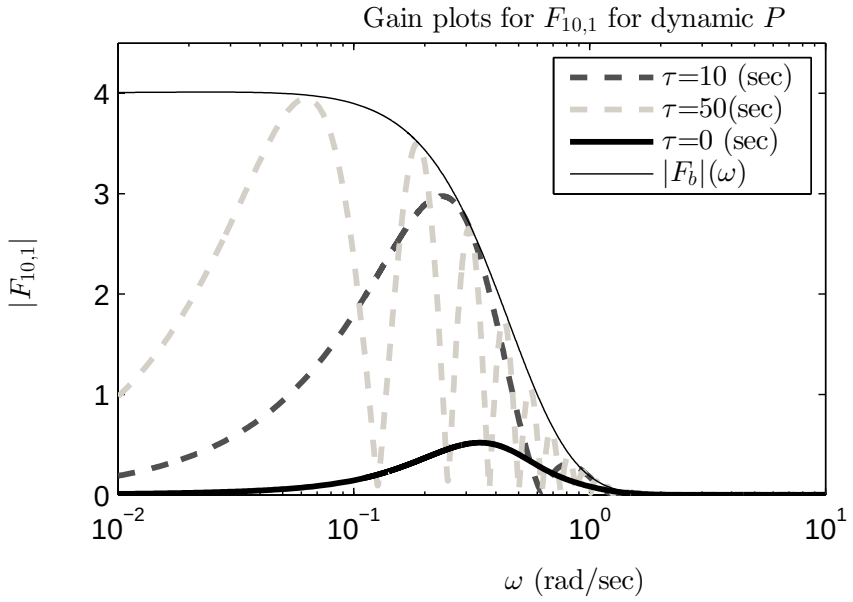

Figure 9: Magnitude plots of $F_{10,1}$ for one-step string relay communications with dynamic P, $n_r = 5$ and $\tau = \{0, 10, 50\}(sec)$. Solid thin line: $|F_b|(\omega)$.

a) *one-step string relay communications*

In Figure 9 the magnitude plots of $F_{10,1}$ are shown for one-step string relay communications with $n_r = 5$, for different values of time delay τ and dynamic P. From (61) we have

$$F_{n,1} = TH\left[(PT)^{n-3}PS + (1-e^{-\tau s})(1-P)(PT)^{n-n_r-1}\right], \tag{83}$$

and a very conservative bound for the magnitude for all ω and independent of τ is given by

$$|F_{n,1}| \leqslant |(PT)^{n-2}HS| + 2|TH(1-P)(PT)^{n-n_r-1}| = |F_b|(\omega). \tag{84}$$

We can see in the figure that for increasing values of the time delay, the value of $\|F_{n,1}\|_\infty$ grows but it does not surpass the maximum value given by $\max_\omega |F_b|(\omega)$, which is independent of τ.

On the other hand, for $P = \eta \in (0,1)$, Theorem 3.3 states that $F_{n,1}(0) = \tau\tilde{H}(0)(1-\eta)\eta^{n-n_r-1}$, which depends linearly on the value of τ. In this sense the leader-velocity tracking strategy (i. e. using dynamic P rather than $P = \eta \in (0,1)$) provides some extra robustness to delays on the broadcast of the leader state.

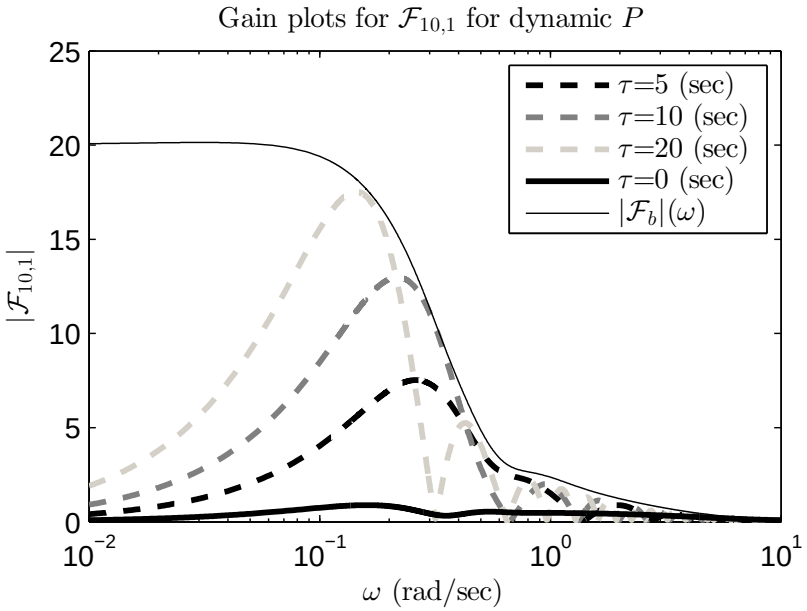

Figure 10: Magnitude plots of $\mathcal{F}_{10,1}$ for one-step string relay communications with dynamic P, $n_r = 5$ and $\tau = \{0, 5, 10, 20\}(sec)$. Solid thin line: $|\mathcal{F}_b|(\omega)$.

Similarly, for the transfer function from a disturbance at the leader to the leader error of the last vehicle, $\mathcal{F}_{10,1}$, we have Figure 10 (again with dynamic P and using $n_r = 5$). In particular

$$\mathcal{F}_{n,1} = SH\frac{1-(PT)^{n-1}}{1-PT} + (1-e^{-\tau s})(1-P)TH\frac{1-(PT)^{n-n_r}}{1-PT}, \tag{85}$$

with a simple bound for all ω, independent of τ given by

$$|\mathcal{F}_{n,1}| \leqslant |SH|\left|\frac{1-(PT)^{n-1}}{1-PT}\right| + 2\,|(1-P)TH|\left|\frac{1-(PT)^{n-n_r}}{1-PT}\right| = |\mathcal{F}_b|(\omega). \tag{86}$$

As in the previous case, we can see from the plots that the magnitude peak $\|\mathcal{F}_{n,1}\|_\infty$ does not depend on the value of the time delay τ when we use leader-velocity tracking (i. e. for dynamic P). Similarly to the previous case, we have that for the leader-velocity tracking strategy, the impact of a single delay of the leader state broadcast on the disturbance amplification for the leader error is bounded independently of the magnitude of time delay for the leader-velocity tracking strategy. This is not the case for leader-predecessor following, as the DC gain given by Theorem 3.3 $\mathcal{F}_{n,1}(0) = \tau\tilde{H}(0)(1-\eta^{n-n_r})$ when $P = \eta \in (0,1)$ grows linearly with the value of delay.

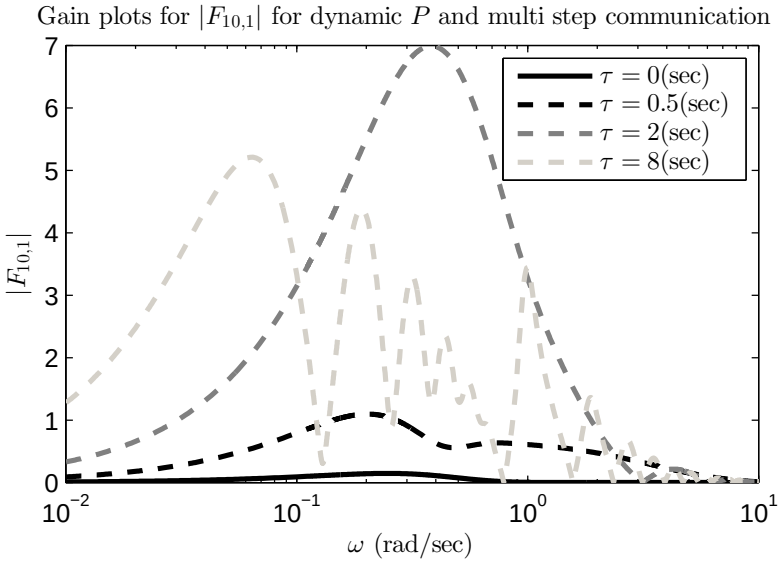

Figure 11: Magnitude plots of $F_{10,1}$ for multi-step string relay communications with dynamic P, and $\tau = \{0, 0.5, 2, 8\}(sec)$.

b) *multi-step string relay communications*

For multi-step string relay communications we have from (65) that for dynamic P

$$F_{n,1} = TH\Big[(1-PT)(PT)^{n-3} - (1-P)e^{-(n-2)\tau s} + (1-PT)(1-P)e^{-\tau s}\frac{((PT)^{n-3} - e^{-(n-3)\tau s})}{PT - e^{-\tau s}}\Big]. \tag{87}$$

Figure 11 shows the magnitude plots of $F_{10,1}$ for different values of the time delay. According to Remark 3.7 the behaviour of the norms is bounded in n for $\tau \neq -P'(0)$. In this case $P'(0) = -2$. It can be noticed in Figure 11 that the case $\tau = 2$(sec) yields the largest $\|F_{10,1}\|_\infty$.

For constant $P = \eta \in (0,1)$ we have, according to Theorem 3.4, that

$$F_{n,1}(0) = \tau\tilde{H}(0)(1-\eta^{n-2}), \tag{88}$$

$$\mathcal{F}_{n,1}(0) = \tau\tilde{H}(0)\left(n-1-\frac{1-\eta^{n-1}}{1-\eta}\right), \tag{89}$$

which both grow linearly with τ.

3.7 CONCLUSION

In this chapter we studied three leader tracking schemes for formation control of vehicle strings. In particular we described the inter-

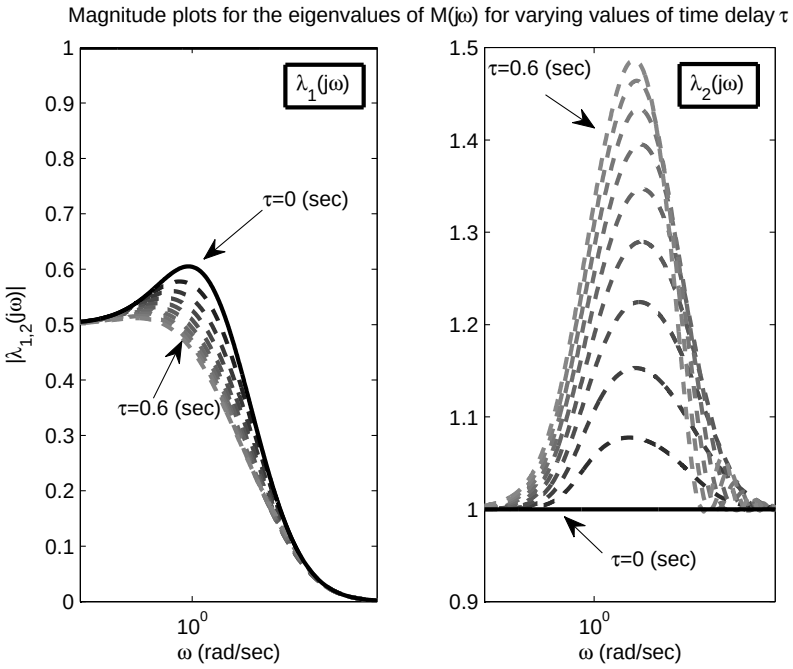

Figure 12: Magnitude plots of the eigenvalues $\lambda_1(j\omega), \lambda_2(j\omega)$ of the matrix $\mathfrak{M}(j\omega)$ from the alternative algorithm for different magnitudes of time delay

vehicle and leader-follower spacings dynamics resulting from the use of the three schemes, including possible time delays. We have shown that these architectures provide tight formations and string stability if the leader state is received instantaneously by the followers. However, if time delays occur in the leader state transmission only one of the schemes, namely leader velocity tracking, is able to maintain a tight formation while achieving string stability in the predecessor errors. An immediate extension to the present work is to obtain conditions for the existence and a methodology for the design of the controllers K_p and K_v in (19) from the velocity tracking scheme. In Chapter 6 we provide some initial thoughts on this topic.

As a final remark we note that the presence of time delays in the broadcast of the leader state has different effects for each architecture, despite the fact that the three share some similarities. In particular, the alternative algorithm for indirect leader state broadcast becomes string unstable for any value of time delay, independent of the vehicle dynamics or the design of the local controllers. This fact suggests that the way in which the leader state is sent to the followers and/or

used by them plays a major role in the capability of a leader tracking architecture for formation control to achieve string stability.

4

FORMATION CONTROL WITH A CYCLIC INTERCONNECTION

4.1 INTRODUCTION

In this chapter we consider a cyclic formation control architecture. For this strategy, the front member of the platoon tracks the position of the last and every other member tracks only its predecessor. With this scheme there is no leader that moves independently. Nevertheless, the initial conditions and parameters of the control architecture allow the vehicles to travel at a desired constant speed in steady state while keeping desired inter-vehicle spacings. In Section 4.2 we give some preliminary assumptions on the vehicle model and cyclic control strategy. We also discuss the initial conditions and control parameters and their relation with the speed of the platoon. In Section 4.3 we obtain closed form expressions for the transfer functions from disturbances at vehicles to inter-vehicle errors when the proposed control is used. The first main contribution of the chapter is contained in Section 4.4. Here we obtain results concerning the stability and string stability of the dynamical system associated with the proposed control architecture. These results are obtained for two different inter-vehicle spacing policies. In particular we consider a constant spacing policy and a constant time-headway spacing policy. In Section 4.5 we extend the results shown before to a cyclic interconnection with an independent leader. We give some numerical examples and comments on the main results in Section 4.6. We conclude this chapter with some final remarks and possible lines of future work in Section 4.7.

4.2 VEHICLE MODEL, CONTROL STRATEGY AND INITIAL CONDITIONS

We consider a platoon of $n \in \mathbb{N}$ identical vehicles, with positions $z_i(t)$, initial positions $z_i(0)$ and initial velocities $\dot{z}_i(0)$ for $1 \leqslant i \leqslant n$,

modeled by linear time invariant systems. In the frequency domain, the models of each member of the platoon are given by

$$Z_i = P(U_i + D_i) + \frac{z_i(0)}{s} + \frac{\dot{z}_i(0)}{s^2} \quad \text{for } 1 \leqslant i \leqslant n, \tag{90}$$

where Z_i denotes the Laplace transform of $z_i(t)$, U_i is the control action and D_i is an input disturbance, both acting on the i-th member. The transfer function P has a single pole at the origin and is strictly proper.

Now, we define the separation errors as

$$\begin{aligned} e_i(t) &= z_{i-1}(t) - z_i(t) - (\varepsilon_i + h\dot{z}_i(t)), \quad \text{for } i = 2, \dots, n, \\ e_1(t) &= z_n(t) - z_1(t) - (\varepsilon_1 + h\dot{z}_1(t)), \end{aligned} \tag{91}$$

where $\varepsilon_i \in \mathbb{R}$, and $h \geqslant 0$ is the time headway parameter.

Remark 4.1. *In this chapter we use P to denote the vehicle model. This is in contrast to the previous and the following chapters where H was and will be used. This change is made to avoid confusions with the common use of h as the time headway parameter in the literature.*

The control objective is to maintain the errors $e_i(t)$ defined in (91) equal to zero whenever possible, which would imply that the vehicles retain a desired formation. We will study the control strategy given by

$$U_i = KE_i, \quad \text{for } i = 1, \dots, n, \tag{92}$$

where K is a strictly proper controller assumed to have a single pole at the origin and E_i is the Laplace transform of the signal $e_i(t)$.

In steady state, that is for $t \to \infty$, we aim to have a tight formation, i. e. $e_i(t) = 0$ and also the same speed $v_p \in \mathbb{R}$ for every vehicle, i. e. $\dot{z}_i(t) = v_p$ for all $i = 1, \dots, n$. Here we follow a similar approach to the one used in (Rogge and Aeyels, 2008). Adding all the right hand sides of (91) and setting $\dot{z}_i(t) = v_p$ yields

$$v_p = -\frac{1}{hn} \sum_{i=1}^{n} \varepsilon_i. \tag{93}$$

For simplicity, we will set $\varepsilon_i = \varepsilon \in \mathbb{R}$ for $i = 2, \dots, n$ and therefore $\varepsilon_1 = -hnv_p - (n-1)\varepsilon$. Additionally, we take initial conditions such that the formation is in steady state, that is $z_{i-1}(0) - z_i(0) = \varepsilon +$

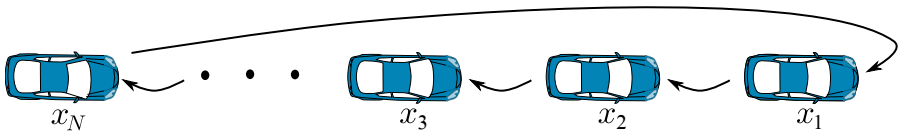

Figure 13: Cyclic platoon of vehicles. x_i: position of the i-th vehicle.

$h\dot{z}_i(0)$ for $i = 2, \dots, n$, $z_n(0) - z_1(0) = \varepsilon_1 + h\dot{z}_1(0)$ and $\dot{z}_i(0) = v_p$ for $i = 1, \dots, n$. Finally, we define the change of coordinates

$$x_i(t) = z_i(t) - z_i(0) - v_p t, \quad \text{for } i = 1, \dots, n, \tag{94}$$

and substituting in (91) yields

$$\begin{aligned} e_i(t) &= x_{i-1}(t) - x_i(t) - h\dot{x}_i(t), \quad \text{for } i = 2, \dots, n, \\ e_1(t) &= x_n(t) - x_1(t) - h\dot{x}_1(t), \end{aligned} \tag{95}$$

With this, we will focus on the effect of the disturbances D_i on the separation errors E_i when the initial conditions and ε_i are set to zero. In the following sections we will have

$$\begin{aligned} E_i &= X_{i-1} - X_i - shX_i, \quad \text{for } i = 2, \dots, n, \\ E_1 &= X_n - X_1 - shX_1 \end{aligned} \quad . \tag{96}$$

The main difference with the basic approach (Seiler et al., 2004), where the leader moves independently, is that the first vehicle now tries to maintain a predefined spacing with respect to the last member of the platoon (See Figure 13). Applications of such a configuration may include subway systems that run on circuits and ring roads around major cities. Nevertheless, the vehicles need not be necessarily arranged in a 2D ring, they can be moving along a straight road and at the same time have a cyclic interconnection.

One potential advantage of such a strategy is the fact that a disturbance at any vehicle will be detected and compensated by every member of the formation. This could provide an extra level of safety when compared to unidirectional strategies where a disturbance at any vehicle is not detected by its predecessors (which could possibly lead to collisions). We will discuss this further in a following section.

4.3 DYNAMICS OF THE INTERCONNECTED SYSTEM

With the control strategy defined in the previous section, the vehicle dynamics are given by

$$\underline{X} = (\mathbf{I} - PK\mathbf{G})^{-1} P\underline{D}, \tag{97}$$

where $\underline{X} = [X_1 \ \cdots \ X_n]^\top$, $\underline{D} = [D_1 \ \cdots \ D_n]^\top$, $\mathbf{I}$ is the $n \times n$ identity matrix and $\mathbf{G} \in \mathbb{C}^{n\times n}$ is the interconnection matrix:

$$\mathbf{G} = \begin{bmatrix} -Q & & & 1 \\ 1 & \ddots & & \\ & \ddots & \ddots & \\ & & 1 & -Q \end{bmatrix}, \tag{98}$$

with $Q = 1 + hs$.

We aim to obtain explicit formulae for the vehicle positions. To do so, we must invert the matrix $\mathbf{I} - PK\mathbf{G}$ in (97). In unidirectional control strategies with a free leader (Seiler et al., 2004; Klinge and Middleton, 2009) the matrix to invert is lower triangular and normally has a straightforward inverse, yielding dynamics for the vehicle positions that are easy to study. In the present case $\mathbf{I} - PK\mathbf{G}$ is circulant and the resulting dynamics will not be straightforward to analyze as will be seen below.

In the following, to simplify the presentation, we will consider strictly proper controllers K that satisfy

$$K = \frac{\tilde{K}}{Q}, \tag{99}$$

with $\tilde{K}$ having no zero at $s = -1/h$. Let $T = PKQ/(1 + PKQ) = P\tilde{K}/(1 + P\tilde{K}) = 1 - S$, and also $\Gamma = T/Q$. Then, we have

$$\mathbf{I} - PK\mathbf{G} = KP \begin{bmatrix} \Gamma^{-1} & & & -1 \\ -1 & \ddots & & \\ & \ddots & \ddots & \\ & & -1 & \Gamma^{-1} \end{bmatrix}, \tag{100}$$

and the corresponding inverse (which can be checked by direct calculation) is given by

$$(\mathbf{I} - PK\mathbf{G})^{-1} = \frac{S}{1-\Gamma^n} \begin{bmatrix} 1 & \Gamma^{n-1} & \dots & \Gamma^2 & \Gamma \\ \Gamma & 1 & \ddots & & \Gamma^2 \\ \vdots & \ddots & \ddots & \ddots & \vdots \\ \Gamma^{n-2} & & \ddots & 1 & \Gamma^{n-1} \\ \Gamma^{n-1} & \Gamma^{n-2} & \dots & \Gamma & 1 \end{bmatrix}. \tag{101}$$

By the structure of the interconnection, this matrix is also circulant and therefore the response of the i—th vehicle to a single disturbance on the k—th vehicle is the same as the response of the $i+l$-th vehicle to a single disturbance on the $k+l$-th vehicle (there is no *leader*). In terms of transfer functions this can be written as

$$\frac{X_i}{D_k} = F = \frac{X_{i+l}}{D_{k+l}}. \tag{102}$$

This is clear from the diagonals with identical elements in the matrix of the right hand side of (101).

As mentioned before, a consequence of the chosen interconnection is that a single disturbance affects every vehicle in the string. From the point of view of control energy this could be seen as a disadvantage, since every vehicle will take an action in response to a disturbance at any vehicle. However, this extra action could mean an increase in safety in comparison to a unidirectional architecture. In a unidirectional architecture, such as the one studied in Chapter 3, a disturbance in the k-th vehicle is not detected nor compensated by the members closer to the leader than the k-th position.

In particular we have that the inter-vehicle spacings when $D_1 \neq 0$ and $D_i = 0$ for $i = 2, \dots, n$ are given by $E_i = X_{i-1} - QX_i = F_i^{(n)} D_1$, with

$$F_i^{(n)} = \frac{SP(1-T)\Gamma^{i-2}}{1-\Gamma^n}, \quad \text{for } i = 2, \dots, n \tag{103}$$

$$E_1 = X_n - QX_1 = \frac{SP(\Gamma^{n-1} - Q)}{1-\Gamma^n} D_1 = F_1^{(n)} D_1. \tag{104}$$

It is important to note that the dynamics of the inter-vehicle spacings have a factor $(1-\Gamma^n)^{-1}$. The poles of this transfer function increase in number and change in location as the string size increases. This

is in great contrast with other unidirectional architectures where the pole locations are unaffected by n. In those cases the dynamics are usually powers of the complementary sensitivity function T (Seiler et al., 2004).

4.4 PROPERTIES OF THE INTERCONNECTED SYSTEM

In this section, we state the main results of the chapter. In particular we analyse the roots of the equation $1 - \Gamma^n = 0$ and their role in the stability of the interconnection.

We will consider two of the most common spacing policies and will obtain stability conditions of the interconnection for both. The following result, taken from (Klinge and Middleton, 2009), shows how the use of a time headway policy can impact the frequency response of the interconnection.

Proposition 4.1. *Let* $T = P\tilde{K}/(1 + P\tilde{K})$, *with* P *and* $\tilde{K}$ *defined in* (90) *and* (99) *respectively.* T *is a stable and strictly proper transfer function such that* $T(0) = 1$, $T'(0) = 0$ *and* $\|T\|_\infty > 1$. *Then, there exists* $h_0 > 0$ *such that* $\|T/(1 + hs)\|_\infty > 1$ *for* $0 \leqslant h < h_0$ *and* $|T(j\omega)/(1 + jh\omega)| < 1$ *for* $\omega > 0$, *whenever* $h > h_0$. *Moreover*

$$h_0 = \sqrt{\sup_\omega \left(\frac{\left| \frac{P\tilde{K}}{1 + P\tilde{K}} \right|^2 - 1}{\omega^2} \right)} \tag{105}$$

We also have the following corollary which provides a bound for h_0. This result will be used at a later stage.

Corollary 4.1. *The value* h_0 *defined in* (105) *satisfies*

$$2h_0^2 \geqslant \frac{d^2}{d\omega^2} \left(\left| \frac{P\tilde{K}}{1 + P\tilde{K}} \right|^2 \right) \Bigg|_{\omega=0}. \tag{106}$$

The final preliminary result needed for the derivation of the main results is given in the following lemma.

Lemma 4.1. *Let* Γ *be a stable and strictly proper transfer function such that* $\|\Gamma\|_\infty > 1$. *Then, there exists an interval* $[\theta_1, \theta_2] \subset [0, 2\pi]$ *with* $\theta_1 \leqslant \theta_2$ *such that* $1 - e^{j\theta}\Gamma = 0$ *has solutions in the open right half plane when* $\theta \in (\theta_1, \theta_2)$. *Moreover, if there exists* ω_c *such that* $|\Gamma_c(j\omega_c)| = 1$ *and* $|\Gamma_c(j\omega_c)|' \neq 0$, *we have* $\theta_1 < \theta_2$.

Proof: See Section A.3 for the proof.

Assumption 4.1. *In the following we will consider* Γ *that satisfies: if there exists* $\omega_c > 0$ *such that* $|\Gamma_c(j\omega_c)| = 1$*, then* $|\Gamma_c(j\omega_c)|' \neq 0$.

4.4.1 *Stability analysis*

To check the stability of the transfer functions $F_i^{(n)}$ in (103) we note that SP and $\Gamma = T/Q$ are stable provided that the controller K is properly designed. By this we refer to having no unstable cancellations in the product KP and $T = KP/(1+KP)$ being stable, which ensures the stability of S (see for example Goodwin et al. (2001)). We will now focus on the behaviour of $(1-T)/(1-\Gamma^n)$ which appears in $F_i^{(n)}$ for $i = 2, \dots, n$. The results are analogous for F_1 and we omit the details for the sake of simplicity in the exposition. We have that

$$\Gamma^n - 1 = \prod_{k=0}^{n-1} \left(\Gamma - e^{\frac{j2k\pi}{n}} \right). \tag{107}$$

Note that this echoes the results derived in (Fax and Murray, 2004), where the term $e^{\frac{j2k\pi}{n}}$ is directly connected to the eigenvalues of the graph Laplacian matrix for the interconnection considered here. Before we state our stability result we include the following preliminary result from complex analysis (Rudin, 1987).

Lemma 4.2. (Simplified Rouche's Theorem) *Let* G *and* F *be stable (no poles in the closed right half plane) transfer functions. If*

$$|F - G| < |F|, \tag{108}$$

for all s *on the imaginary axis, then* F *and* G *have the same number of zeros in the open right half plane.*

Now we have the following result.

Theorem 4.1. *Let* T *and* $Q = 1 + hs$ *be defined as in Proposition 4.1, and let* $\Gamma = T/Q$*. Then, there exists* $h_0 > 0$ *such that the following holds:*
1) if $h > h_0$*, then* $(1-T)/(1-\Gamma^n)$ *has all of its poles in the open left half plane;*
2) if $h < h_0$ *then there exists* $n_c \in \mathbb{N}$ *such that for all* $n > n_c$*,* $(1-T)/(1-\Gamma^n)$ *has poles in the right half plane.*

Proof: 1) If $h > h_0$, Proposition 4.1 states that $|\Gamma| < 1$ for all $\omega > 0$. Now we show that $(1-T)/(1-\Gamma)$ is stable. If we recall that $T(0) = 1$ and $T'(0) = 0$ we have that $1 - T$ has two zeros at $s = 0$. Since Γ is stable, $\Gamma(0) = 1$ and $|\Gamma| < 1$ for all $\omega > 0$, we have that for all $c \in (0,1)$, $|c\Gamma| < 1$ for all $\omega \geqslant 0$. This in turn implies that $|1-(1-c\Gamma)| < 1$ for $\omega \in \mathbb{R}$ and Rouche's Theorem (Lemma 4.2) ensures that $1 - c\Gamma$ and 1 have the same number of zeros in the closed right half plane. By continuity of the roots, $1 - \Gamma$ only has unstable roots at the stability boundary and given that $|\Gamma| < 1$ for all $\omega > 0$ this root can only be located at $s = 0$. Computing $\Gamma' = T'/Q - TQ'/Q^2$ implies that $\Gamma'(0) = -h$ and therefore $1 - \Gamma$ has only one root at $s = 0$ if $h > 0$. Consequently $(1-T)/(1-\Gamma)$ is stable. It remains to show that $1/\prod_{k=1}^{n-1}\left(\Gamma - e^{\frac{j2k\pi}{n}}\right)$ has poles only in the left half plane. For this, we note that the Nyquist plot of $-e^{\frac{j2k\pi}{n}}\Gamma$ does not encircle the point $s = -1$ for any value of $\frac{2k\pi}{n}$ with $k = 1, \ldots, n-1$ as $|\Gamma| < 1$ for $\omega > 0$. Given that Γ is open loop stable $(1 - e^{\frac{j2k\pi}{n}}\Gamma)^{-1}$ is also stable for $k = 1, \ldots, n-1$.

2) If $h < h_0$, Proposition 4.1 states that $\|\Gamma\|_\infty > 1$. We write

$$\frac{1-T}{1-\Gamma^n} = \frac{1-T}{1-\Gamma}\prod_{k=1}^{n-1}(1 - e^{\frac{j2k\pi}{n}}\Gamma)^{-1} \tag{109}$$

where $\frac{2k\pi}{n} \in (0, 2\pi)$ when $k = 1, \ldots, n-1$. According to Lemma 4.1, given that in this case $\|\Gamma\|_\infty > 1$, there exists an interval (θ_1, θ_2) such that $1 - e^{j\theta}\Gamma$ has zeros in the right half plane when $\theta \in (\theta_1, \theta_2)$. Now, if $\frac{2\pi}{n} < \frac{\theta_2 - \theta_1}{2}$ there is at least one point of the sequence $\{\frac{2k\pi}{n}\}$ for $k = 1, \ldots, n-1$ that belongs to (θ_1, θ_2). Therefore, for all $n > n_c = \left\lfloor \frac{4\pi}{\theta_2 - \theta_1} \right\rfloor + 1$ the transfer function $(1-T)/(1-\Gamma^n)$ has poles in the right half plane. □

Part 1) of the last theorem implies that the condition $|\Gamma| < 1$ for all $\omega > 0$ is sufficient for stability of the transfer functions $F_i^{(n)}$ in (103). Part 2) states that if the time headway parameter satisfies $0 \leqslant h < h_0$, there exists a critical number n_c for which any interconnection with a string size greater than n_c will be unstable.

Remark 4.2. *If $h = h_0$ it is possible to have $\Gamma(j\omega_c) = e^{j\theta}$ for some $\omega_c > 0$. If this is the case, there could be a value of k and n such that $\Gamma(j\omega_c) - e^{\frac{j2k\pi}{n}} = 0$, or equivalently $\theta = 2k\pi/n$ implying that there is a pair of pure imaginary complex poles at $\pm j\omega_c$.*

4.4.2 *String stability analysis*

Now we show that the interconnection can also be made string stable. We understand string stability as having certain sequences of transfer functions from disturbances to errors with a uniform bound on their magnitude peak; this bound is also independent of the string length (Middleton and Braslavsky, 2010). We use Definition 3.1 from Chapter 3.

In the present case we have the following result.

Theorem 4.2. *Let* $\Gamma = T/Q$ *with* T *defined as in Lemma 3.1 with* $T'(0) = 0$ *and* $Q = 1 + hs$, *with* $h > h_0$ *(with* h_0 *defined in Proposition 4.1). Consider* $F_i^{(n)}$ *defined in* (103) *for all* i, n *with* $i \leqslant n$. *Then the following hold:*
1) $F_i^{(n)}(0) = 0, \quad \forall n \in \mathbb{N}$ *and* $i = 1, \dots, n$.*;*
2) There exists $c > 0$ *such that* $\|F_i^{(n)}\|_\infty \leqslant c$ *for all* i, n, $i \leqslant n$.

Proof: 1) For $i \geqslant 2$ we have

$$F_i^{(n)}(0) = \lim_{s\to 0} \frac{SP(1-T)\Gamma^{i-2}}{1-\Gamma^n} = \Gamma(0)^{i-2} \lim_{s\to 0} SP \lim_{s\to 0} \frac{1-T}{1-\Gamma^n} \tag{110}$$

Given that $Q(0) = 1$, $T(0) = 1$, we have that $\Gamma(0) = 1$. Also, we have $S(0) = 1 - T(0) = 0$ and $S'(0) = T'(0)$, and therefore S has two zeros at $s = 0$. Since P has a single pole at $s = 0$ we have that $\lim_{s\to 0} SP = 0$. Now, $(1-T)/(1-\Gamma^n)$ is of the form $0/0$ when $s \to 0$ and the following limit can be computed using L'Hôpital's rule

$$\lim_{s\to 0} \frac{1-T}{1-\Gamma^n} = \lim_{s\to 0} \frac{T'}{n\Gamma^{n-1}\Gamma'}. \tag{111}$$

Since $T'(0) = 0$ and $Q' = h$ it follows that $\Gamma' = T'/Q - TQ'/Q^2$ and $\Gamma'(0) = -h$. With this, evaluating the last limit yields $F_i^{(n)}(0) = 0$ for $i \geqslant 2$. For $F_1^{(n)}$ defined in (104) we have

$$F_1^{(n)}(0) = \lim_{s\to 0} \frac{SP(\Gamma^{n-1} - Q)}{1-\Gamma^n} = \lim_{s\to 0} SP \lim_{s\to 0} \frac{\Gamma^{n-1} - Q}{1-\Gamma^n} \tag{112}$$

The second limit is again of the form $0/0$ and using L'Hôpital's rule

$$\lim_{s\to 0} \frac{\Gamma^{n-1} - Q}{1-\Gamma^n} = \lim_{s\to 0} \frac{(n-1)\Gamma^{n-2}\Gamma' - h}{-n\Gamma^{n-1}\Gamma'} = \frac{-nh}{nh} = -1. \tag{113}$$

Since $\lim_{s\to 0} SP = 0$, we have that $F_1^{(n)}(0) = 0$.

2) First we consider $i \geqslant 2$ fixed. From 1) we have that $F_i^{(n)}(0) = 0$. From Proposition 4.1, we have $\|\Gamma\|_\infty \leqslant 1$, and for $\omega > 0$

$$\left|\frac{SP(1-T)\Gamma^{i-2}}{1-\Gamma^n}\right| \leqslant |SP|\left|\frac{1-T}{1-\Gamma^n}\right|. \tag{114}$$

The product SP is stable and proper by design, therefore $\|SP\|_\infty \leqslant c_1$ with $c_1 > 0$. Since $\lim_{s\to 0}\frac{1-T}{1-\Gamma^n} = 0$, as seen in the previous point, and $|\Gamma| < 1$ for all $\omega > 0$, we have that $\left|\frac{1-T}{1-\Gamma^n}\right|$ is well defined for every $\omega \geqslant 0$. Now, since $|\Gamma| < 1$ for $\omega > 0$

$$\left|\frac{1-T}{1-\Gamma^n}\right| \leqslant \frac{|1-T|}{1-|\Gamma|^n} \leqslant \frac{|1-T|}{1-|\Gamma|^2}, \tag{115}$$

for all $\omega \geqslant 0$. Since $T(0) = 1$ and $T'(0) = 0$, the factor $|1-T|$ has at least two zeros at $\omega = 0$. We will show that $1-|\Gamma|^2$ does not have more than two zeros at $\omega = 0$, given that $h > h_0$. In particular, since $\Gamma(0) = 1$, $1-|\Gamma|^2$ has at least one zero at $\omega = 0$. We will show that

$$\frac{d^2}{d\omega^2}(1-|\Gamma|)^2\big|_{\omega=0} \neq 0. \tag{116}$$

Let $g_1(\omega) = |1/Q|^2$ and $g_2(\omega) = |T|^2$ which yields $1-|\Gamma|^2 = 1 - g_1(\omega)g_2(\omega)$. We have that $g_1(\omega) = 1/(1+\omega^2h^2)$ and consequently $g_1'(0) = 0$. Assuming that $g_2'(0) = 0$ (otherwise this would imply that $1-|\Gamma|^2$ has only one zero at $\omega = 0$, and therefore there is nothing to prove), and given that $g_1(0) = g_2(0) = 1$ we have that

$$\frac{d^2}{d\omega^2}(1-|\Gamma|)^2\big|_{\omega=0} = -g_1''(0) - g_2''(0). \tag{117}$$

In particular $g_1''(0) = -2h^2$ and Corollary 4.1 states that

$$2h_0^2 \geqslant \frac{d^2}{d\omega^2}|T|^2_{\omega=0} = g_2''(0). \tag{118}$$

By hypothesis $h > h_0$, and we have that $2h^2 > g_2''(0)$. This implies that $1-|\Gamma|^2$ has at most two zeros at $\omega = 0$. Consequently there exists $c_2 > 0$ independent of n such that

$$\frac{|1-T|}{|1-\Gamma^n|} \leqslant \frac{|1-T|}{1-|\Gamma|^2} < c_2 \quad \text{for all } \omega \geqslant 0. \tag{119}$$

It follows that $\|F_i^{(n)}\|_\infty \leqslant c_1c_2$ for all $n \in \mathbb{N}$ and $i \geqslant 2$.

Following a similar approach for $F_1^{(n)}$ defined in (104) we have

$$|F_1^{(n)}| = \left|\frac{SP(\Gamma^{n-1} - Q)}{1-\Gamma^n}\right| = \left|\frac{SP(\Gamma^{n-1} - 1 + 1 - Q)}{1-\Gamma^n}\right|. \tag{120}$$

By the triangle inequality

$$|F_1^{(n)}| \leqslant \left|\frac{SP(\Gamma^{n-1} - 1)}{1-\Gamma^n}\right| + \left|\frac{SP(1-Q)}{1-\Gamma^n}\right|. \tag{121}$$

The second term in the right hand side of (121) satisfies for all $\omega \geqslant 0$

$$\left|\frac{SP(1-Q)}{1-\Gamma^n}\right| \leqslant \frac{|sh SP|}{1-|\Gamma|^2}, \tag{122}$$

where we used the fact that $1 - Q = -sh$. The factor $shSP$ is proper and has two zeros at $s = 0$ (since SP is strictly proper and already has one zero at $s = 0$). From the discussion for $i \geqslant 2$ we have that $1 - |\Gamma|^2$ has at most two zeros at $\omega = 0$, therefore we know that there exists $c_{31} > 0$ independent of n such that

$$\left|\frac{SP(1-Q)}{1-\Gamma^n}\right| \leqslant c_{31} \quad \text{for all } \omega \geqslant 0. \tag{123}$$

For the first term in (121) we have

$$\begin{aligned}\left|\frac{SP(\Gamma^{n-1} - 1)}{1-\Gamma^n}\right| &\leqslant \frac{|SP(\Gamma - 1)|}{1-|\Gamma|}\frac{|1 + \Gamma + \ldots + \Gamma^{n-2}|}{1 + |\Gamma| + \ldots + |\Gamma|^{n-1}} \\ &\leqslant \frac{|SP(\Gamma - 1)(1 + |\Gamma|)|}{1-|\Gamma|^2}\frac{1 + |\Gamma| + \ldots + |\Gamma|^{n-2}}{1 + |\Gamma| + \ldots + |\Gamma|^{n-1}},\end{aligned} \tag{124}$$

and using a similar reasoning to previous cases we have that $|SP(\Gamma - 1)|$ has at least two zeros at $\omega = 0$ and $1 - |\Gamma|^2$ has at most two zeros at $\omega = 0$. Hence, there exists $c_{32} > 0$ independent of n such that

$$\frac{|SP(\Gamma - 1)(1 + |\Gamma|)|}{1-|\Gamma|^2} < c_{32} \quad \text{for all } \omega \geqslant 0. \tag{125}$$

Finally, using the fact

$$\frac{1 + |\Gamma| + \ldots + |\Gamma|^{n-2}}{1 + |\Gamma| + \ldots + |\Gamma|^{n-1}} \leqslant 1 \quad \text{for all } \omega \geqslant 0, \tag{126}$$

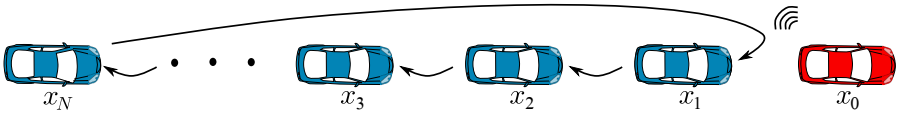

Figure 14: Cyclic platoon of vehicles. x_i: position of the i-th vehicle. Red vehicle: indepent leader which broadcasts its position to every follower within the cyclic interconnection.

we can conclude that there exists $c = c_{31} + c_{32} > 0$ independent of n, i such that

$$|F_1^{(n)}| \leqslant c_3 \quad \text{for all } \omega \geqslant 0. \tag{127}$$

□

Part 1) of the previous theorem shows that the transfer functions $\{F_i^{(n)}\}$ have 0 DC-gain independent of the size of the string and the dynamics of the vehicles and controllers (besides the poles at the origin). Part 2) shows that the sequences $\{F_i^{(n)}\}$ are string stable. In other words, the effect of a disturbance on the first vehicle D_1 on the inter-vehicle spacing of the i-th vehicle $E_i = X_{i-1} - X_i$ does not grow with an increase of the string size. Finally, Part 3) can be interpreted as the effect that a single disturbance to the first vehicle has on the inter-vehicle spacings of every vehicle is bounded independent of the string size.

4.5 CYCLIC INTERCONNECTION WITH A LEADER

In this section we consider the addition of an extra (possibly fictitious) vehicle, with position $z_0(t)$, that moves independently and such that every other member of the formation also tracks its position (See Figure 14). We also consider a constant inter-vehicle spacing policy, that is $h = 0$. If we let $\varepsilon_i^0 = i\varepsilon$ be a fixed desired constant spacing from the i-th follower to the leader, then we define

$$e_i^0(t) = z_0(t) - z_i(t) - i\varepsilon, \quad \text{for } i = 1, \dots, n, \tag{128}$$

$$e_i(t) = z_{i-1}(t) - z_i(t) - \varepsilon, \quad \text{for } i = 2, \dots, n, \tag{129}$$

$$e_1(t) = z_n(t) - z_1(t) + (n-1)\varepsilon. \tag{130}$$

We consider initial positions such that the platoon starts at the desired formation, that is

$$z_i(0) = -i\varepsilon, \quad \text{for } i = 0, \dots, n, \tag{131}$$

and we also consider the platoon to be initially at rest, i.e. $\dot{z}_i(0) = 0$ for all $i = 0, \dots, n$.. Now, we use the change of variables

$$x_i(t) = z_i(t) - z_i(0), \quad \text{for } i = 1, \dots, n, \tag{132}$$

which yields

$$X_i = P(U_i + D_i), \quad \text{for } i = 0, \dots, n, \tag{133}$$

where U_i and D_i are the input and disturbance at the i-th vehicle, and

$$E_i = X_{i-1} - X_i, \quad \text{for } i = 2, \dots, n, \tag{134}$$
$$E_1 = X_n - X_1, \tag{135}$$
$$E_i^0 = X_0 - X_i, \quad \text{for } i = 1, \dots, n. \tag{136}$$

The control strategy is now given by

$$U_i = K(\eta E_i + (1-\eta)E_i^0), \quad \text{for } 2 \leqslant i \leqslant n, \tag{137}$$
$$U_1 = K(\eta X_n + (1-\eta)E_1^0 - \eta X_1), \tag{138}$$
$$U_0 = 0, \tag{139}$$

where $\eta \in (0, 1)$.

Remark 4.3. *Note that the selection $U_0 = 0$ implies that the leader vehicle moves independently and its position is completely determined by its initial condition and the input signal D_0 as $X_0 = PD_0$. Moreover, the control strategy is such that every follower aims to maintain constant inter-vehicle spacing with respect to its immediate predecessor and with the leader.*

Now we proceed in a similar fashion as in Section 4.3. With this control strategy, the vehicle dynamics $\underline{X} = [X_0\ X_1\ \cdots\ X_n]^\top \in \mathbb{C}^{n+1}$ are given by

$$\underline{X} = (\mathbf{I} - PK\mathbf{G}_0)^{-1} P\underline{D}, \tag{140}$$

with $\mathbf{G}_0 \in \mathbb{C}^{n+1\times n+1}$ the new interconnection matrix:

$$\mathbf{G}_0 = \begin{bmatrix} 0 & \underline{0}^\top \\ (1-\eta)\underline{1} & \boldsymbol{\Theta} \end{bmatrix}, \tag{141}$$

where $\underline{0} \in \mathbb{R}^n$ is the all zeros vector, $\underline{1} \in \mathbb{R}^n$ is the all ones vector, and

$$\boldsymbol{\Theta} = \begin{bmatrix} -1 & & & \eta \\ \eta & \ddots & & \\ & \ddots & \ddots & \\ & & \eta & -1 \end{bmatrix}. \tag{142}$$

Now we compute

$$\begin{aligned}(\mathbf{I} - PK\mathbf{G}_0)^{-1} &= \begin{bmatrix} 1 & \underline{0}^\top \\ -(1-\eta)PK\underline{1} & \boldsymbol{\Theta}_0 \end{bmatrix}^{-1} \\ &= \begin{bmatrix} 1 & \underline{0}^\top \\ (1-\eta)PK\boldsymbol{\Theta}_0^{-1}\underline{1} & \boldsymbol{\Theta}_0^{-1} \end{bmatrix}\end{aligned} \tag{143}$$

with

$$\begin{aligned}\boldsymbol{\Theta}_0^{-1} &= \begin{bmatrix} S^{-1} & & & -\eta PK \\ -\eta PK & \ddots & & \\ & \ddots & \ddots & \\ & & -\eta PK & S^{-1} \end{bmatrix}^{-1} \\ &= \frac{S}{1-(\eta T)^n}\begin{bmatrix} 1 & (\eta T)^{n-1} & \cdots & (\eta T)^2 & \eta T \\ \eta T & 1 & \ddots & & (\eta T)^2 \\ \vdots & \ddots & \ddots & \ddots & \vdots \\ (\eta T)^{n-2} & & \ddots & 1 & (\eta T)^{n-1} \\ (\eta T)^{n-1} & (\eta T)^{n-2} & \cdots & \eta T & 1 \end{bmatrix},\end{aligned} \tag{144}$$

for $S = 1/(1+PK)$ and $T = 1 - S$.

Now, we define $\mathcal{F}_{i,k}^{(n)}$ as the transfer function from a disturbance D_k at the k-th vehicle to the i-th inter-vehicle spacing E_i, which can be written as $E_i = X_{i-1} - X_i = \mathcal{F}_{i,k}^{(n)} D_k$. We have the following result

Proposition 4.2. *The transfer functions* $\mathcal{F}_{i,k}^{(n)}$ *satisfy*

$$\mathcal{F}_{1,0}^{(n)} = \frac{SP}{1-\eta T} \tag{145}$$

$$\mathcal{F}_{i,0}^{(n)} = 0, \quad \textit{for } i > 1. \tag{146}$$

Proof: Since the sum of every row of $\mathbf{\Theta}_0^{-1}$ in (144) is equal to

$$\frac{S}{1-(\eta T)^n} \sum_{i=0}^{n-1} (\eta T)^i, \tag{147}$$

we have that

$$\mathbf{\Theta}_0^{-1} \underline{1} = \frac{S}{1-(\eta T)^n} \sum_{i=0}^{n-1} (\eta T)^i \underline{1} = \frac{S}{1-\eta T} \underline{1}. \tag{148}$$

This implies that for $\underline{D} = [D_0 \quad 0 \quad \cdots \quad 0]^\top$,

$$E_1^0 = X_0 - X_1 = \left(1-(1-\eta)PK\frac{S}{1-\eta T}\right) PD_0 = \frac{SP}{1-\eta T} D_0, \tag{149}$$

and $E_i = X_{i-1} - X_i = 0, \quad \text{for } i > 1.$ □

Remark 4.4. *If we recall that* $X_0 = PD_0$ *is the trajectory of the leader, we see that the every follower has the same transient when there are no other disturbances in the platoon. This can also be seen as all the followers moving as a unit when the only disturbance in the system is one at the leader. This is an interesting feature when using this interconnection. (An immediate question is how model uncertainty, or non homogeneity, might affect this property).*

The effect of a disturbance on the first follower, D_1, is given by

$$E_1 = \mathcal{F}_{1,1}^{(n)} D_1 = \frac{-SP}{1-(\eta T)^n} D_1,$$

$$E_i = \mathcal{F}_{i,1}^{(n)} D_1 = \frac{SP(1-\eta T)(\eta T)^{i-1}}{1-(\eta T)^n} D_1, \quad \text{for } i > 1. \tag{150}$$

By the symmetry of the interconnection we only need to study the transfer functions $F_{i,1}^{(n)}$.

4.5.1 *Stability analysis*

In a similar way as in the leaderless cyclic case, the stability of the interconnection is determined by the stability of the transfer function $\frac{1-T}{1-(\eta T)^n}$. We have the following result

Theorem 4.3. *Let* T *be defined as in Proposition 4.1 and* $\eta \in (0,1)$*. The following holds:*
1) if $|\eta| < \|T\|_\infty^{-1}$ *then* $(1-T)/(1-(\eta T)^n)$ *has all of its poles in the open left half plane;*
2) if $|\eta| > \|T\|_\infty^{-1}$ *then there exists* $n_c \in \mathbb{N}$ *such that for all* $n > n_c$*,* $(1-T)/(1-(\eta T)^n)$ *has poles in the right half plane.*

Proof: 1) The condition $|\eta| < \|T\|_\infty^{-1}$ implies that $\|\eta T\|_\infty < 1$ and moreover $\|(\eta T)^n\|_\infty < 1$. Hence, we have that that $|1-(1-\eta T)^n| < 1$ for all $\omega \in \mathbb{R}$ and Lemma 4.2 ensures that $(1-(\eta T)^n)^{-1}$ is stable. Since $1-T$ is stable, we have that $(1-T)/(1-(\eta T)^n)$ has all of its poles in the open left half plane.

2) The condition $|\eta| > \|T\|_\infty^{-1}$ implies that $\|\eta T\|_\infty > 1$ and the proof of part 2) of Theorem 4.1 applies directly substituting ηT for Γ. □

This result coincides with the sufficient conditions on η for string stability in a unidirectional leader following scheme (See for example Seiler et al. (2004)). The case $\eta = \|T\|_\infty^{-1}$ will yield instability for the particular values of $n \in \mathbb{N}$ which satisfy the equation $1-(\eta T(j\omega_c)^n) = 0$ with ω_c being the frequency where $|T(j\omega_c)| = \|T\|_\infty$.

4.5.2 *String stability analysis*

Following similar steps as in the analysis for string stability in the leaderless cyclic case, we obtain the following result for disturbances at the first follower ($D_1 \neq 0$):

Theorem 4.4. *Let* T *be defined as in Lemma 3.1 and* $\eta \in (0,1)$*. Consider* $\mathcal{F}_{i,1}^{(n)}$ *defined in* (150) *for all* i, n *with* $i \leqslant n$*. Then the following hold:*
1) $\mathcal{F}_{i,1}^{(n)}(0) = 0, \quad \forall i = 1, \ldots, n.$*;*
2) if $|\eta| < \|T\|_\infty^{-1}$*, then there exists* $c > 0$ *such that* $\|\mathcal{F}_{i,1}^{(n)}\|_\infty < c$ *for all* $i, n \in \mathbb{N}$*,* $i \leqslant n$*.*

Proof: 1) Since $\eta < 1$ and $T(0) = 1$, and recalling from part 1) of Theorem 4.1 that SP has one zero at $s = 0$, direct substitution of $s = 0$ into (150) implies that $\mathcal{F}_{i,1}^{(n)}(0) = 0, \quad \forall i = 1, \ldots, n.$

2) From 1) we have that $\mathcal{F}_{i,1}^{(n)}(0) = 0$. The condition $|\eta| < \|T\|_\infty^{-1}$ implies that $\|(\eta T)^k\|_\infty < 1$ for all $k \geqslant 1$. Moreover, $\|SP\|_\infty < c_1$ (See part 2) of Theorem 4.2) and $\|(1-\eta T)\|_\infty = c_2$. Therefore

$$\left|\frac{SP(1-\eta T)(\eta T)^{i-1}}{1-(\eta T)^n}\right| \leqslant \frac{c_1 c_2}{|1-(\eta T)^n|}. \tag{151}$$

Given that $\|\eta T\|_\infty < 1$, we have that $1-(\eta T(j\omega))^n = 0$ has no solutions for $\omega \in \mathbb{R}$ and therefore

$$\frac{c_1 c_2}{|1-(\eta T)^n|} < \frac{c_1 c_2}{\min_\omega |1-(\eta T(j\omega))^n|} < \frac{c_1 c_2}{1-|(\eta T(j\omega_c))|}, \tag{152}$$

where ω_c satisfies $|T(j\omega_c)| = \|T\|_\infty$. It follows that there exists $c > 0$ such that

$$\|\mathcal{F}_{i,1}^{(n)}\|_\infty < c, \tag{153}$$

for all i, n with

$$c = \frac{c_1 c_2}{1-|(\eta T(j\omega_c))|}. \tag{154}$$

□

Part 1) of the last result is analogous to Theorem 4.2 for the leaderless cyclic case. Part 2) shows that the interconnection is string stable for disturbances in any follower and also gives a bound for the maximum disturbance amplification. The case $\|\eta T\|_\infty = 1$ is not considered since it may yield instability for some values of n. In particular, if $\eta T = e^{j\phi}$ for some ω_c, the factor

$$\frac{1-\eta T}{1-(\eta T)^n}, \tag{155}$$

in (150) may have an unstable pole at $\omega = \omega_c$ if $e^{jn\phi} = 1$ and $e^{j\phi} \neq 1$.

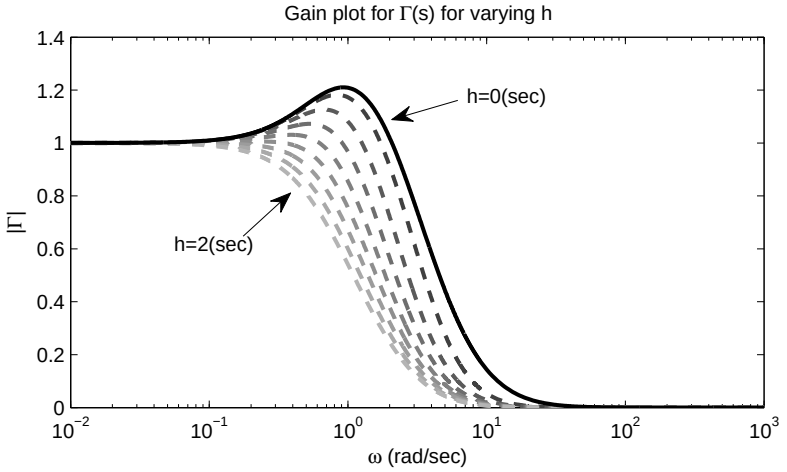

Figure 15: Magnitude plots of $\Gamma = T/(1 + sh)$ for different values of h. Solid line $h = 0(sec)$. Lightest gray and dashed line $h = 2(sec)$.

4.6 NUMERICAL EXAMPLES

In this section we present numerical examples and simulations that illustrate the results of the chapter. We consider the vehicle dynamics and local controllers

$$P = \frac{1}{s(0.1s+1)}, \tag{156}$$

$$\tilde{K} = \frac{2s+1}{s(0.05s+1)}. \tag{157}$$

In Figure 15 we have the magnitude plots of $\Gamma = PK/(1 + PKQ)$ for different values of h. It can be noted that for increasing values of the time headway constant h, the magnitude peak decreases from $\|\Gamma\|_\infty = 1.2103$ for $h = 0$ to $\|\Gamma\|_\infty = 1$ after some value of $h > 0$. In particular we can compute h_0 defined in Proposition 4.1 as

$$h_0 = \sqrt{\sup_\omega \left(\frac{|P\tilde{K}/(1+P\tilde{K})|^2 - 1}{\omega^2} \right)} = \sqrt{2} \approx 1.4142. \tag{158}$$

This value is in agreement with Figure 15 from where it can be estimated that $h_0 < 2$. Now, according to Proposition 4.1 for $h > \sqrt{2}$ we will have $|\Gamma| < 1$ for $\omega > 0$.

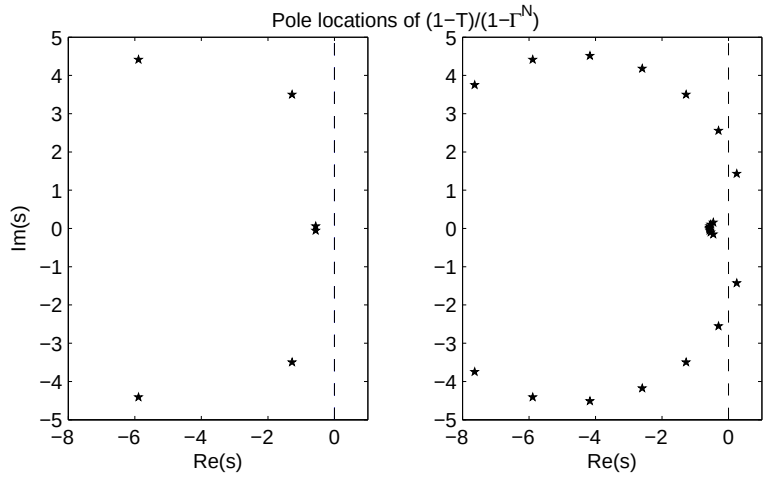

Figure 16: Pole locations for $\frac{1-T}{1-\Gamma^n}$ with $h = 0(sec)$. Dashed line: Stability boundary. Left: $n = 3$. Right $n = 9$.

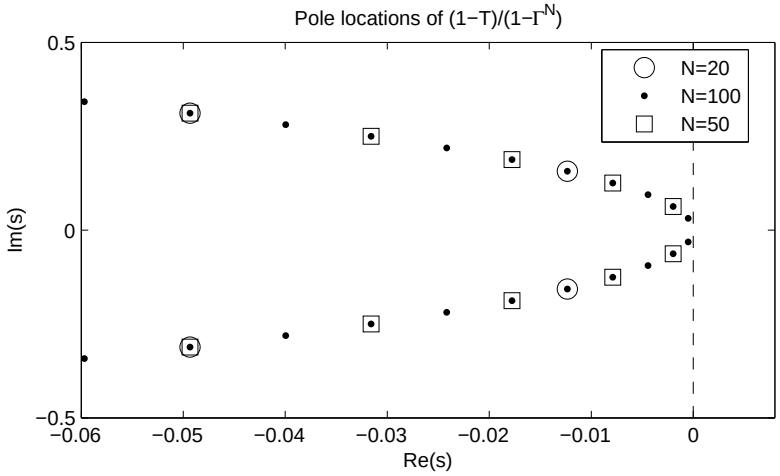

Figure 17: Pole locations for $\frac{1-T}{1-\Gamma^n}$ with $h = 2(sec)$. Dashed line: Stability boundary. Circles: n=20. Squares: n=50. Dots: n=100.

4.6.1 *Stability analysis*

Leaderless case: In Figure 16 the pole locations of the transfer function $\frac{1-T}{1-\Gamma^n}$, with $h = 0$, are plotted for $n = 3$ and $n = 9$. For $n = 3$ all the poles are in the open left half plane, however, for $n = 9$ there is a pair of complex poles with a positive real part. Part 2) of Theorem 4.1 predicts that instability occurs for large enough string size when $h = 0$. For $h = 2$ Figure 17 shows the locations of some of the poles of the transfer function $\frac{1-T}{1-\Gamma^n}$. It can be seen that the poles remain to the left of the stability boundary for $n = 20, 50, 100$. It can also be noted that for $n = 100$ there exist two poles that are closer to the boundary

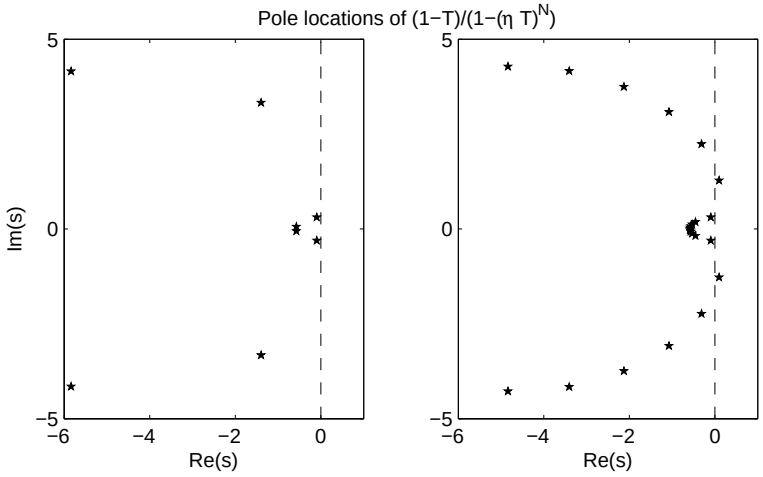

Figure 18: Pole locations for $\frac{1-T}{1-(\eta T)^n}$ with $\eta = 0.9$. Dashed line: Stability boundary. Left: $n = 3$. Right $n = 9$.

than the poles for $n = 20, 50$. It can be inferred that slower dynamics will occur with an increase of the string size. This can be predicted if we note that a factor $e^{j\frac{2k\pi}{n}} - \Gamma$ tends to $1 - \Gamma$ when n grows large and $k = 1$. Since $1 - \Gamma$ has a zero at $s = 0$, slow poles for increasing n should be expected.

Leader case: According to Theorem 4.3 the stability of the interconnection is ensured for $|\eta| < \|T\|_\infty^{-1}$. In this particular case $\|T\|_\infty \approx 1.2$. Figure 18 shows the pole locations of the transfer function $\frac{1-T}{1-(\eta T)^n}$, with $\eta = 0.9$, for $n = 3$ and $n = 9$. As predicted, since $\eta > 1/1.2 \approx 0.83$, the system is unstable after the string size increases over a critical value. On the other hand, Figure 19 shows the pole locations of $\frac{1-T}{1-(\eta T)^n}$ when $\eta = 0.5$ for $n = 20, 50, 100$. It can be seen that the system remains stable even for a string size as large as $n = 100$. Moreover, the poles of the transfer function do not approach the stability boundary as the size of the string increases.

4.6.2 *String stability*

Leaderless case: The transfer functions $F_2^{(n)}$, reflect the effect of disturbances on the inter-vehicle spacing of the second member of the string with respect to its immediate predecessor, for different string sizes. For $h = 2$, we obtain the corresponding magnitude plots, which are shown in Figure 20. We can see that they are all bounded as predicted by Theorem 4.2 with the bound $F_b(\omega) = |SP|\frac{|1-T|}{1-|\Gamma|^2}$.

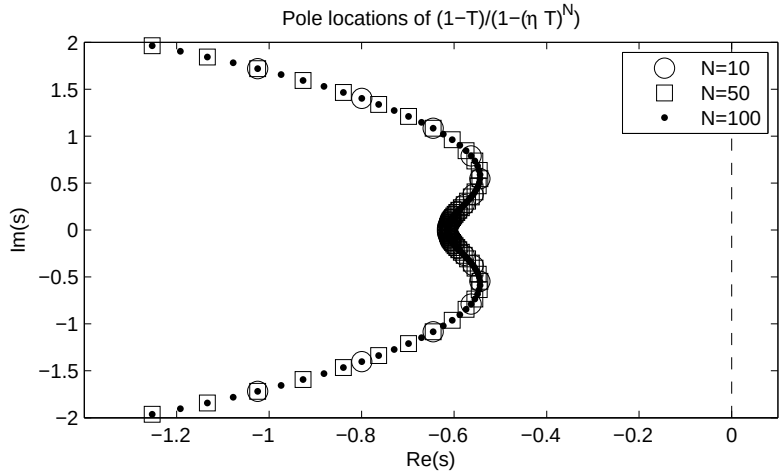

Figure 19: Pole locations for $\frac{1-T}{1-(\eta T)^n}$ with $\eta = 0.5$. Dashed line: Stability boundary. Circles: n=20. Squares: n=50. Dots: n=100.

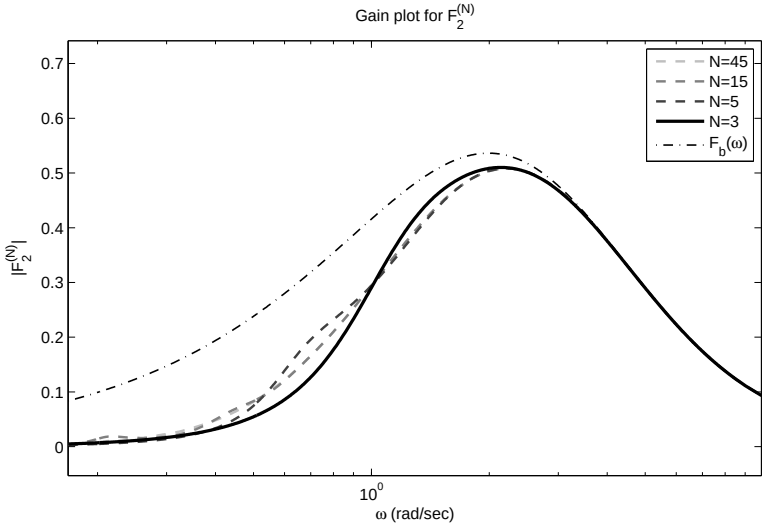

Figure 20: Magnitude plots of $F_2^{(n)}$, when $h = 2(sec)$, for an increasing number of vehicles. $F_b(\omega)$: Bound for $|F_2^{(n)}|$ independent of n.

Leader case: The transfer functions $\mathcal{F}_{2,1}^{(n)}$, reflect the effect of disturbances on the inter-vehicle spacing of the second follower of the leader of the string with respect to its immediate predecessor, for different string sizes. For $\eta = 0.5$, we obtain the corresponding magnitude plots, which are shown in Figure 21. We can see that they are all bounded as predicted by Theorem 4.4 with the bound $F_b(\omega) = |SP|\frac{|1-\eta T|}{1-\eta||T||_\infty}$.

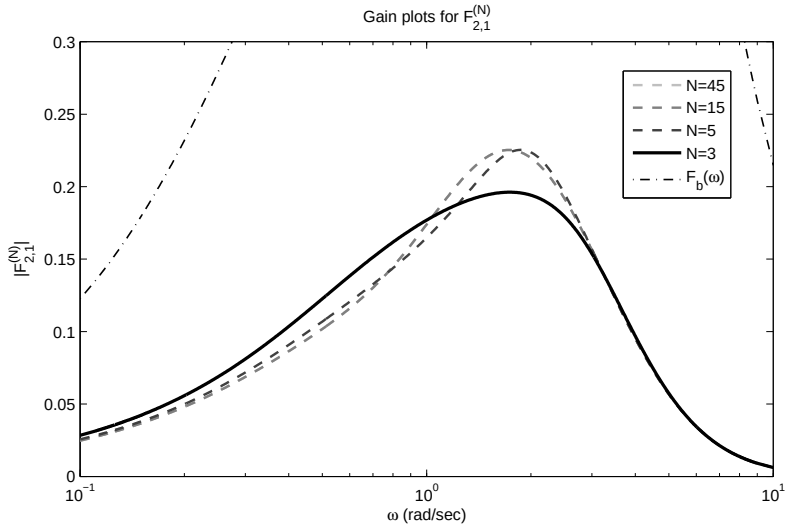

Figure 21: Magnitude plots of $\mathcal{F}_{2,1}^{(n)}$, when $\eta = 0.5$, for an increasing number of vehicles.

4.7 CONCLUSIONS

In this chapter we provided stability and string stability results for a cyclic interconnection of vehicles. In particular we showed that if the spacing policy is constant, the formation becomes unstable for any string size greater than a critical value n_c. For the time headway spacing policy we show that it is possible to achieve stability and string stability of the interconnection, provided that the time headway constant is chosen appropriately.

Numerical examples illustrated these results and showed some of the drawbacks of the interconnection such as slower dynamics when the string size increases.

The use of an independent leader who is tracked by the remaining members of the vehicle string was also studied. We showed that similar results to the leaderless case apply, guaranteeing stability for any string size and string stability when the design parameter $\eta < \|T\|_\infty^{-1}$. The added benefits are a simpler trajectory of the vehicles when the leader starts a manoeuvre and the dynamics do not become slower as the string size increases.

An immediate extension to this work would be to study a cyclic and bidirectional interconnection with and without a leader. Other lines of work may include the inclusion of time delays in the measurements and non homogeneity of the vehicle models and controllers.

5

FORMATION CONTROL WITH A BIDIRECTIONAL INTERCONNECTION

5.1 INTRODUCTION

In this chapter we present preliminary results on a type of bidirectional formation control architecture. In such architectures almost every member of the platoon is controlled using measurements that contain (directly or indirectly) information from members that are behind them and also from members that are in front of them. Although this architecture has been reported to possess some disadvantages (see for example Seiler et al. (2004); Barooah et al. (2009)), it can be used to allow every member of the platoon compensate for a disturbance at any particular vehicle.

In Section 5.2 we define the particular architecture to be studied (nearest neighbour bidirectional). We also present the resulting dynamics of the platoon in the frequency domain as a collection of transfer functions from disturbances to positions. One of the main properties of this interconnection is that the location of the poles of the associated transfer functions will vary with the number of vehicles $n \in \mathbb{N}$ (similar to the cyclic case in Chapter 4). In Section 5.3 we discuss some conditions for establishing the stability of the whole interconnection and some other dynamical properties.

The novelty of the approach presented here lies in the direct method for the computation of the transfer functions from disturbances to vehicle positions. We obtain closed form expressions for these transfer functions and a way to directly compute the location of their poles. As discussed in Chapter 2, the work in (Barooah et al., 2009) discusses a method to study the behaviour of the least stable pole of a simple bidirectional interconnection. For this they obtain a PDE associated to the limit of a bidirectional platoon of large size. Our method avoids using such approximations and allows for further insight into the possible resulting dynamics. In Section 5.4 we present a performance study of the interconnection by considering the resulting dynamics for the inter-vehicle spacings. We present numerical examples and

comments on the main results shown in Section 5.5. Section 5.6 contains some final remarks and possible lines of future work.

5.2 FORMATION CONTROL DEFINITION AND RESULTING VEHICLE DYNAMICS

Again, as in the previous chapters, we consider a platoon of $n \in \mathbb{N}$ identical vehicles travelling in a straight line. In this chapter we will consider the frequency domain model for the vehicles given by

$$X_i = H(U_i + D_i), \tag{159}$$

where X_i is the Laplace transform of the position of the i-th vehicle, D_i is the Laplace transform of its input disturbance and U_i is the Laplace transform of its control action. We consider H to be a transfer function with a pole at $s = 0$. For the bidirectional architecture that we want to study, the control signals U_i are defined as

$$U_i = K(PX_{i-1} - X_i + FX_{i+1}), \quad 1 < i < n, \tag{160}$$

$$U_1 = D_1, \tag{161}$$

$$U_n = D_n, \tag{162}$$

where P and F are proper and stable transfer functions such that $P(0) + F(0) = 1$ (see Remark 3.2) and K is a controller with a pole at $s = 0$ that stabilizes H in closed loop.

If we consider that every vehicle starts from rest and is positioned initially in the desired formation, then the dynamics of the vehicles' positions can be written as

$$\underline{X} = (\mathbf{I} - KH\mathbf{G})^{-1}H\underline{D}, \tag{163}$$

where $\underline{X} = [X_1 \ \cdots \ X_n]^\top$, $\underline{D} = [D_1 \ \cdots \ D_n]^\top$, $\mathbf{I}$ is the $n \times n$ identity matrix and $\mathbf{G} \in \mathbb{C}^{n\times n}$ is given by

$$\mathbf{G} = \begin{bmatrix} 0 & & & & \\ P & -1 & F & & \\ & \ddots & \ddots & \ddots & \\ & & P & -1 & F \\ & & & & 0 \end{bmatrix}. \tag{164}$$

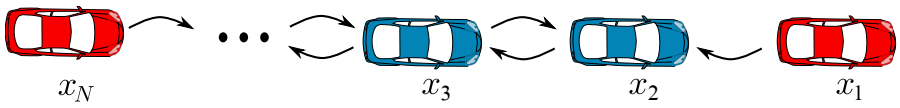

Figure 22: Bidirectional platoon of vehicles. x_i: position of the i-th vehicle. Red vehicles move independently.

Remark 5.1. *In this scheme we consider that the leader and the last vehicle of the platoon move independent of the string (See Figure 22). Therefore, for consistency, they must follow the same trajectory. For this we set* $D_1 = D_n = D$ *and* $\mathbf{G}_{1,1} = \mathbf{G}_{n,n} = 0$. *The main reason for this assumption is that of simplicity on the following derivations. In a practical sense this is not an unreasonable setting and it has been studied in other works (Barooah et al., 2009). It will be the aim of future research to consider the case without an independent last vehicle.*

Now, in order to obtain closed form expressions for every element of the matrix $(\mathbf{I} - KH\mathbf{G})^{-1}HD$ we can write $(\mathbf{I} - KH\mathbf{G})^{-1}$ in the following way

$$(\mathbf{I} - KH\mathbf{G})^{-1} = \begin{bmatrix} 1 & \zeta_{n-2}^\top & 0 \\ -PKHe_1 & (KH)\mathbf{\Phi} & -FKHe_{n-2} \\ 0 & \zeta_{n-2}^\top & 1 \end{bmatrix}^{-1} \tag{165}$$

$$= \begin{bmatrix} 1 & \zeta_{n-2}^\top & 0 \\ P\mathbf{\Phi}^{-1}e_1 & (KH)^{-1}\mathbf{\Phi}^{-1} & F\mathbf{\Phi}^{-1}e_{n-2} \\ 0 & \zeta_{n-2}^\top & 1 \end{bmatrix}, \tag{166}$$

where $\zeta_{n-2}^\top \in \mathbb{R}^{n-2}$ is a vector of zeros, $e_k \in \mathbb{R}^{n-2}$ is a canonical vector of $\mathbb{R}^{n-2}$ (only the k-th entry is non zero and equal to 1) and $\mathbf{\Phi}$ is the $n-2 \times n-2$ tridiagonal matrix

$$\mathbf{\Phi} = \begin{bmatrix} T^{-1} & -F & & \\ -P & \ddots & \ddots & \\ & \ddots & \ddots & -F \\ & & -P & T^{-1} \end{bmatrix}, \tag{167}$$

with $T = KH/(1+KH)$. The elements of $\mathbf{\Phi}^{-1}$ are given by the formula (which is obtained by using equation (5.1) in Da Fonseca and Petronilho (2005))

$$(\mathbf{\Phi}^{-1})_{i,j} = \begin{cases} \frac{1}{\sqrt{PF}} \left(\frac{F}{\sqrt{PF}} \right)^{j-i} \frac{V_{i-1}(\Gamma) V_{n-2-j}(\Gamma)}{V_{n-2}(\Gamma)} & \text{if } i \leqslant j \\ \frac{1}{\sqrt{PF}} \left(\frac{P}{\sqrt{PF}} \right)^{i-j} \frac{V_{j-1}(\Gamma) V_{n-2-i}(\Gamma)}{V_{n-2}(\Gamma)} & \text{if } i > j \end{cases}, \tag{168}$$

where

$$\Gamma = T^{-1}/(2\sqrt{PF}), \tag{169}$$

and $V_k(x)$ is the Chebyshev polynomial of the second kind of order k.

Remark 5.2. *Here we note an important distinction from the unidirectional schemes. Similar to the cyclic case, every vehicle position transfer function depends on the size n of the platoon, whereas in the unidirectional case this is only the case for the last member of the platoon (since it is the n—th member). This implies that the approach to study string stability in the unidirectional case cannot be used in a straightforward manner in the bidirectional case.*

5.3 LOCATION OF THE INTERCONNECTION POLES

Given that we have obtained explicit expressions for the position transfer functions of every vehicle, we can study them in order to find where the poles of the system are located. In the unidirectional case the dynamics of the interconnection are defined by the local feedbacks and the controller/vehicle-model pair $H(s)K(s)$ through $(1+H(s)K(s))^{-1}$. In contrast, the bidirectional case studied here has poles that depend not only on the mentioned parameters but also on the number of vehicles. Additionally, this dependence is not straightforward as in the unidirectional case for the last member. As a first step, we can write the Chebyshev polynomials as (Zwillinger, 2002):

$$V_k(\Gamma) = 2^k \prod_{m=1}^{k} \left(\Gamma - \cos\left(\frac{m\pi}{k+1} \right) \right). \tag{170}$$

Now, we note that for a fixed $k \in \mathbb{N}$, the set of numbers

$$\mathcal{Y} = \left\{ \cos\left(\frac{m\pi}{k+1}\right), m = 1, \dots, k \right\} \subset \mathbb{R}, \tag{171}$$

is symmetrically distributed in $(-1, 1)$, i. e. if $y \in \mathcal{Y}$ then $-y \in \mathcal{Y}$. With this, if we use the definition of Γ in (169) we can rewrite

$$V_k(\Gamma) = \frac{1}{(PF)^{k/2} T^k} \prod_{m=1}^{\lfloor k/2 \rfloor} \left(1 - 4\cos^2\left(\frac{m\pi}{k+1}\right) PFT^2\right) \tag{172}$$

By substituting (172) into (168) we obtain

$$(\Phi^{-1})_{i,j} = \begin{cases} T(FT)^{j-i} \dfrac{\tilde{V}_{i-1}\tilde{V}_{n-2-j}}{\tilde{V}_{n-2}} & \text{if } i \leqslant j \\ T(PT)^{i-j} \dfrac{\tilde{V}_{j-1}\tilde{V}_{n-2-i}}{\tilde{V}_{n-2}} & \text{if } i > j, \end{cases}, \tag{173}$$

where

$$\tilde{V}_k = \prod_{m=1}^{\lfloor k/2 \rfloor} \left(1 - 4\cos^2\left(\frac{m\pi}{k+1}\right) PFT^2\right). \tag{174}$$

The poles of the transfer functions $(\Phi^{-1})_{i,j}$, will be poles of the transfer functions F, P and T, and points in the set

$$\Lambda_n := \left\{ s \in \mathbb{C} : \frac{1}{4P(s)F(s)T(s)^2} = \cos^2\left(\frac{m}{n-1}\pi\right), m = 1, \dots \right.$$
$$\left. \dots, \lfloor (n-2)/2 \rfloor \right\}, \tag{175}$$

which are the points $s \in \mathbb{C}$ where $\tilde{V}_{n-2}$ vanishes. Note that not all the elements of Λ_n have to be a pole of $(\Phi^{-1})_{i,j}$. In some cases, there may be cancellations with the numerators in (168). Since P, F and T are assumed to be stable (otherwise the interconnection would be unstable), the stability of the resulting interconnected system is determined by the set Λ_n being contained completely within the open left half-plane of $\mathbb{C}$. We have the following result regarding the stability of the set Λ_n.

Proposition 5.1. *Let T, P and F be stable transfer functions. If the transfer function $-4PFT^2$ has a gain margin greater than 1, then every $s \in \Lambda_n$ defined in (175) satisfies $\Re\{s\} < 0$ for all $n \in \mathbb{N}$.*

Proof: The set Λ_n in (175) is defined from the zeros of $1-\alpha 4PFT^2$, with $\alpha = \cos^2(m\pi/(n-1))$ for $m = 1,\dots,n$. Now $\alpha \in (0,1)$ for any possible value of the integers m and n and therefore the Nyquist stability criterion implies that a gain margin of 1 for $-4PFT^2$ will ensure that every $s \in \Lambda_n$ has negative real part for all $n \in \mathbb{N}$. □

The last result states that if the selection of the controller K and the filters P and F yields a gain margin greater than 1 for $-4PFT^2$, every point $s \in \Lambda_n$ also satisfies $\Re\{s\} < 0$.

On the contrary, if the gain margin of $-4PFT^2$ is less than 1, there exists n_c such that for $n > n_c$ the set Λ_n will contain elements in the open right half plane of $\mathbb{C}$.

For the particular case where the gain margin of $-4PFT^2$ is equal to 1 we have that the least stable pole of all the transfer functions from disturbances to vehicle positions should approach $s = 0$ as the number of vehicles increases. This due to the fact that

$$\alpha = \cos^2(m\pi/(n-1)), \tag{176}$$

approaches 1 when $n, m \to \infty$. In (Barooah et al., 2009), this is shown to be true for a particular selection of vehicle models (double integrators) and for static gains as controllers. Moreover, the result was obtained by approximating the dynamics of a large platoon using a PDE. In contrast, our derivations allow for more insight on the properties of the interconnection, without using an approximation and for a wider range of vehicle models and controllers.

Remark 5.3. *The following derivation suggests that for static symmetric gains, i. e.* $P = F = 0.5$ *for all* s*, slow oscillations may occur in the transient response of the interconnection.*

Let $P = F = 0.5$, then there exists $n_o \in \mathbb{N}$ such that for $n > n_o$ the set Λ_n defined in (175) contains a pair of complex conjugate points. For $P = F = 0.5$, the elements of Λ_n are given by the roots of the equation

$$1-\alpha T^2 = (1-\sqrt{\alpha}T)(1+\sqrt{\alpha}T) = 0, \tag{177}$$

with $\alpha = \cos^2(m\pi/(n-1))$ for $m = 1,\dots,n$. For $\alpha = 1$ we have

$$1-T^2 = (1-T)(1+T) = 0. \tag{178}$$

Now, from the controller and vehicle model properties (KH has two integrators) we have that $T(0) = 1$, $T'(0) = 0$ and $T''(0) \neq 0$, which in turn implies that $(1 - T) = 0$ has $s = 0$ as a solution twice. According to (Krall, 1970) $s = 0$ is an *isolated breakaway point* with multiplicity 2 for the equation $1 - \sqrt{\alpha}T = 0$. Theorem 3.4 of (Krall, 1970) states that the corresponding root locus of $1 - \sqrt{\alpha}T = 0$ either arrives vertically and departs horizontally, or vice versa at $s = 0$. Since T is designed such that Λ_n has all of its elements in the left half plane for all values of $\alpha \in (0, 1)$, there exists $\alpha_0 < 1$ for which $1 - \sqrt{\alpha_0}T = 0$ has a complex conjugate pair of roots in the open left half plane whenever $\alpha_0 < \alpha < 1$ (or else one of the roots at $s = 0$ for $\alpha = 1$ would depart horizontally into the right half plane). Finally, if $m = 1$, $\alpha = \cos^2(\pi/(n-1))$ tends to 1 as n increases and there exists n_o such that $\alpha \geqslant \alpha_o$.

In Theorem 1 of (Barooah and Hespanha, 2005) it is shown with a similar argument that HK having three or more integrators (and therefore $T''(0) = 0$) would imply instability of the interconnection if $P = F = 0.5$. This comes from the fact that now $s = 0$ would be a triple breakaway point. According to Theorem 3.2 in (Krall, 1970) the root locus will always yield a root in the right half plane for some value of α. However, this is only true in the static symmetric case $P = F = 0.5$. In the following section we will show that the proper design of P and F can enable the use of more integrators in the product HK for stability and also avoid oscillating modes in the interconnection.

5.4 INTER-VEHICLE SPACING DYNAMICS

The inter-vehicle spacings that result from the use of the studied bidirectional interconnection are given by

$$\underline{E}^{pre} = \begin{bmatrix} 0 & & & \\ 1 & -1 & & \\ & \ddots & \ddots & \\ & & 1 & -1 \end{bmatrix} \underline{X}. \tag{179}$$

We will focus our attention on the response of the interconnection to the movements of the leader and last vehicles, which are assumed

to be equal (for this we set $D_1 = D_n = D$). Setting the disturbances at followers to 0, that is $D_i = 0$ for $i = 2, \dots, n-1$, we have

$$\underline{E}^{pre} = \begin{bmatrix} 0 & & & \\ 1 & -1 & & \\ & \ddots & \ddots & \\ & & 1 & -1 \end{bmatrix} \left(\begin{bmatrix} 1 \\ P\Phi^{-1}e_1 \\ 0 \end{bmatrix} + \begin{bmatrix} 0 \\ F\Phi^{-1}e_{n-2} \\ 1 \end{bmatrix} \right) HD \tag{180}$$

$$= \begin{bmatrix} 0 & & & \\ 1 & -1 & & \\ & \ddots & \ddots & \\ & & 1 & -1 \end{bmatrix} \begin{bmatrix} 1 \\ \Phi^{-1}(Pe_1 + Fe_{n-2}) \\ 1 \end{bmatrix} HD. \tag{181}$$

Since $\Phi^{-1}e_1$ and $\Phi^{-1}e_{n-2}$ correspond to the first and last column of Φ^{-1} we have from (168) that

$$\Phi^{-1}e_1 = \frac{1}{\sqrt{PF}V_{n-2}(\Gamma)} \begin{bmatrix} V_{n-2-1}(\Gamma) \\ \left(\frac{P}{\sqrt{PF}}\right) V_{n-2-2}(\Gamma) \\ \vdots \\ \left(\frac{P}{\sqrt{PF}}\right)^{n-2-1} V_{n-2-n+2}(\Gamma) \end{bmatrix}, \tag{182}$$

$$\Phi^{-1}e_{n-2} = \frac{1}{\sqrt{PF}V_{n-2}(\Gamma)} \begin{bmatrix} \left(\frac{F}{\sqrt{PF}}\right)^{n-2-1} V_{n-2-n+2}(\Gamma) \\ \vdots \\ \left(\frac{F}{\sqrt{PF}}\right) V_{n-2-2}(\Gamma) \\ V_{n-2-1}(\Gamma) \end{bmatrix}. \tag{183}$$

With this, the inter-vehicle spacings take the form

$$\underline{E}^{pre} = \left(\begin{bmatrix} 0 \\ 1 - \frac{P}{\sqrt{PF}} \frac{V_{n-3}(\Gamma)}{V_{n-2}(\Gamma)} \\ \frac{P}{\sqrt{PF}} \left(\frac{V_{n-3}(\Gamma) - \frac{P}{\sqrt{PF}} V_{n-4}(\Gamma)}{V_{n-2}(\Gamma)} \right) \\ \left(\frac{P}{\sqrt{PF}} \right)^2 \left(\frac{V_{n-4}(\Gamma) - \frac{P}{\sqrt{PF}} V_{n-5}(\Gamma)}{V_{n-2}(\Gamma)} \right) \\ \vdots \\ \left(\frac{P}{\sqrt{PF}} \right)^{n-3} \left(\frac{V_1(\Gamma) - \frac{P}{\sqrt{PF}} V_0(\Gamma)}{V_{n-2}(\Gamma)} \right) \\ \left(\frac{P}{\sqrt{PF}} \right)^{n-2} \left(\frac{1}{V_{n-2}(\Gamma)} \right) \end{bmatrix} + \right.$$

$$\left. \begin{bmatrix} 0 \\ -\left(\frac{F}{\sqrt{PF}} \right)^{n-2} \left(\frac{1}{V_{n-2}(\Gamma)} \right) \\ \left(\frac{F}{\sqrt{PF}} \right)^{n-3} \left(\frac{\frac{F}{\sqrt{PF}} V_0(\Gamma) - V_1(\Gamma)}{V_{n-2}(\Gamma)} \right) \\ \vdots \\ \left(\frac{F}{\sqrt{PF}} \right)^2 \left(\frac{\frac{F}{\sqrt{PF}} V_{n-5}(\Gamma) - V_{n-4}(\Gamma)}{V_{n-2}(\Gamma)} \right) \\ \frac{F}{\sqrt{PF}} \left(\frac{\frac{F}{\sqrt{PF}} V_{n-4}(\Gamma) - V_{n-3}(\Gamma)}{V_{n-2}(\Gamma)} \right) \\ \frac{F}{\sqrt{PF}} \frac{V_{n-3}(\Gamma)}{V_{n-2}(\Gamma)} - 1 \end{bmatrix} \right) HD, \tag{184}$$

or for the k–th vehicle, $k \geqslant 2$, $E_k^{pre}/D = HM_k(s,n)$, with

$$M_k(s,n) = \left(\frac{P}{\sqrt{PF}} \right)^{k-2} \left(\frac{V_{n-k}(\Gamma) - \frac{P}{\sqrt{PF}} V_{n-k-1}(\Gamma)}{V_{n-2}(\Gamma)} \right) + \left(\frac{F}{\sqrt{PF}} \right)^{n-k} \left(\frac{\frac{F}{\sqrt{PF}} V_{k-3}(\Gamma) - V_{k-2}(\Gamma)}{V_{n-2}(\Gamma)} \right). \tag{185}$$

We note that all the predecessor errors for $k \geqslant 2$ depend on the number of vehicles n that form the platoon which justifies the notation for $M_k(s,n)$.

5.4.1 *Steady state analysis for step* D

We next study the DC-gain of the inter-vehicle spacings transfer functions. First, we recall that H has a pole at $s = 0$. Therefore, for stability

of the inter-vehicle spacings we must check that we can factor a zero at $s = 0$ from the right hand side of (185). If we write

$$M_k(s,n) = \left(\frac{P}{\sqrt{PF}}\right)^{k-2} \frac{Q_k(s,n)}{V_{n-2}(\Gamma)}, \tag{186}$$

we need to check if

$$\begin{aligned} Q_k(s,n) =& V_{n-k}(\Gamma) - \frac{P}{\sqrt{PF}} V_{n-k-1}(\Gamma) \\ & - \left(\frac{F}{\sqrt{PF}}\right)^{n-2} \left(V_{k-2}(\Gamma) - \frac{F}{\sqrt{PF}} V_{k-3}(\Gamma)\right), \end{aligned} \tag{187}$$

has a zero at $s = 0$ since $P(0) \neq 0, F(0) \neq 0$ and $\Gamma(0) \geqslant 1$, which implies $V_{n-2}(\Gamma(0)) \neq 0$ (recalling that all the roots of the Chebyshev polynomials are contained in $(-1,1)$).

At $s = 0$ with $y = 1/(2\sqrt{P(0)F(0)})$ and recalling that $T(0) = 1$ and $P(0) + F(0) = b + c = 1$ we have that

$$\begin{aligned} Q_k(0,n) =& V_{n-k}(y) - 2ybV_{n-k-1}(y) \\ & - (2yc)^{n-2} \left(V_{k-2}(y) - 2ycV_{k-3}(y)\right). \end{aligned} \tag{188}$$

Since $P/\sqrt{PF} = \sqrt{PF}/F$, we have that $2yb = 1/(2yc)$. Moreover, the Chebyshev polynomials of the second kind satisfy the recurrence relation

$$V_{i+1}(y) = 2yV_i(y) - V_{i-1}(y), \tag{189}$$

$$V_{i-1}(y) = 2yV_i(y) - V_{i+1}(y), \tag{190}$$

and iterating on the terms of the right hand side of (188) we have

$$\begin{aligned} V_{n-k}(y) - 2ybV_{n-k-1}(y) =& 2yc(V_{n-k-1}(y) - 2ybV_{n-k-2}(y)) \\ =& (2yc)^{n-k-2}, \end{aligned} \tag{191}$$

$$\begin{aligned} V_{k-2}(y) - 2ycV_{k-3}(y) =& V_{k-2}(y) - 2yV_{k-3}(y) + 2ybV_{k-3}(y) \\ =& 2yb(V_{k-3}(y) - 2ycV_{k-4}(y)) \\ =& (2yb)^{k-4}. \end{aligned} \tag{192}$$

Therefore, substituting in (188) we see that $Q_k(0,n) = 0$ for any selection of $P(s)$ and $F(s)$ satisfying $P(0) + F(0) = 1$. With this we ensure that the inter-vehicle spacing transfer function for the k-th vehicle

$$\frac{E_k^{pre}}{D} = HM_k(s,n), \tag{193}$$

does not have a pole at $s = 0$.

In order to compute the DC-gain of $E_k^{pre}(s)/D$ we need to evaluate

$$\lim_{s\to 0} H(s)M_k(s,n) = \left(\frac{b}{\sqrt{bc}}\right)^{k-2} \frac{\tilde{H}(0)}{V_{n-2}(y)} \lim_{s\to 0} \frac{Q_k(s,n)}{s}, \tag{194}$$

where $H(s) = \tilde{H}(s)/s$, $\tilde{H}(0) \neq 0$. We already showed that $Q_k(0,n) = 0$ and then L'Hôpital's rule implies

$$\lim_{s\to 0} \frac{Q_k(s,n)}{s} = \lim_{s\to 0} Q_k'(s,n). \tag{195}$$

We will consider particular cases.

5.4.1.1 *Static gains*

For static gains we have the following result.

Proposition 5.2. *If* $P(s) = b \in \mathbb{R}$ *and* $F(s) = c \in \mathbb{R}$ *for all* $s \in \mathbb{C}$*, we have that* $Q_k'(0,n) = 0$.

Proof: Since P and F are constant, in this case we have

$$(V_i(\Gamma))' = V_i'(\Gamma)\Gamma', \tag{196}$$

$$\Gamma' = -T(s)^{-2}T'(s)/(2\sqrt{bc}). \tag{197}$$

Recalling that $T'(0) = 0$, direct differentiation and evaluation at $s = 0$ in (187) yields the desired result. □

5.4.1.2 *Symmetric dynamic gains*

If we consider $P(s) = F(s)$, then $\Gamma = 1/(2PT)$ with $P(0) = 0.5$. Now $Q_k(s,n)$ simplifies to

$$Q_k(s,n) = V_{n-k}(\Gamma) - V_{n-k-1}(\Gamma) + V_{k-3}(\Gamma) - V_{k-2}(\Gamma). \tag{198}$$

The derivative of $Q_k(s,n)$ with respect to s takes the form

$$Q_k'(s,n) = \Gamma'(V_{n-k}'(\Gamma) - V_{n-k-1}'(\Gamma) + V_{k-3}'(\Gamma) - V_{k-2}'(\Gamma)), \tag{199}$$

and at $s = 0$, $Q'_k(0, n)$ will vanish if either $\Gamma'(0) = 0$ or

$$V'_{n-k}(1) - V'_{n-k-1}(1) + V'_{k-3}(1) - V'_{k-2}(1) = 0. \tag{200}$$

The last expression is due to the fact that $P(0) = 0.5$ and hence $\Gamma(0) = 1$. For Γ' in this case we obtain

$$\Gamma' = 0.5\left(\frac{1}{PT}\right)' = -0.5\frac{P'T + PT'}{(PT)^2} \Rightarrow \Gamma'(0) = -2P'(0), \tag{201}$$

recalling that $T(0) = 1$ and $T'(0) = 0$. For the expression in (200) we need to compute the derivatives of the Chebyshev polynomials. A formula for this is given by (Zwillinger, 2002)

$$V'_n(x) = \frac{(n+1)W_{n+1}(x) - xV_n(x)}{(x^2-1)}, \tag{202}$$

where $W_n(x)$ is the Chebyshev polynomial of the first kind of order n. We note that at $x = 1$ we must take limits

$$\begin{aligned} V'_n(1) &= \lim_{x\to 1} \frac{(n+1)W_{n+1}(x) - xV_n(x)}{(x^2-1)} \\ &= \frac{1}{2}\lim_{x\to 1} \frac{(n+1)W_{n+1}(x) - xV_n(x)}{x-1}. \end{aligned} \tag{203}$$

Since $W_n(1) = 1$ and $V_n(1) = n+1$ the last limit is of the form $0/0$ and using L'Hôpital's rule once more we get

$$V'_n(1) = \frac{1}{2}\lim_{x\to 1}(n+1)W'_{n+1}(x) - V_n(x) - xV'_n(x). \tag{204}$$

As the limits exist and using the fact (Zwillinger, 2002)

$$W'_n(x) = nV_{n-1}(x), \tag{205}$$

we can write

$$V'_n(1) = \frac{(n+1)^2V_n(1) - (n+1) - V'_n(1)}{2}, \tag{206}$$

and therefore

$$V'_n(1) = \frac{n(n+1)(n+2)}{3}. \tag{207}$$

With this formula we can see that

$$V'_{n-k}(1) - V'_{n-k-1}(1) + V'_{k-3}(1) - V'_{k-2}(1) = (n-k)(n-k+1) + (k-1)(k-2), \tag{208}$$

which can only be zero if $n = 1$ or $k = n/2+1$ (which is only possible if n is even).

In general $Q'_k(0,n)$ for the symmetric dynamic gains will be zero if and only if $P'(0) = 0$. If this is not the case, the DC-gain of the inter-vehicle spacings is proportional to n which implies inter-vehicle spacings that grow with the number of vehicles (string instability).

It should also be noted that if $k = n/2+1$, from (187) we have that in this symmetric case

$$\begin{aligned} Q_{n/2+1}(s,n) =& V_{n/2-1}(\Gamma) - V_{n/2-2}(\Gamma) - V_{n/2-1}(\Gamma) + V_{n/2-2}(\Gamma) \\ =& 0, \quad \forall s \in \mathbb{C}, \end{aligned} \tag{209}$$

which means that the two central vehicles move with the same transient response when n is even.

5.4.1.3 *Arbitrary dynamic gains*

In the general case, if we let $\gamma = F/\sqrt{PF} = \sqrt{PF}/P$ we have

$$\begin{aligned} Q'_k(s,n) =& V'_{n-k}(\Gamma)\Gamma' + \gamma^{-2}\gamma' V_{n-k-1}(\Gamma) - \gamma^{-1} V'_{n-k-1}(\Gamma)\Gamma' \\ & - (n-2)\gamma^{n-3}\gamma'(V_{k-2}(\Gamma) - \gamma V_{k-3}(\Gamma)) \\ & + \gamma^{n-2}(V'_{k-2}(\Gamma)\Gamma' - \gamma' V_{k-3}(\Gamma) - \gamma V'_{k-3}(\Gamma)\Gamma'). \end{aligned} \tag{210}$$

It can be noted that all the terms of this expression possess either Γ' or γ' as a factor. These derivatives are given by

$$\Gamma' = -\frac{1}{2\sqrt{PF}T^2}T' - \frac{P'F + PF'}{4T(PF)^{3/2}} = -\Gamma\left(\frac{T'}{T} + \frac{P'F + PF'}{2PF}\right), \tag{211}$$

$$\gamma' = \frac{F'}{\sqrt{PF}} - \frac{F(P'F + PF')}{2(PF)^{3/2}} = \gamma\left(\frac{F'}{F} - \frac{P'F + PF'}{2PF}\right) = \gamma\left(\frac{PF' - P'F}{2PF}\right). \tag{212}$$

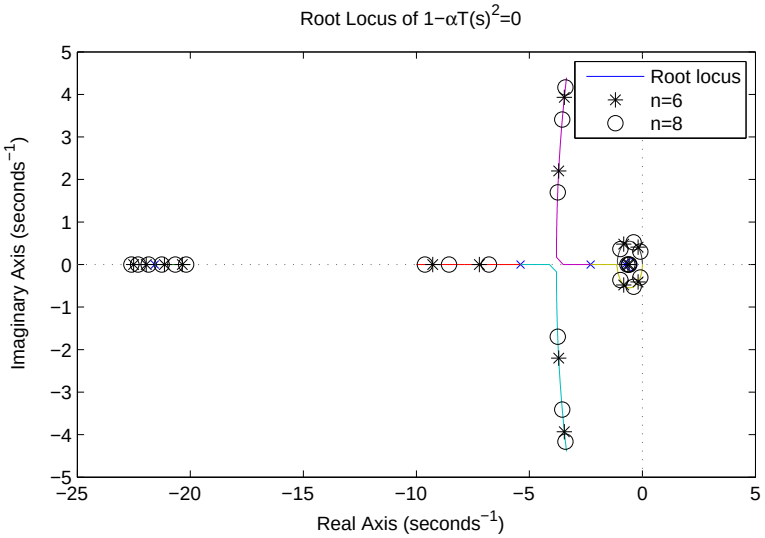

Figure 23: Root locus of $1 - \alpha T^2 = 0$.

At $s = 0$, recalling that $T(0) = 1$, $T'(0) = 0$, $\Gamma(0) \geqslant 1$, $\gamma(0) \neq 0$, $P(0) = b$ and $F(0) = c$ we have

$$\Gamma'(0) = -\Gamma(0)\frac{cP'(0) + bF'(0)}{2bc}, \tag{213}$$

$$\gamma'(0) = \gamma(0)\frac{bF'(0) - cP'(0)}{2bc}. \tag{214}$$

It follows immediately that $P'(0) = F'(0) = 0$ implies $Q'_k(0, n) = 0$.

In general, if the previous condition does not hold we see that for $k = 2$

$$\begin{aligned} Q'_2(s, n) =& V'_{n-2}(\Gamma)\Gamma' + \gamma^{-2}\gamma' V_{n-3}(\Gamma) - \gamma^{-1}V'_{n-3}(\Gamma)\Gamma' \\ & - (n-2)\gamma^{n-3}\gamma' \\ Q'_2(s, n) =& \Gamma'[V'_{n-2}(\Gamma) - \gamma^{-1}V'_{n-3}(\Gamma)] \\ & + \gamma'\gamma^{-2}[V_{n-3}(\Gamma) - (n-2)\gamma^{n-1}], \end{aligned} \tag{215}$$

noting that $V_{-1}(\Gamma) = 0$ and $V_0(\Gamma) = 1$.

In a similar fashion for $k = n$

$$\begin{aligned} Q'_n(s, n) =& -\gamma^{n-3}[(n-2)\gamma'(V_{n-2}(\Gamma) - \gamma V_{n-3}(\Gamma)) \\ & + \gamma(V'_{n-2}(\Gamma)\Gamma' - \gamma' V_{n-3}(\Gamma) - \gamma V'_{n-3}(\Gamma)\Gamma')], \end{aligned} \tag{216}$$

These expressions are hard to handle in general. We will use some examples to illustrate the general case.

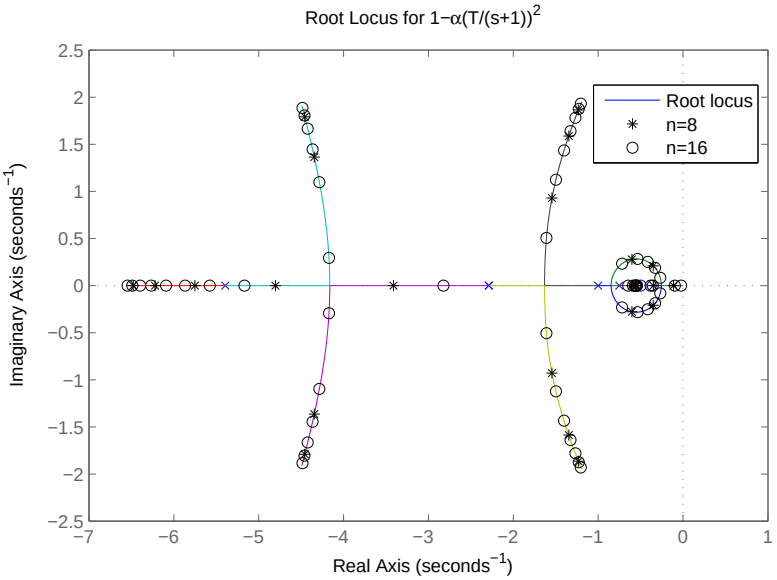

Figure 24: Root locus of $1 - \alpha \left(\frac{T}{s+1}\right)^2 = 0$.

5.5 NUMERICAL EXAMPLES

Now we present some simulations that illustrate the results of this chapter. We consider vehicle dynamics, local controllers and filters

$$H = \frac{1}{s(0.1s+1)}, \quad K = \frac{2s+1}{s(0.05s+1)}, \tag{217}$$

$$P = \frac{a}{bs+1}, \quad F = \frac{c}{ds+1}, \tag{218}$$

where $a, b, c, d \in \mathbb{R}$ are real parameters.

5.5.1 *Pole locations*

We consider different filters P and F in order to see their effect on the pole locations of the interconnection (defined by the set Λ_n in (175)).

Static gains: For this case we consider $a = c = 0.5$ and $b = d = 0$. Then Λ_n contains the points that solve

$$1 - \cos^2\left(\frac{m}{n-1}\pi\right) T^2 = 0, \quad m = 1, \ldots, \left\lfloor \frac{n-2}{2} \right\rfloor. \tag{219}$$

Figure 23 shows the root locus (generated using the function `rlocus` in Matlab®) for this equation when $\alpha \in (0, 1)$. It can be seen that the points of Λ_n will be contained in the open left half plane for every n.

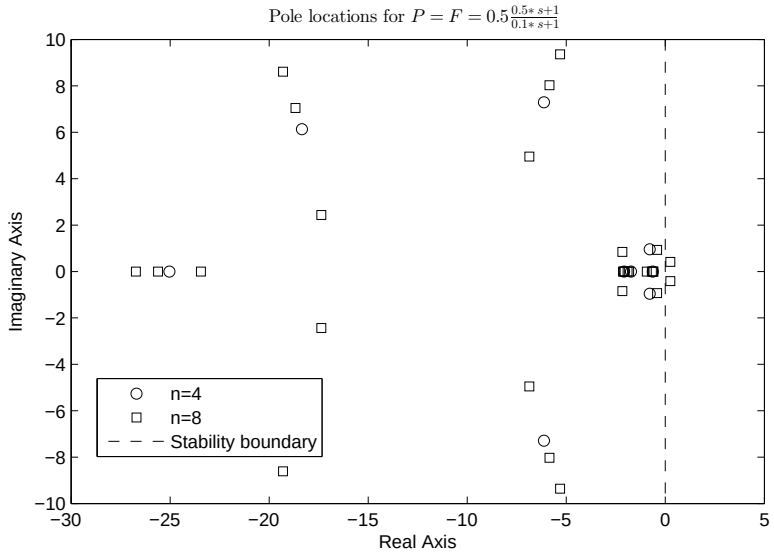

Figure 25: Λ_n for $F = P = \frac{0.5(0.5s+1)}{0.1s+1}$.

However, it can be noted that for this case, an increase of n implies that slow oscillatory modes will be present in the dynamics of the vehicles.

Symmetric dynamic gains: For this case we consider $a = c = 0.5$ and $b = d = 1$. The new Λ_n will be given by the solutions of

$$1 - \cos^2\left(\frac{m}{n-1}\pi\right)\left(\frac{T}{s+1}\right)^2 = 0, \quad m = 1, \ldots, \left\lfloor \frac{n-2}{2} \right\rfloor. \tag{220}$$

The new root locus and some pole locations for particular values of n can be seen in Figure 24. The addition of the poles at $s = -1$ in the filters F and B allows us to avoid the presence of slow oscillatory modes as the string size n increases. However, the least stable pole of the interconnection approaches $s = 0$ as n increases.

Although the use of dynamic P and F brings a certain benefit to the interconnection dynamics, a poor choice of them can produce instability. In particular, according to Proposition 5.1 we must have a gain margin of $-4PFT^2$ greater than 1 for stability, which has been the case so far. For the opposite case, for example, the selections $F = P = \frac{0.5(0.5s+1)}{0.1s+1}$, we have a gain margin for $-4PFT^2$ less than 1 and the interconnection becomes unstable for a certain number of vehicles. This can be seen in Figure 25. The points in Λ_4 are inside of the open left half plane. However, there are a few points in Λ_8 with positive real part.

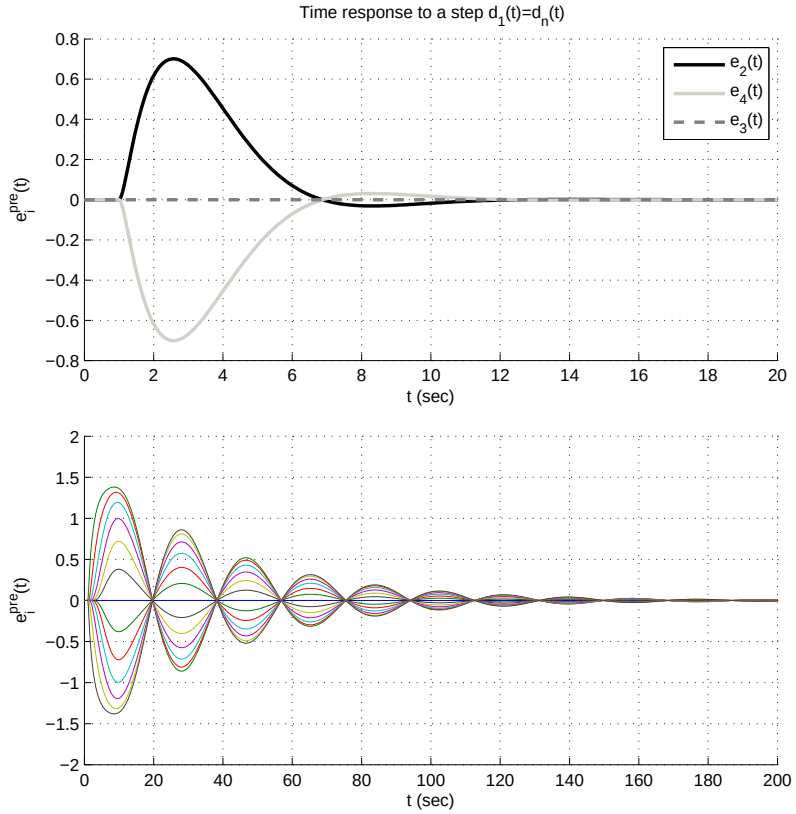

Figure 26: Time responses of the inter-vehicle spacings to a step in the front and rear vehicle. Symmetric static gains $P = F = 0.5$ for all s. Top: $n = 4$. Bottom: $n = 14$.

5.5.2 *Time response*

We consider a step disturbance at the front and rear vehicle, that is $d_1 = d_n = \mu(t-1)$. We also consider the vehicles to start from rest and at the desired formation. We will focus on the inter-vehicle spacings for different selections of the filters P and F.

Static gains: For $a = c = 0.5$ and $b = d = 0$ we have the time response of the interconnection for $n = 4$ and $n = 14$ in Figure 26. For $n = 4$ (Figure 26 top) we have that the second and third vehicle move with the same trajectory, which can be observed from $e_3^{pre}(t) = x_2(t) - x_3(t) = 0$. This was predicted by (209). For $n = 14$ (Figure 26 bottom), with the same design parameters, we have that the response becomes noticeable slower and oscillating, as predicted by Remark 5.3. Additionally, we can see that there is 0 DC gain independently of the string size, as predicted by Proposition 5.2.

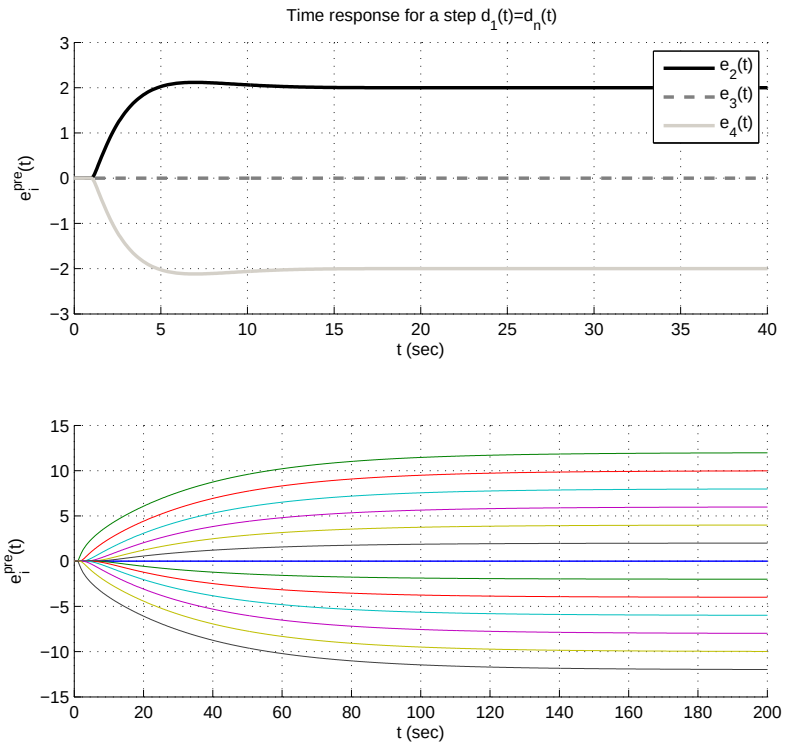

Figure 27: Time responses of the inter-vehicle spacings to a step in the front and rear vehicle. Symmetric dynamic gains $P = F = 0.5/(s+1)$. Top: $n = 4$. Bottom: $n = 14$.

Symmetric dynamic: Now we consider $a = c = 0.5$ and $b = d = 1$. Figure 27 shows the time response of the inter-vehicle spacings for $n = \{4, 14\}$. We can see that in this case the 0 DC gains are lost, as predicted by the derivations in Section 5.4.1.2. In particular, for 0 DC gains we must have $P'(0) = F'(0) = 0$, which is not the case for the current selections. Additionally, we can see that the inter-vehicle spacings grow with the string size which can be interpreted as string instability. This was predicted by (208).

Assymetric dynamic with 0 DC gain: Here we consider $P = 0.5$ and $F = 0.5T$. It is clear that $P'(0) = F'(0) = 0$. According to (213) and (214) this conditions are sufficient to have 0 DC gain. Figure 28 top confirms this for $n = 4$.

General assymetric dynamic: Here we select $P = 0.5/(s+1)$ and $F = 0.5T$. In this case $P'(0) \neq 0$. From our derivations at the end of Section 5.4.1.3 it was not clear whether the DC gain could be 0 in this case. Figure 28 bottom suggests that this is not the case.

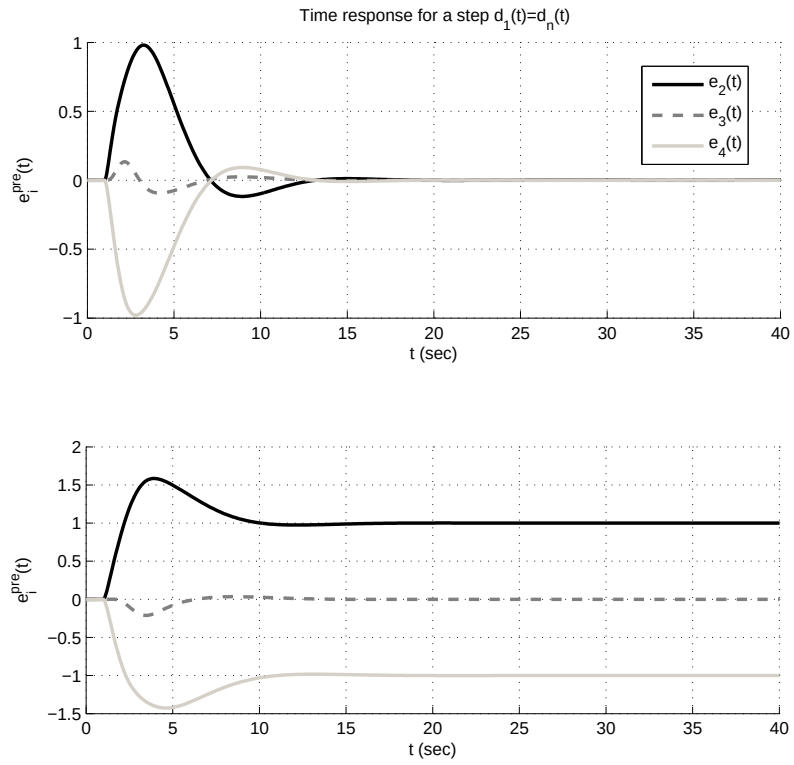

Figure 28: Time responses of the inter-vehicle spacings to a step in the front and rear vehicle for $n = 4$. Asymmetric dynamic gains. Top: $P = 0.5$ and $F = 0.5T$. Bottom: $P = 0.5/(s+1)$ and $F = 0.5T$..

5.6 CONCLUSION

In this chapter we provided closed form expressions in the frequency domain for the transfer functions from disturbances to positions in a bidirectional formation control scheme. We derived conditions on the design parameters (controllers and filters) that dictate the stability and presence of oscillations in the dynamics. These results extend on previous works that were obtained with the use of approximations and for specific choices of the vehicle model and controllers.

We also obtained expressions for the inter-vehicle spacings of the interconnection and derived conditions on the design parameters to have some desirable properties in the interconnection. We used some numerical examples to illustrate our results and highlight the properties of bidirectional architectures.

There are numerous ways in which this work can be extended. For example, the use of an independent leader that every follower can

track, while maintaining the bidirectional structure for the remaining vehicles. Also, to consider a last vehicle that tracks the position of its predecessor, instead of following the same trajectory as the front vehicle. Other lines of research include the use of cyclic bidirectional schemes, the effect of time delays and disturbances at any follower.

6

MISCELLANEOUS TOPICS

6.1 INTRODUCTION

In this chapter we present a miscellaneous collection of results related to formation control architectures. These results are either not fully developed yet or are complementary to those presented in the previous chapters of this thesis. In Section 6.2 we consider the dynamics of a two lane formation control architecture. In Section 6.3 we study a case of a leader following formation control architecture with non-homogeneous weights. In particular, we consider homogeneous vehicle and controller dynamics for every vehicle. However, the weights on the measurements that every controller uses to compute the control action vary along the string. Section 6.4 contains a discussion on the design of the controller pair K_p and K_v used in the implementation of a leader velocity tracking scheme (such as the one defined in Section 3.3 of Chapter 3). Section 6.5 contains some final remarks for this chapter.

6.2 FORMATION CONTROL FOR A 2-LANE PLATOON

We consider two parallel strings of cars travelling in a straight line, where each member has dynamics modelled by H and a local compensator given by K. As a first step in studying the behaviour of these vehicles we assume that every car that is not in the front of a string has access to the longitudinal position of the two vehicles that are immediately in front of it and the vehicle that is directly on its side (see Figure 29). The initial idea for a 2-lane formation control architecture is to extend a simple predecessor following scheme. For this we take a weighted average of the three available relative errors, that is the front, diagonal and side errors, as the input to a compensator K. In particular, let n be the number of cars per string and

$$\underline{X} = [X_1 \quad X_2 \quad \dots \quad X_{2n}], \tag{221}$$

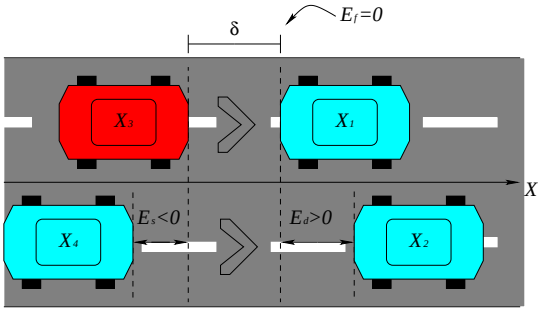

Figure 29: Example of relative errors measured by the red car X_3 for a desired spacing δ.

the vector with the positions of each car where X_1 and X_2 are the leaders and X_{2i-1} and X_{2i} are their $(i-1)$-th followers respectively for $i = 1, \dots, n$. Additionally let $\underline{D}(s)$ be the vector of input disturbances for each vehicle with the indexing used before. Then, assuming that every vehicle starts from rest and at the desired formation, the control signals are given by

$$U_i(s) = K(\eta_s E_i^{side} + \eta_d E_i^{diag} + \eta_f E_i^{fro}), \tag{222}$$

where U_i is the output of the compensator for the i-th vehicle, η_s, η_f and η_d are real numbers such that $\eta_s + \eta_f + \eta_d = 1$, and

$$E_i^{side} = \begin{cases} X_{i+1} - X_i, & \text{if } i \text{ is odd} \\ X_{i-1} - X_i, & \text{if } i \text{ is even} \end{cases} \tag{223}$$

$$E_i^{diag} = \begin{cases} X_{i-1} - X_i, & \text{if } i > 2 \text{ is odd} \\ X_{i-3} - X_i), & \text{if } i > 2 \text{ is even} \end{cases} \tag{224}$$

$$E_i^{fro} = X_{i-2} - X_i, \quad \text{for } i > 2, \tag{225}$$

are the relative side, diagonal and front errors respectively (see Figure 29 for an example of these errors for X_3) and the real numbers. Finally, the leader of each string has only access to the position of the car on its side, i.e. $U_i = KE_i^{side}$ for $i = 1, 2$.

Now, the interconnection described by (222) and the previous discussion yields the transfer function from $\underline{D}$ to $\underline{X}$:

$$\underline{X} = (\mathbf{I}_{2n,2n} - HK\mathbf{G})^{-1} H\underline{D}, \tag{226}$$

where $\mathbf{I}_{k,k}$ is the $k \times k$ identity matrix and $\mathbf{G}$ is the constant block matrix:

$$\mathbf{G} = \begin{bmatrix} \mathbf{G_l} & & & \\ \mathbf{G_f} & \mathbf{G_s} & & \\ \ddots & \ddots & & \\ & & \mathbf{G_f} & \mathbf{G_s} \end{bmatrix}, \quad \mathbf{G_l} = \begin{bmatrix} -1 & 1 \\ 1 & -1 \end{bmatrix},$$
$$\mathbf{G_f} = \begin{bmatrix} \eta_f & \eta_d \\ \eta_d & \eta_f \end{bmatrix}, \quad \mathbf{G_s} = \begin{bmatrix} -1 & \eta_s \\ \eta_s & -1 \end{bmatrix}. \tag{227}$$

If we define

$$\begin{aligned} \mathbf{A} &= (\mathbf{I}_{2,2} - HK\mathbf{G_l})^{-1}, \\ \mathbf{B} &= HK\mathbf{G_f}, \\ \mathbf{C} &= (\mathbf{I}_{2,2} - HK\mathbf{G_s})^{-1}, \end{aligned} \tag{228}$$

where $\mathbf{I}_{2,2}$ is the 2×2 identity matrix, then we have

$$\underline{X} = \begin{bmatrix} \mathbf{A}^{-1} & & & \\ -\mathbf{B} & \mathbf{C}^{-1} & & \\ \ddots & \ddots & & \\ & & -\mathbf{B} & \mathbf{C}^{-1} \end{bmatrix}^{-1} H\underline{D}, \tag{229}$$

and direct inversion gives us

$$\underline{X} = \begin{bmatrix} \mathbf{A} & 0_{2,2n-2} \\ \mathbf{\Phi A} & \mathbf{\Theta C} \end{bmatrix} H\underline{D}, \tag{230}$$

where $0_{2,2n-2}$ is the $2 \times 2n-2$ matrix of zeros,

$$\mathbf{\Phi} = \begin{bmatrix} \mathbf{CB} \\ \vdots \\ (\mathbf{CB})^{n-1} \end{bmatrix}, \tag{231}$$

and,

$$\boldsymbol{\Theta} = \begin{bmatrix} \mathbf{I}_{2,2} & & & \\ \mathbf{CB} & \ddots & & \\ \vdots & \ddots & \ddots & \\ (\mathbf{CB})^{n-2} & \dots & \mathbf{CB} & \mathbf{I}_{2,2} \end{bmatrix}. \tag{232}$$

We are interested in the spacing errors from one car to its in-lane predecessor, i.e. $E_k = X_{k-2} - X_k$ for $k = 3 \dots 2n$. Defining $\mathbf{T} = \mathbf{CB}$ and $\mathbf{S} = \mathbf{I}_{2,2} - \mathbf{CB}$, then these errors are given by

$$\begin{aligned} \begin{bmatrix} E_3 \\ \vdots \\ E_{2n} \end{bmatrix} &= \begin{bmatrix} \mathbf{I}_{2,2} & -\mathbf{I}_{2,2} & & \\ & \ddots & \ddots & \\ & & \mathbf{I}_{2,2} & -\mathbf{I}_{2,2} \end{bmatrix} \underline{X}, \\ &= \begin{bmatrix} \mathbf{SA} & -\mathbf{C} & & \\ \mathbf{TSA} & \mathbf{SC} & \ddots & \\ \vdots & \vdots & \ddots & \ddots \\ \mathbf{T}^{n-2}\mathbf{SA} & \mathbf{T}^{n-3}\mathbf{SC} & \dots & \mathbf{SC} & -\mathbf{C} \end{bmatrix} H\underline{D}. \end{aligned} \tag{233}$$

Moreover, we can rewrite $\mathbf{A}$ and $\mathbf{C}$ as

$$\mathbf{A} = \frac{1}{1+2KH}\left(\mathbf{I}_{2,2} + KH\begin{bmatrix} 1 & 1 \\ 1 & 1 \end{bmatrix}\right), \tag{234}$$

$$\mathbf{C} = \frac{1}{(1+KH)^2 - (\eta_s KH)^2}\left(\mathbf{I}_{2,2} + KH\begin{bmatrix} 1 & \eta_s \\ \eta_s & 1 \end{bmatrix}\right). \tag{235}$$

Disturbance propagation

Let's consider disturbances of the form $\underline{D} = d[\boldsymbol{v}_1^T \quad \dots \quad \boldsymbol{v}_n^T]^T$, where $d \in \mathbb{R}$ is a scalar disturbance and $\boldsymbol{v}_i \in \mathbb{R}^2$ for $i = 1, \dots n$. Then, the error dynamics are given by

$$\begin{bmatrix} E_3 \\ \vdots \\ E_{2n} \end{bmatrix} = \begin{bmatrix} \mathbf{I_2} \\ \mathbf{T} \\ \vdots \\ \mathbf{T}^{n-2} \end{bmatrix} \mathbf{S}\mathbf{A}dH\boldsymbol{v}_1 + \begin{bmatrix} -\mathbf{I_2} & & & \\ \mathbf{S} & -\mathbf{I_2} & & \\ \vdots & \ddots & \ddots & \\ \mathbf{T}^{n-3}\mathbf{S} & \dots & \mathbf{S} & -\mathbf{I_2} \end{bmatrix} \mathbf{C}dH \begin{bmatrix} \boldsymbol{v}_2 \\ \vdots \\ \boldsymbol{v}_n \end{bmatrix}. \tag{236}$$

Given the symmetry of the configuration we will be interested in only the response to the disturbances $z_a = [1 \quad 1]^T$ or $z_s = [1 \quad -1]^T$, since every $\boldsymbol{v}_i \in \mathbb{R}^2$ can be decomposed as a linear combination of these two vectors. By direct computation with $\mathbf{A}$, $\mathbf{B}$ and $\mathbf{C}$ defined in (228) we have that

$$\mathbf{A}z_s = z_s, \tag{237}$$

$$\mathbf{A}z_a = z_a \frac{1}{1 + 2KH}, \tag{238}$$

$$\mathbf{B}z_s = z_s KH(\eta_f + \eta_d), \tag{239}$$

$$\mathbf{B}z_a = z_a KH(\eta_f - \eta_d), \tag{240}$$

$$\mathbf{C}z_s = z_s \frac{1}{1 + (1 - \eta_s)KH}, \tag{241}$$

$$\mathbf{C}z_a = z_a \frac{1}{1 + (1 + \eta_s)KH}, \tag{242}$$

and for simplicity, we define the transfer functions T_{sy}, T_{as}, S_{sy} and S_{as} such that

$$T_{sy} z_s = \mathbf{T} z_s = \frac{(\eta_f + \eta_d)KH}{1 + (1 - \eta_s)KH} z_s, \tag{243}$$

$$T_{as} z_a = \mathbf{T} z_a = \frac{(\eta_f - \eta_d)KH}{1 + (1 + \eta_s)KH} z_a, \tag{244}$$

$$S_{sy} z_s = \mathbf{S} z_s = \left(1 - T_{sy}\right) z_s, \tag{245}$$

$$S_{as} z_a = \mathbf{S} z_a = \left(1 - T_{as}\right) z_a. \tag{246}$$

As every $\nu_i \in \mathbb{R}^2$ satisfies $\nu_i = a_i z_s + b_i z_a$, with $\xi_i = \begin{bmatrix} a_i & b_i \end{bmatrix} \in \mathbb{R}^2$, we can decompose the dynamics of the disturbance as

$$\begin{bmatrix} E_3 \\ \vdots \\ E_{2n} \end{bmatrix} = \begin{bmatrix} 1 \\ T_{sy} \\ \vdots \\ T_{sy}^{n-2} \end{bmatrix} S_{sy} dH z_s a_1 + \begin{bmatrix} 1 \\ T_{as} \\ \vdots \\ T_{as}^{n-2} \end{bmatrix} \frac{S_{as} dH z_a}{1 + 2KH} b_1 +$$

$$\begin{bmatrix} -1 & & & \\ S_{sy} & -1 & & \\ \vdots & \ddots & \ddots & \\ T_{sy}^{n-3} S_{sy} & \dots & S_{sy} & -1 \end{bmatrix} \frac{dH z_s}{1 + (1 - \eta_s)KH} \begin{bmatrix} a_2 \\ \vdots \\ a_n \end{bmatrix} +$$

$$\begin{bmatrix} -1 & & & \\ S_{as} & -1 & & \\ \vdots & \ddots & \ddots & \\ T_{as}^{n-3} S_{as} & \dots & S_{as} & -1 \end{bmatrix} \frac{dH z_a}{1 + (1 + \eta_s)KH} \begin{bmatrix} b_2 \\ \vdots \\ b_n \end{bmatrix}. \tag{247}$$

Now, it remains to analyse the behaviour of the sensitivity functions that are the elements of the matrices obtained above. For some values of the parameters η_s, η_f, η_d we can apply the results of (Seiler et al., 2004) in a direct fashion, that is, the interconnection will be string unstable if either $\|T_{sy}\|_\infty$ or $\|T_{as}\|_\infty$ is greater than 1. Moreover, if as usual the pair HK has two integrators, $T_{sy}(0) = 1$ for any choice of the other parameters and $\|T_{sy}\|_\infty > 1$. Unfortunately, under these considerations, there is not much incentive to use this interconnection. However it should be possible to add common methods to solve the

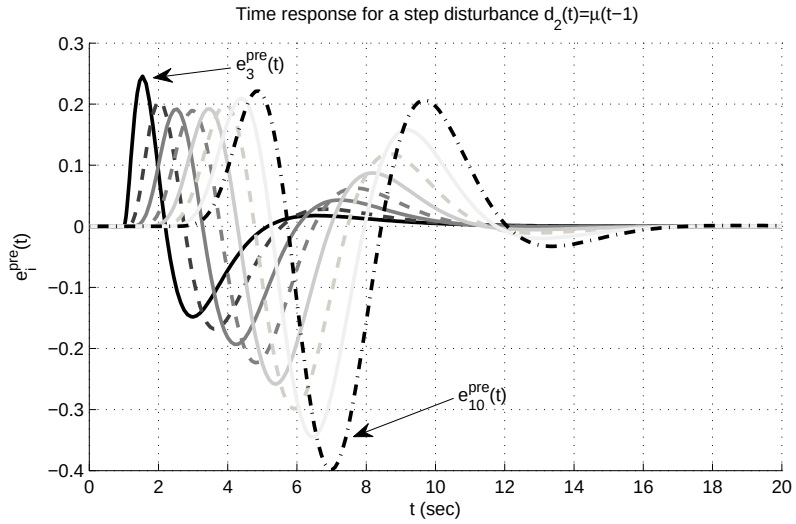

Figure 30: Time response of the inter-vehicle spacings (front) for a single lane platoon with a step disturbance $d_2(t) = \mu(t-1)$.

string instability issue (leader information and or use of a constant time-headway spacing policy). A possible benefit of the use of two lanes is that an asymmetric disturbance (for example one that only affects a single vehicle) could have a smaller effect along the string in comparison with a single lane platoon affected by the same disturbance.

Example

We consider a single and 2-lane platoon with identical vehicles and local controllers

$$H = \frac{1}{s(0.1s+1)}, \quad K = \frac{2s+1}{s(0.05s+1)}, \tag{248}$$

such that the single lane uses a predecessor follower scheme (no leader state broadcast). We want to compare the inter-vehicle spacing errors for the last member(s) of the platoon when the number of vehicles in both cases is 10. For the 2-lane platoon this means two lanes with 5 vehicles each. We consider a single step disturbance at the second member of the string in the single lane platoon and in the third member (second of the first lane) for the 2-lane platoon. Figure 30 shows the transient response for a step disturbance at the second member of the single lane platoon $d_2(t) = \mu(t-1)$. As we

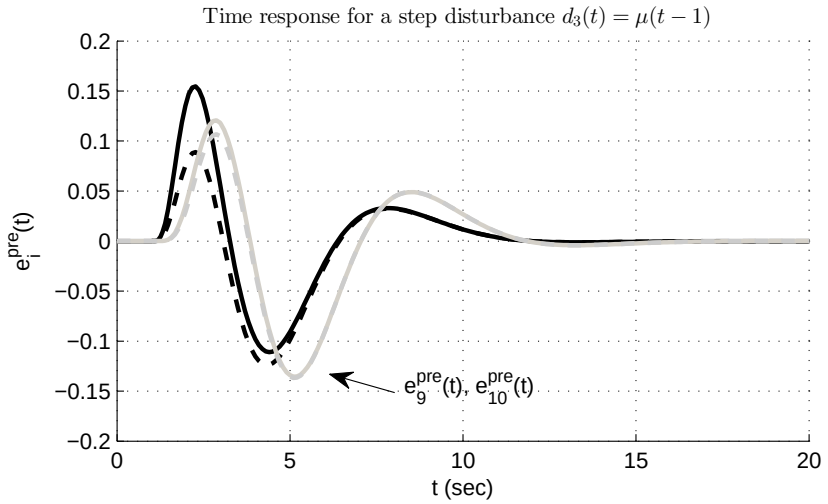

Figure 31: Time response of the inter-vehicle spacings (front) for a 2-lane platoon with a step disturbance $d_3(t) = \mu(t-1)$.

know from results in (Seiler et al., 2004) this interconnection is string unstable for any selection of the design parameters. In particular, the inter-vehicle spacing at the 10-th member of the string has a negative peak of approximately -0.4 units. In comparison, for a 2-lane platoon with parameters $\eta_f = 0.5$, $eta_d = 0.25$ and $eta_s = 0.25$, we have the time response for a step disturbance at the vehicle with index $i = 3$, $d_3(t) = \mu(t-1)$ (which corresponds to the first follower of the first left leader, the red car in Figure 29) shown in Figure 31. The two grey lines correspond to the transients for the inter-vehicle spacings of the last two members of the 2-lane platoon and none of them goes below -0.15 units. However, this transients are larger than the transients for the two vehicles immediately in front of them. As noted before, this interconnection is string stable unless other design choices are made. This comparison can be made in the frequency domain by further studying the expressions obtained in this section.

6.3 LEADER FOLLOWING WITH NON-HOMOGENEOUS WEIGHTS

We consider a single string of n cars with the vehicle models, controllers and notations from Chapter 3. We also assume that the vehicles start at rest and in the desired formation. If we define the control action

$$U_i = K(\eta_i E_i^{pre} + (1-\eta_i)E_i^{lea}), \tag{249}$$

where U_i is the output of the compensator of the i-th car, $E_i^{pre} = X_{i-1} - X_i$ and $E_i^{lea} = X_1 - X_i$ are its relative front and leader errors respectively and η_i are stable transfer functions for $i = 3 \dots N$. For $i = 2$ we have $U_2 = KE_2^{pre}$. Then, the interconnection described by (249) and the previous discussion yield the transfer function from $\underline{D}$ to $\underline{X}$:

$$\underline{X} = (\mathbf{I} - HK\mathbf{G})^{-1} H\underline{D}, \tag{250}$$

where $\mathbf{I}$ is the $n \times n$ identity matrix and $\mathbf{G}$ is the constant matrix:

$$\mathbf{G} = \begin{bmatrix} 0 & & & & \\ 1 & -1 & & & \\ 1-\eta_3 & \eta_3 & -1 & & \\ \vdots & & \ddots & \ddots & \\ 1-\eta_N & & \dots & \eta_N & -1 \end{bmatrix}. \tag{251}$$

The main difference with the derivations in Chapter 3 come from the second diagonal of $\mathbf{G}$. That particular case was similar to having $\eta_i = \eta$ for all $i \geqslant 3$.

If we define as usual $T = HK(1 + HK)^{-1}$, and $S = 1 - T$, we have

$$\underline{X} = \begin{bmatrix} S & & & & \\ -T & 1 & & & \\ (\eta_3 - 1)T & -\eta_3 T & 1 & & \\ \vdots & & \ddots & \ddots & \\ (\eta_N - 1)T & & & -\eta_N T & 1 \end{bmatrix}^{-1} S^{-1} H\underline{D}. \tag{252}$$

Since the matrix to be inverted is lower triangular, we can easily express the dynamics of the vehicle positions. In the following we will

focus on the effect of the disturbance on the first vehicle D_1 and assume that for all $i > 1$, $D_i = 0$ for all s. Then, we have that

$$\underline{X} = \begin{bmatrix} 1 \\ T \\ \tilde{T}_3 \\ \tilde{T}_4 \\ \vdots \\ \tilde{T}_N \end{bmatrix} HD_1, \tag{253}$$

where

$$\tilde{T}_k = T - \sum_{i=3}^{k} \left(T^{k-i+1} S \prod_{j=i}^{k} \eta_j \right), \tag{254}$$

for $k = 3, \ldots, N$.

Now, we are interested in the spacing errors from one car to its immediate predecessor, i.e. $E_k^{pre} = X_{k-1} - X_k$ for $k = 2, \ldots, N$. Then these errors are given by

$$\begin{bmatrix} E_2^{pre} \\ \vdots \\ E_N^{pre} \end{bmatrix} = \begin{bmatrix} 1 & -1 & & \\ & \ddots & \ddots & \\ & & 1 & -1 \end{bmatrix} \underline{X} = \begin{bmatrix} S \\ T - \tilde{T}_3 \\ \tilde{T}_3 - \tilde{T}_4 \\ \vdots \\ \tilde{T}_{N-1} - \tilde{T}_N \end{bmatrix} HD_1. \tag{255}$$

We can rewrite the right hand side as

$$\begin{bmatrix} S \\ T - \tilde{T}_3 \\ \tilde{T}_3 - \tilde{T}_4 \\ \vdots \\ \tilde{T}_{N-1} - \tilde{T}_N \end{bmatrix} HD_1 = \begin{bmatrix} 1 \\ \mathcal{T}_3 \\ \vdots \\ \mathcal{T}_N \end{bmatrix} SHD_1, \tag{256}$$

where $\mathcal{T}_k$ satisfies

$$\mathcal{T}_k = \eta_k T + (\eta_k T - 1) \sum_{i=3}^{k-1} \left(T^{k-i} \prod_{j=i}^{k-1} \eta_j \right), \tag{257}$$

for $k = 3, \ldots, N-1$, with $\mathcal{T}_3 = \eta_3 T$. If $\eta_3 = \eta_4 = \ldots = \eta_N = \tilde{\eta}$, then $\mathcal{T}_k = (\tilde{\eta}T)^{k-1}$. This is in agreement with results presented in (Seiler et al., 2004).

Now, we study a possible selection for the sequence $\{\eta_k\}$. From a practical point of view (for example optimization of fuel consumption as mentioned in Chapter 1 and (Bonnet and Fritz, 2000)) it would be ideal to have $E_i^{pre} = 0$ for all s and all $i \geqslant 2$. However, $E_2^{pre} = SHD_1$ and $E_3^{pre} = \eta_3 TSHD_1$ for any possible selection of η_k or controller. Regardless, for $i = 4$ we have

$$\mathcal{T}_4 = \eta_4 T + (\eta_4 T - 1)T\eta_3, \tag{258}$$

and solving $\mathcal{T}_4 = 0$ yields

$$\eta_4 = \frac{\eta_3}{1 + \eta_3 T}. \tag{259}$$

For $i = 5$ we have

$$\begin{aligned}\mathcal{T}_5 =& \eta_5 T + (\eta_5 T - 1)(\eta_3 \eta_4 T^2 + \eta_4 T),\\ =& \eta_5 T + (\eta_5 T - 1)\eta_4 T(1 + \eta_3 T),\end{aligned} \tag{260}$$

and using η_4 obtained in (259) we have

$$\mathcal{T}_5 = \eta_5 T + (\eta_5 T - 1)\eta_3 T. \tag{261}$$

Solving $\mathcal{T}_5 = 0$ now yields

$$\eta_5 = \frac{\eta_3}{1 + \eta_3 T}. \tag{262}$$

It is straightforward to compute that for a fixed η_3, the selection

$$\eta_k = \frac{\eta_3}{1 + \eta_3 T}, \quad k \geqslant 4 \tag{263}$$

yields $\mathcal{T}_k = 0$ for all s. For movements of the leader, this selection allows a response of the vehicle platoon that resembles the movement of a train (with the exception of the first two followers). It must be noted that the selection of η_3 can be any stable transfer function and it must be selected in order that $\eta_3/(1 + \eta_3 T)$ is also stable.

The selection of the sequence $\{\eta_k\}$ was made with the aim of obtaining $E_k^{pre} = 0$ for all s whenever possible for disturbances (or move-

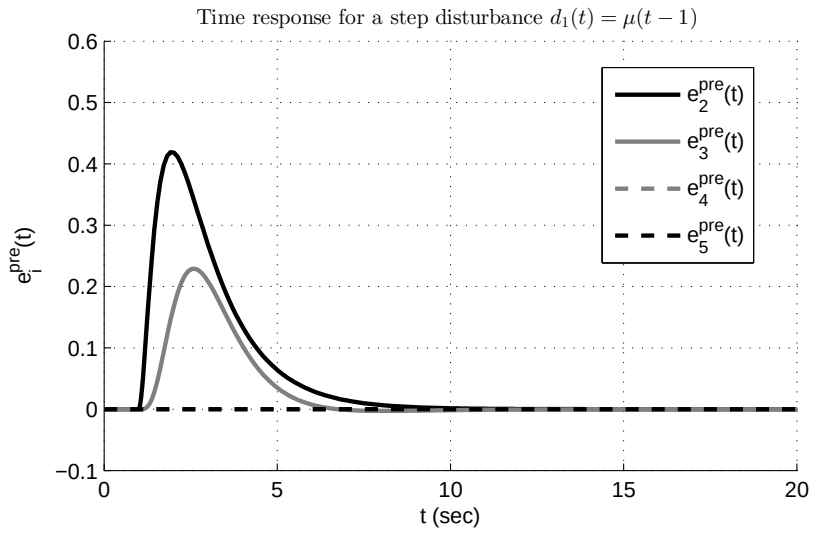

Figure 32: Time response of the inter-vehicle spacings with a step disturbance at the leader $d_1(t) = \mu(t-1)$ for a platoon with non-homogeneous weights η_k.

ment) at the leader. These selections may not provide a satisfactory response of the vehicle string for disturbances at the followers.

Example

We use the same vehicle model and controller as before. Additionally we set $\eta_3 = 0.5$ and consequently

$$\eta_k = \frac{1}{2+T}, \quad k > 3 \tag{264}$$

which is stable for the particular selection of K and H. For a step input to the lead vehicle, $d_1(t) = \mu(t-1)$ we obtain the transient response shown in Figure 32. All the inter-vehicle spacings $e_i^{pre}(t)$ are 0 for $i > 3$ as desired and imposed in the derivation of the sequence η_k.

As dealing with the expressions for the response of the platoon for disturbances to the followers requires more derivations, we will illustrate this case with a simulation. In Figure 33 we can see the time response of the platoon to a disturbance at the second vehicle $d_2(t) = \mu(t-1)$. The inter-vehicle spacings along the string have magnitude peaks that are smaller than the peak for $e_2^{pre}(t)$. This suggests that the sequences of transfer functions from disturbances at the followers to other followers are string stable. A future extension is then

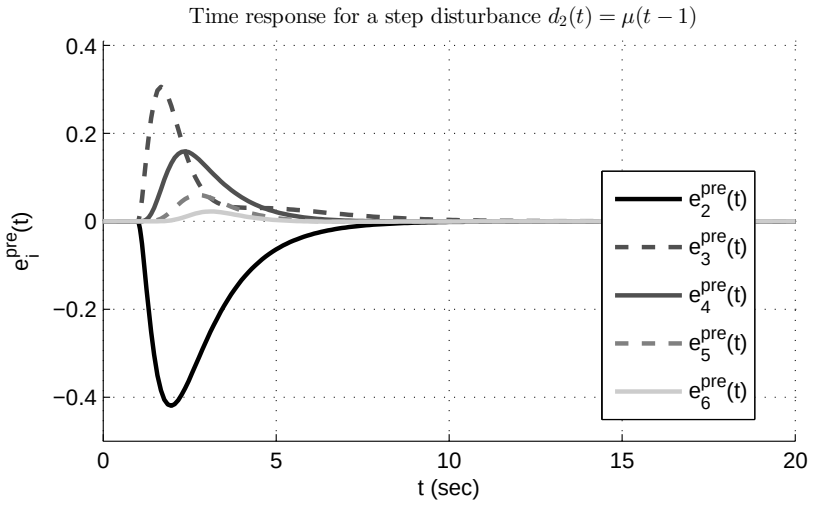

Figure 33: Time response of the inter-vehicle spacings with a step disturbance at the second member $d_2(t) = \mu(t-1)$ for a platoon with non-homogeneous weights η_k.

to compute such sequences for arbitrary parameter values, and find the conditions for string stability.

6.4 CONTROLLER STRUCTURE FOR LEADER VELOCITY TRACKING SCHEME

In this section we aim to obtain some preliminary insight on how to select (design) the controllers for the leader velocity tracking scheme K_p and K_v defined in (19) on Chapter 3. The goal of these selections is to achieve string stability in the interconnection.

First, we study some properties of PT, where

$$P = \frac{K_p}{K_p + sK_v} \tag{265}$$

is real rational, stable and $P(0) = T(0) = 1$. According to Lemma 3.1 PT satisfies

$$\int_0^\infty \ln|P(j\omega)T(j\omega)|\frac{d\omega}{\omega^2} \geqslant \frac{\pi}{2}\frac{d}{ds}(PT)\Big|_{s=0}. \tag{266}$$

Since we must have two integrators in the product KH (controller-car model), $T'(0) = 0$, which yields

$$\int_0^\infty \ln|P(j\omega)T(j\omega)|\frac{d\omega}{\omega^2} \geqslant \frac{\pi}{2}P'(0). \tag{267}$$

A necessary condition for string stability, according to Theorem 3.2, is then given by $P'(0) < 0$, since otherwise this would imply that $\|PT\|_\infty > 1$. The transfer function P is defined in terms of K_p and K_v. Therefore, the discussion should focus on the design of K_p and K_v to achieve the condition $P'(0) < 0$, string stability, and stability of the interconnection.

6.4.1 *Integral action on the controller*

In general situations, it is required that the controller for each vehicle has an integrator. We consider the controller architecture given by

$$U_i = K_p(X_{i-1} - X_i) + sK_v(X_1 - X_i), \tag{268}$$

for $i > 2$. An equivalent controller is defined by $K = K_p + sK_v$ and this controller must stabilize the vehicle model in closed loop and must have a pole at $s = 0$. First, to obtain the pole at $s = 0$ we might choose to add a pole at $s = 0$ in K_p, K_v or both. Now, we will show that a sole integrator in K_p will yield string instability regardless of the resulting K. In particular, if $K_p = \tilde{K}_p/s$, where $\tilde{K}_p(0) = k_p$, $k_p \in \mathbb{R} - \{0\}$, then

$$\frac{d}{ds}P = \frac{-2sK_v}{\tilde{K}_p + s^2K_v} - s^2\frac{d}{ds}\left(\frac{K_v}{\tilde{K}_p + s^2K_v}\right). \tag{269}$$

Since $K_v(0) < \infty$, we have that $P'(0) = 0$, which in turn implies that $\|PT\|_\infty > 1$. On the other hand, a sole integrator in K_v would yield an equivalent controller that does not have infinite gain at $\omega = 0$. If we include a pole at $s = 0$ in both K_p and K_v we have that

$$P'(0) = -\frac{\tilde{K}_v(0)}{\tilde{K}_p(0)}. \tag{270}$$

We must have $\tilde{K}_v(0)/\tilde{K}_p(0) > 0$ in order to satisfy the condition for string stability $P'(0) < 0$.

6.4.2 *Controller implementation*

Since we have two degrees of freedom in K_p and K_v we have a broad set of possible selections for these controllers given a K designed to

achieve a stable closed loop in each vehicle. For instance we can take two PI controllers

$$K_p = k_p \frac{\tau_p s + 1}{s}, \tag{271}$$

$$K_v = k_v \frac{\tau_v s + 1}{s}, \tag{272}$$

$$P'(0) = -\frac{k_v}{k_p} \tag{273}$$

which together yield the equivalent controller

$$K = \frac{1}{s}(k_p + s(k_v \tau_v s + k_p \tau_p + k_v)). \tag{274}$$

We can obtain the same equivalent controller with the selections

$$K_p = \frac{k_p}{s}, \tag{275}$$

$$K_v = \frac{k_v \tau_v s + k_p \tau_p + k_v}{s}, \tag{276}$$

$$P'(0) = -\frac{k_v + k_p \tau_p}{k_p}. \tag{277}$$

One difference resides on the resulting filter P. From the string stability point of view, the second implementation is a more sensible choice. This can be seen intuitively from the Bode integral and more clearly if we look at the resulting expression

$$P = \frac{k_p}{k_p + s(k_v \tau_v s + k_p \tau_p + k_v)}. \tag{278}$$

6.4.3 *Controller design example*

A priori, a reasonable design choice for the controller is for it to yield real closed loop poles, avoiding resonating complex pairs. Considering the simple vehicle model

$$H = \frac{1}{s(\tau s + 1)}, \tag{279}$$

where $\tau > 0$ and a PID equivalent controller

$$K = \alpha \frac{s^2 + \beta s + \gamma}{s}, \tag{280}$$

with $\alpha, \beta, \gamma \in \mathbb{R}$, yields the complementary sensitivity function

$$T = \frac{\alpha(s^2 + \beta s + \gamma)}{s^2(\tau s + 1) + \alpha(s^2 + \beta s + \gamma)}. \tag{281}$$

The three parameters α, β and γ allow us to freely place the closed loop poles. In particular we can choose

$$K_p = \frac{\alpha\gamma}{s}, \tag{282}$$

$$K_v = \frac{\alpha s + \alpha\beta}{s}, \tag{283}$$

which yields

$$P = \frac{\alpha\gamma}{\alpha(s^2 + \beta s + \gamma)}. \tag{284}$$

Now, we have that

$$PT = \frac{\alpha\gamma}{s^2(\tau s + 1) + \alpha(s^2 + \beta s + \gamma)}. \tag{285}$$

For simplicity we cancel the vehicle stable pole by choosing $K = k_k(\tau_k s + 1)(\tau s + 1)/s$. By setting

$$K_p = \frac{k_k}{s}, \quad K_v = k_k \frac{\tau\tau_k s + \tau + \tau_k}{s}, \tag{286}$$

we obtain

$$PT = \frac{k_k}{(\tau s + 1)(s^2 + k_k\tau_k s + k_k)}. \tag{287}$$

As it was expected $P(0)T(0) = 1$ independently of the parameter selection. There are some easy selections to satisfy the necessary condition for string stability $\|PT\|_\infty \leqslant 1$, such as forcing real closed loop poles (or at most highly damped complex pairs).

Example

For our normal vehicle and controller models

$$H = \frac{1}{s(0.1s + 1)}, \quad K = \frac{2s + 1}{s(0.05s + 1)}, \tag{288}$$

we have in the examples from Chapter 3 that a possible selection for K_p and K_v such that $K = K_p + sK_v$ is

$$K_p = \frac{1}{s(0.05s+1)}, \quad K_v = \frac{2}{s(0.05s+1)}, \tag{289}$$

which together yield

$$P = \frac{K_p}{K_p + sK_v} = \frac{1}{2s+1}. \tag{290}$$

Here, it is interesting to note that PT in this case is

$$PT = \frac{1}{2s+1}T, \tag{291}$$

and according to the result for minimum time-headway h_0 for string stability from (Klinge and Middleton, 2009) and in Proposition 4.1 from Chapter 4 $h_0 = \sqrt{2}$ for this T. Then $|PT| < 1$ for all $\omega > 0$. Therefore, a possible way to find K_p and K_v is to choose K that stabilizes H in closed loop and then select $P = 1/(1+hs)$ with $h > h_0$ (which ensures $P'(0) = -h < 0$). This yields

$$P = \frac{1}{1+hs} = \frac{K_p}{K_p + sK_v} \Rightarrow K_p + sK_v = K_p + shK_p, \tag{292}$$

and we have $K_v = hK_p$. Moreover $K = K_p + sK_v = K_p(1+sh)$, which ensures that for every proper and well designed K, there always exists K_p strictly proper that ensures the string stability of the leader velocity tracking architecture. If it is possible to find strictly proper K_p and K_v satisfying the same is an open question.

6.5 CONCLUSION

In this chapter we presented three topics related to formation control architectures. The results and considerations are likely to be the starting point for new lines of work.

For a 2-lane immediate predecessor following formation control architecture we obtained expressions for the resulting dynamics of the inter-vehicle spacings. These expressions are decomposed in a way that it is possible to analyse the effect of symmetrical and asymmetrical disturbances in the two leaders of the 2-lane platoon. Although the behaviour of this 2-lane formation is similar to a single lane one,

the expressions obtained suggest that there are certain benefits in the disturbance compensation. It would be of interest to study extensions that consider the mitigation of string instability (such as leader state broadcast and/or use of constant time-headway policies).

For a single lane leader following scheme with non-homogeneous weights we obtained expressions for the dynamics of the vehicles. Moreover, we obtained a sequence of weights that achieve a train-like behaviour of the string as a response to disturbances or movement of the lead vehicle. An immediate extension of this is to study the response of the system to disturbances at any follower.

Finally, we presented a discussion on the design process for the controllers used to implement the leader velocity tracking architecture presented in Chapter 3.

7

CONCLUSIONS AND FUTURE LINES OF WORK

The work presented in this thesis includes several theoretical results concerning formation control architectures for platooning. We have provided stability and string stability results for three important topologies: leader unidirectional, cyclic unidirectional and bidirectional. The importance of these strategies comes from the simplicity of their definitions and their effectiveness in achieving the platooning goal of coordinated movement of the vehicle string.

Although we have extended recent known results for these architectures we also provided novel results concerning the dynamical properties of the platoons. These technical results consider design aspects such as spacing policies, coordination requirements and communication issues (time delays), highlighting how the stability properties are affected by them.

In particular we have established that for unidirectional leader following architectures, the exclusive use of the leader velocity as the state to be broadcast to the followers provides string stability under reduced coordination requirements if certain conditions on the design parameters are satisfied. Followers do not need to know the number of vehicles in the string nor the sizes of the inter-vehicle spacings that every other follower keeps with their immediate predecessors. In a practical implementation this fact would allow new vehicles to merge with the platoon in a simple fashion, measuring the distance to the last vehicle and listening to the leader's velocity broadcast. Moreover, the string stability property achieved with the leader velocity tracking strategy is robust to the presence of certain time delays in the communication. We have explicitly shown that a time delay of the velocity reception that is linearly proportional to the followers position (i. e. the time delay is $k\tau$ with $\tau > 0$ and k is the position along the string of the vehicle) does not affect the string stability of the inter-vehicle spacing transfer functions. Additionally, we studied an alternative communication scheme for the leader state. This was considered as a solution to the problem in a leader position tracking scheme where every follower needed to know the number of vehicles ahead and

Chapter 3

their desired inter-vehicle spacings. Although the strategy was an effective way to solve this problem, it failed to provide string stability when time delays were present in the broadcast for any selection of the design parameters. This conclusion gives more value to the strategy of using only the leader velocity to obtain string stability. Finally, we recall that these results give conditions on the design parameters for achieving string stable interconnections. A heuristic discussion on the existence of transfer functions that satisfy the conditions was given in Chapter 6 in which partial solutions and avenues for further research were highlighted. Simple cases for the vehicle model and numerical examples suggest that it is always possible to find controllers to achieve the condition. An immediate extension of this work is to obtain theoretical results that ensure the existence of such controllers. A further extension based on the previous one is to develop design techniques in order to optimize the performance of the vehicle platoon, while maintaining the string stability properties and robustness to time delays.

Chapter 4

For a leaderless cyclic interconnection we have shown, echoing results from Fax and Murray (2004), that instability of the interconnected system will occur when the string size surpasses a critical number. This result considers a constant spacing policy and almost general vehicle and controller models (HK has two poles at $s = 0$), extending known results for constant controller gains where instability was not an issue (Rogge and Aeyels (2008)). Moreover, by modifying the spacing policy to be of the constant time-headway kind, we obtained stability and string stability results tied to the value of the time-headway parameter h. In particular, if $h > h_0$ where h_0 is a critical time-headway value (Klinge and Middleton (2009)) depending on the design parameters, the cyclic interconnection is string stable and stable for any string size n. Finally, in an effort to combine the knowledge from leader following strategies, we studied the effect of adding an independent leader which broadcasts its state to every member of the cyclic platoon. We concluded that stability and string stability are achievable with a constant spacing policy, provided that the design parameters satisfy simple conditions. A straightforward extension of these results is to consider the presence of time delays in the leader broadcast in a similar fashion to the work described in Chapter 3.

Chapter 5

The final main contribution of this work considered the study of a bidirectional strategy. The motivation for this comes from results that

utilize approximations to study the behaviour of the least stable pole of a bidirectional interconnection (Barooah and Hespanha (2005)). Moreover, a bidirectional strategy, where vehicles use front and back measurements for their control, provides compensation to all vehicles for disturbances at any vehicle, unlike unidirectional strategies. With this in mind, we used a direct method to compute the dynamics of the vehicles in the case where the first and last vehicles follow the same trajectory independently of the other string members. We obtained closed form expressions for the transfer functions from disturbances to vehicle positions, and consequently also from disturbances to inter-vehicle spacings. Although the expressions obtained are slightly harder to study than in unidirectional cases, they allow the study of the location of the interconnection poles in a straightforward manner. Standard control design tools such as root locus plots and stability margins can be applied to the key design parameters of the interconnection. Additionally we obtained results that echo the ones reported with the use of approximations, namely, that in the case of static symmetric weights for the bidirectional measurements, the least stable pole approaches the origin of the complex plane as the size of the vehicle string increases. We extended this result including a simple analysis of the trajectory in the complex plane that the least stable pole(s) take when the size of the string increases. It can be concluded that slow oscillatory modes will be dominant in the transient response of the interconnection.

The expressions obtained in this case considered general stable filters for the local measurements of the inter-vehicle spacings at every vehicle. These filters allow for modifying the stability margins and the dominant dynamics of the transfer functions that describe the interconnection. Numerical examples show some of the flexibilities of the proposed architecture and suggest some of the future directions for this line of work. Moreover, it is of great interest to obtain general string stability results for this case, specifically, considering techniques that are successful in other topologies such as leader state broadcast or the use of constant time-headway spacing policies. A more straightforward extension considers the use of a vehicle in the last position of the string that follows the trajectory of its predecessor. This adds more complexity to the resulting closed form expressions for the dynamics, but is a more realistic assumption.

Most of the results presented in this thesis may be extended for very small changes on the topology or the design parameters (vehicle models, controllers, spacing policy, combined topologies such as cyclic-bidirectional, etc.). We note that the first important step to obtain our results was to compute

$$\underline{\tilde{X}} = (\mathbf{I} - H K \mathbf{G})^{-1} H \underline{D}, \tag{293}$$

where $\mathbf{G}$ is a $n \times n$ matrix, describing most of the characteristics of the interconnection to be studied (and possible sensor or communication disruption between the vehicles). In particular, we obtained conditions on the design parameters which give a boundedness property to a sequence of transfer functions that arise from the matrix $(\mathbf{I} - H K \mathbf{G})^{-1} H$ as the string size grows. The inverse $(\mathbf{I} - H K \mathbf{G})^{-1}$ is not straightforward to obtain in some cases, as seen for example in the bidirectional case. However, perturbations of a well studied $\mathbf{G}$ matrix allow us to consider many other interconnections. For instance, given a $\mathbf{G} \in \mathbb{C}^{n \times n}$ that yields a stable and string stable interconnection, what are the conditions on $\mathcal{G} \in \mathbb{C}^{n \times n}$ such that $\mathbf{G}\mathcal{G}$ or $\mathbf{G} + \mathcal{G}$ maintain the stability and string stability?. Similar lines of work could include the study of model uncertainty in the vehicle, actuators or sensors.

We finalise with an observation on the applicability of the results. The main motivation of this work comes from vehicular platooning problems. However, the results obtained are general enough to consider interconnections of dynamical systems other than vehicles. As noted in the literature review, multi-agent systems have been widely studied and are the focus of ongoing research in different fields. Our derivations could be of use in such efforts.

A

APPENDIX

A.1 PROOF OF THEOREM 3.3

1) The proof is similar to part 1) of Theorems 3.1 and 3.2. The evaluation of the transfer functions at $s = 0$ is straightforward.

2) For dynamic P, such that $P(0) = 1$ we can rewrite (61) as

$$\begin{aligned} F_{n,1} = \big[&H(1-P)(PT)^{n-n_r-1}T + (PT)^{n-2}HS \\ &- e^{-\tau s}H(1-P)(PT)^{n-n_r-1}T\big]. \end{aligned} \tag{294}$$

We have that SH and $H(1-P)$ are bounded at $s = 0$ since the integrator of H is canceled by the zero at $s = 0$ of S and $(1-P)$ respectively. Now, Proposition 3.1 can be applied to every term of (294) and $\{F_{n,1}\}$ is string stable.

For $P = \eta \in (0,1)$, we can once again rewrite $F_{n,1}$

$$F_{n,1} = \left[(\eta T)^{n-2}HS + (1-e^{-\tau s})H\frac{(1-\eta)}{\eta}(\eta T)^{n-n_r}\right]. \tag{295}$$

The limit

$$\lim_{s\to 0}(1-e^{-\tau s})H = \lim_{s\to 0}\frac{(1-e^{-\tau s})}{s}\tilde{H} = \tilde{H}(0)\tau, \tag{296}$$

shows that $\|(1-e^{-\tau s})H\|_\infty$ is well defined and depends on the value of τ. Proposition 3.1 can now be applied since $\|\eta T\|_\infty \leqslant 1$ and $\|SH\|_\infty$ and $\|(1-e^{-\tau s})H(1-\eta)/\eta\|_\infty$ are well defined. Thus the sequence $\{F_{n,1}\}$ is string stable when $P = \eta \in (0,1)$.

3) For the leader error transfer function $\mathcal{F}_{n,1}$ we focus our attention on the second term of (63), noting that the first is exactly $\mathcal{F}_{n,1}$ of the perfect communication case in (58). Since we assume that $\|PT\|_\infty \leqslant 1$, and $PT \neq 1$ for $s = j\omega$, $\omega > 0$, the norm $\|(1-P)/(1-PT)\|_\infty$ is well defined. Recalling that $\|(1-e^{-\tau s})H\|_\infty < \infty$, we have that $\|(1-e^{-\tau s})H(1-P)/(1-PT)\|_\infty < \infty$ and Proposition 3.1 shows that the sequence $\{\mathcal{F}_{n,1}\}$ is string stable. □

A.2 PROOF OF THEOREM 3.4

1) First, we will show that the term $(1-PT)(PT)^{n-3}-(1-P)e^{-\tau(n-2)s}$ inside of the brackets in (65) has two zeros at $s=0$ when P is dynamic. Differentiating we obtain

$$\begin{aligned}&\Big((1-PT)(PT)^{n-3}-(1-P)e^{-\tau(n-2)s}\Big)'=\\&(n-3)(1-PT)(PT)^{n-4}(PT)'-(PT)'(PT)^{n-3}+\\&+P'e^{-\tau(n-2)s}+\tau(n-2)(1-P)e^{-\tau(n-2)s}.\end{aligned}\tag{297}$$

Since S has two zeros at the origin we have that $T'(0)=-S'(0)=0$ which in turn implies $(PT)'(0)=P'(0)$. Recalling that $P(0)=1$ we have that

$$\begin{aligned}&\frac{d}{ds}\Big((1-PT)(PT)^{n-3}-(1-P)e^{-\tau(n-2)s}\Big)\Big|_{s=0}=\\&-P'(0)+P'(0)=0,\end{aligned}\tag{298}$$

and, due to the fact that the third term inside the brackets of (65) has two zeros at $s=0$, we have that $F_{n,1}(0)=0$ and consequently $\mathcal{F}_{n,1}(0)=0$.

The derivation for $P=\eta\in(0,1)$ can be carried out in a similar fashion and we omit it here.

2) The first two terms inside the brackets of (65) satisfy the hypothesis of Proposition 3.1 for any P. The third term requires further study. For dynamic P, such that $P'(0)\neq-\tau$, we have the limit

$$\lim_{s\to0}\frac{1-PT}{PT-e^{-\tau s}}=-\frac{P'(0)}{P'(0)+\tau}.\tag{299}$$

Also, $PT-e^{-\tau s}$ has only one zero at $s=0$ and no other zeros for $s=j\omega$, $\omega>0$. Therefore

$$\|(1-PT)(PT-e^{-s\tau})\|_\infty<\infty,\tag{300}$$

and Proposition 3.1 implies string stability of $\{F_{n,1}\}$.

Remark A.1. *If the conditions for part 2) of Theorem 3.4 are not met we have string instability. If* $PT - e^{-\tau s}$ *has a zero at* $s = j\omega_c$*, that is* $P(j\omega_c)T(j\omega_c) = e^{j\tau\omega_c}$*, string stability is lost since we can only claim*

$$\lim_{s\to j\omega_c} \frac{(PT)^{n-3} - e^{-(n-3)\tau s}}{PT - e^{-\tau s}} = n - 3. \tag{301}$$

If $\tau = -P'(0)$*, that is, the critical value of time delay, string instability arises once again. The limit*

$$\lim_{s\to 0} \frac{(PT)^{n-3} - e^{-(n-3)\tau s}}{PT - e^{-\tau s}} = n - 3, \tag{302}$$

yields a magnitude peak of the last term inside the brackets of (65) *that grows with* n*.*

3) If P is dynamic, we note that for $\tau > 0$, $1 - e^{-(n-1)\tau s}$ has zeros at arbitrarily low values of ω for increasing n and $e^{-\tau s} - PT$ will not cancel them in (66). Now, it remains to compute the limit for the first term of (66)

$$\lim_{s\to 0} H\frac{(1 - (PT)^{n-1})(e^{-\tau s} - T)}{e^{-\tau s} - PT} = \frac{(1-n)\tau\tilde{H}(0)P'(0)}{\tau + P'(0)}. \tag{303}$$

This limit shows that for small frequencies $|\mathcal{F}_{n,1}(j\omega)|$ will grow unbounded with n, regardless of the selection of the dynamic P and the value of $\tau > 0$. Moreover we will have an even worse response if τ gets closer to $-P'(0)$, which is expected from the analysis carried out for $F_{n,1}$.

For $P = \eta \in (0, 1)$, the DC gain of $\mathcal{F}_{n,1}$ is

$$\mathcal{F}_{n,1}(0) = \sum_{i=2}^{n} \tau\tilde{H}(0)(1 - \eta^{i-2}) = \tau\tilde{H}(0)\left(n - 1 - \frac{1-\eta^{n-1}}{1-\eta}\right). \tag{304}$$

This value grows with the platoon size n and implies string instability of $\{\mathcal{F}_{n,1}\}$ □

A.3 PROOF OF LEMMA 4.1

We write $\Gamma(s) = r(s)/m(s)$ where $r(s)$ and $m(s)$ are two polynomials without common factors and $m(s)$ is Hurwitz. Then, the solutions of $1 - e^{j\theta}\Gamma = 0$ are the roots of the polynomial $p(s) = m(s) - e^{j\theta}r(s)$.

According to Proposition 3.4.5 in (Hinrichsen and Pritchard, 2005), if a polynomial, $p(s)$, with complex coefficients is Hurwitz then

$$\frac{d}{d\omega}\arg(p(j\omega)) > 0, \quad \forall \omega \in \mathbb{R}. \tag{305}$$

We will show, given that Γ is stable, strictly proper and $\|\Gamma\|_\infty > 1$, that there exists an interval $\theta \in (\theta_1, \theta_2)$ with $\theta_2 > \theta_1$ where condition (305) is violated. First, we write $p(j\omega)$ as

$$p(j\omega) = |m(j\omega)|e^{j\psi_m(\omega)}(1 + |\Gamma(j\omega)|e^{j\phi(\omega)}) \tag{306}$$

where we factor $m(j\omega) = |m(j\omega)|e^{j\theta_m(\omega)}$ and add the arguments as $\phi(\omega) = \psi_r(\omega) - \psi_m(\omega) + \pi + \theta$. The argument of $p(j\omega)$ is

$$\begin{aligned}\arg(p(j\omega)) &= \psi_m(\omega) + \arg(1 + |\Gamma(j\omega)|e^{j\phi(\omega)}) \\ &= \psi_m(\omega) + \arg(1 + |\Gamma(j\omega)|(\cos(\phi(\omega)) + j\sin(\phi(\omega)))).\end{aligned} \tag{307}$$

Computing the derivative using the formula of Proposition 3.4.5 in (Hinrichsen and Pritchard, 2005) (we omit the arguments (ω) for clarity)

$$\begin{aligned}\frac{d}{d\omega}\arg(p(j\omega)) &= \Re\left\{\frac{p'(j\omega)}{p(j\omega)}\right\} \\ &= \psi_m' + \frac{|\Gamma|'\sin(\phi) + |\Gamma|\phi'(\cos(\phi) + |\Gamma|)}{(1 + |\Gamma|\cos(\phi))^2 + |\Gamma|^2\sin^2(\phi)}.\end{aligned} \tag{308}$$

Since $\Gamma(s)$ is strictly proper and $\|\Gamma\|_\infty > 1$, there exists ω_c such that $|\Gamma|(\omega_c) = 1$. If $|\Gamma|'(\omega_c) \neq 0$ we compute the limit

$$\begin{aligned}&\lim_{\omega\to\omega_c}\frac{d}{d\omega}\arg(p(j\omega)) = \\ &\quad= \psi_m'(\omega_c) + \frac{|\Gamma|'(\omega_c)\sin(\phi_c) + \phi'(\omega_c)(\cos(\phi_c) + 1)}{2(1 + \cos(\phi_c))} \\ &\quad= \psi_m'(\omega_c) + \frac{\phi'(\omega_c)}{2} + |\Gamma|'(\omega_c)\frac{\sin(\phi_c)}{2(1 + \cos(\phi_c))},\end{aligned} \tag{309}$$

where $\phi_c = \lim_{\omega\to\omega_c}\phi(\omega)$. In particular, the values $\psi_m'(\omega_c)$, $\phi'(\omega_c)$ and $|\Gamma|'(\omega_c)$ do not depend on the parameter θ and are bounded. However, the expression

$$\frac{\sin(\phi_c)}{2(1 + \cos(\phi_c))} = \frac{\sin(\psi_r(\omega_c) - \psi_m(\omega_c) + \pi + \theta)}{2(1 + \cos(\psi_r(\omega_c) - \psi_m(\omega_c) + \pi + \theta))}, \tag{310}$$

takes every possible value of the real numbers as θ varies. Therefore, there exists an interval (θ_1, θ_2) with $\theta_1 < \theta_2$ such that $\frac{d}{d\omega}(\arg(p(j\omega)))$ is negative, when $\omega = \omega_c$ and $\theta \in (\theta_1, \theta_2)$, which yields the desired result. If $|\Gamma|'(\omega_c) = 0$, we can only claim the existence of θ_1 such that $1 - e^{j\theta_1}\Gamma = 0$ when $\omega = \omega_c$. Hence, the result follows with $\theta_2 = \theta_1$. □

REFERENCES

K. J. Aström and B. Wittenmark. *Computer-controlled systems: theory and design*. Courier Corporation, 2011.

B. Bamieh, F. Paganini, and M. Dahleh. Distributed control of spatially invariant systems. *Automatic Control, IEEE Transactions on*, 47 (7):1091–1107, Jul 2002. ISSN 0018-9286. doi: 10.1109/TAC.2002.800646.

B. Bamieh, M. R. Jovanovic, P. Mitra, and S. Patterson. Effect of topological dimension on rigidity of vehicle formations: Fundamental limitations of local feedback. In *Decision and Control, 2008. CDC 2008. 47th IEEE Conference on*, pages 369–374. IEEE, 2008.

B. Bamieh, M. R. Jovanovic, P. Mitra, and S. Patterson. Coherence in large-scale networks: Dimension-dependent limitations of local feedback. *Automatic Control, IEEE Transactions on*, 57(9):2235–2249, 2012.

P. Barooah and J. P. Hespanha. Error amplification and disturbance propagation in vehicle strings with decentralized linear control. In *Decision and Control, 2005 and 2005 European Control Conference. CDC-ECC'05. 44th IEEE Conference on*, pages 4964–4969. IEEE, 2005.

P. Barooah, P. G. Mehta, and J. P. Hespanha. Mistuning-based control design to improve closed-loop stability margin of vehicular platoons. *Automatic Control, IEEE Transactions on*, 54(9):2100–2113, 2009.

J. Bender and R. Fenton. A study of automatic car following. In *Vehicular Technology Conference, 1968. 19th IEEE*, volume 19, pages 134–140, 1968. doi: 10.1109/VTC.1968.1621915.

M. Bongini, M. Fornasier, and D. Kalise. (un)conditional consensus emergence under perturbed and decentralized feedback controls. *RICAM report 2014-14*, 2014. URL http://www.ricam.oeaw.ac.at/publications/reports/14/rep14-14.pdf.

C. Bonnet and H. Fritz. Fuel consumption reduction in a platoon: Experimental results with two electronically coupled trucks at close spacing. Technical report, SAE Technical Paper, 2000.

N. K. Bose, B. Buchberger, and J. Guiver. *Multidimensional systems theory and applications*. Springer Science & Business Media, 2003.

C. Canudas de Wit and B. Brogliato. Stability issues for vehicle platooning in automated highway systems. In *Control Applications, 1999. Proceedings of the 1999 IEEE International Conference on*, volume 2, pages 1377–1382. IEEE, 1999.

C. C. Chien and P. Ioannou. Automatic vehicle-following. In *American Control Conference, 1992*, pages 1748 –1752, june 1992.

K. C. Chu. Decentralized control of high-speed vehicular strings. *Transportation Science*, 8(4):361–384, 1974. doi: 10.1287/trsc.8.4.361.

P. A. Cook. Stable control of vehicle convoys for safety and comfort. *IEEE transactions on automatic control*, 52(3):526–531, 2007.

F. Cucker and S. Smale. Emergent behavior in flocks. *Automatic Control, IEEE Transactions on*, 52(5):852–862, May 2007. ISSN 0018-9286. doi: 10.1109/TAC.2007.895842.

C. Da Fonseca and J. Petronilho. Explicit inverse of a tridiagonal k-toeplitz matrix. *Numerische Mathematik*, 100(3):457–482, 2005.

R. D'Andrea and R. Chandra. Control of spatially interconnected discrete-time systems. In *Decision and Control, 2002, Proceedings of the 41st IEEE Conference on*, volume 1, pages 240–245 vol.1, Dec 2002. doi: 10.1109/CDC.2002.1184498.

W. Dunbar and D. Caveney. Distributed receding horizon control of vehicle platoons: Stability and string stability. *Automatic Control, IEEE Transactions on*, 57(3):620–633, March 2012. ISSN 0018-9286. doi: 10.1109/TAC.2011.2159651.

J. Eyre, D. Yanakiev, and I. Kanellakopoulos. A simplified framework for string stability analysis of automated vehicles. *Vehicle System Dynamics*, 30(5):375–405, 1998. doi: 10.1080/00423119808969457. URL http://dx.doi.org/10.1080/00423119808969457.

J. Fax and R. Murray. Information flow and cooperative control of vehicle formations. *Automatic Control, IEEE Transactions on*, 49(9): 1465–1476, 2004. ISSN 0018-9286. doi: 10.1109/TAC.2004.834433.

J. Forrester. *Industrial Dynamics*. Cambridge, MA: M.I.T. Press, 1961.

G. H. Golub and C. F. Van Loan. *Matrix computations*, volume 3. JHU Press, 2012.

G. C. Goodwin, S. F. Graebe, and M. E. Salgado. *Control system design*, volume 240. Prentice Hall New Jersey, 2001.

J. Hedrick, D. McMahon, V. Narendran, and D. Swaroop. Longitudinal vehicle controller design for ivhs systems. In *American Control Conference, 1991*, pages 3107–3112, June 1991.

J. Hedrick, M. Tomizuka, and P. Varaiya. Control issues in automated highway systems. *Control Systems, IEEE*, 14(6):21–32, Dec 1994. ISSN 1066-033X. doi: 10.1109/37.334412.

D. Hinrichsen and A. J. Pritchard. *Mathematical systems theory I : modelling, state space analysis, stability and robustness*. Texts in applied mathematics. Springer, New York, NY, 2005. ISBN 3-540-44125-5.

R. Horn and C. Johnson. *Matrix Analysis*. Cambridge University Press, 1999.

Z. Hurák and M. Šebek. 2d polynomial approach to stability of platoons of vehicles. In *Estimation and Control of Networked Systems*, pages 227–232, 2010.

M. R. Jovanovic and B. Bamieh. On the ill-posedness of certain vehicular platoon control problems. *Automatic Control, IEEE Transactions on*, 50(9):1307–1321, 2005.

M. Khatir and E. Davidson. Bounded stability and eventual string stability of a large platoon of vehicles using non-identical controllers. In *Decision and Control, 2004. CDC. 43rd IEEE Conference on*, volume 1, pages 1111 –1116 Vol.1, dec. 2004. doi: 10.1109/CDC.2004.1428841.

R. Kianfar, P. Falcone, and J. Fredriksson. A control matching-based predictive approach to string stable vehicle platooning. In *The19th World Congress of the International Federation of Automatic Control*, 2014.

S. Klinge and R. Middleton. Time headway requirements for string stability of homogeneous linear unidirectionally connected systems. In *Decision and Control, 2009 held jointly with the 2009 28th Chinese Control Conference. CDC/CCC 2009. Proceedings of the 48th IEEE Conference on*, pages 1992 –1997, dec. 2009. doi: 10.1109/CDC.2009.5399965.

S. Knorn. *A two-dimensional systems stability analysis of vehicle platoons*. PhD thesis, National University of Ireland Maynooth, 2013.

A. M. Krall. The root locus method: A survey. *SIAM Review*, 12(1):64–72, 1970. doi: 10.1137/1012002. URL http://dx.doi.org/10.1137/1012002.

G. Lafferriere, A. Williams, J. Caughman, and J. Veerman. Decentralized control of vehicle formations. *Systems & Control Letters*, 54(9): 899 – 910, 2005. ISSN 0167-6911. doi: http://dx.doi.org/10.1016/j.sysconle.2005.02.004.

G. Lee and S. Kim. A longitudinal control system for a platoon of vehicles using a fuzzy-sliding mode algorithm. *Mechatronics*, 12(1):97 – 118, 2002. ISSN 0957-4158. doi: http://dx.doi.org/10.1016/S0957-4158(00)00063-5. URL http://www.sciencedirect.com/science/article/pii/S0957415800000635.

I. Lestas and G. Vinnicombe. Scalability in heterogeneous vehicle platoons. In *American Control Conference, 2007. ACC '07*, pages 4678 –4683, july 2007. doi: 10.1109/ACC.2007.4283022.

W. Levine and M. Athans. On the optimal error regulation of a string of moving vehicles. *Automatic Control, IEEE Transactions on*, 11(3): 355 – 361, jul 1966. ISSN 0018-9286. doi: 10.1109/TAC.1966.1098376.

Y. Li, M. Cantoni, and E. Weyer. On water-level error propagation in controlled irrigation channels. In *Decision and Control, 2005 and 2005 European Control Conference. CDC-ECC '05. 44th IEEE Conference on*, pages 2101–2106, Dec 2005. doi: 10.1109/CDC.2005.1582471.

F. Lin, M. Fardad, and M. R. Jovanovic. Optimal control of vehicular formations with nearest neighbor interactions. *Automatic Control, IEEE Transactions on*, 57(9):2203–2218, 2012.

X. Liu, A. Goldsmith, S. Mahal, and J. Hedrick. Effects of communication delay on string stability in vehicle platoons. In *Intelligent*

Transportation Systems, 2001. Proceedings. 2001 IEEE, pages 625 –630, 2001. doi: 10.1109/ITSC.2001.948732.

J. P. Maschuw, G. C. Kessler, and D. Abel. Lmi-based control of vehicle platoons for robust longitudinal guidance. In *IFAC World Congress*, volume 17, pages 12111–12116, 2008.

S. Melzer and B. Kuo. Optimal regulation of systems described by a countably infinite number of objects. *Automatica*, 7(3): 359 – 366, 1971. ISSN 0005-1098. doi: http://dx.doi.org/10.1016/0005-1098(71)90128-2. URL http://www.sciencedirect.com/science/article/pii/0005109871901282.

R. Middleton. Trade-offs in linear control system design. *Automatica*, 27(2):281 – 292, 1991. ISSN 0005-1098.

R. Middleton and J. Braslavsky. String instability in classes of linear time invariant formation control with limited communication range. *Automatic Control, IEEE Transactions on*, 55(7):1519 –1530, july 2010. ISSN 0018-9286. doi: 10.1109/TAC.2010.2042318.

R. Olfati-Saber, J. Fax, and R. Murray. Consensus and cooperation in networked multi-agent systems. *Proceedings of the IEEE*, 95(1):215–233, Jan 2007. ISSN 0018-9219. doi: 10.1109/JPROC.2006.887293.

L. Peppard. String stability of relative-motion pid vehicle control systems. *Automatic Control, IEEE Transactions on*, 19(5):579–581, Oct 1974. ISSN 0018-9286. doi: 10.1109/TAC.1974.1100652.

L. Peppard and V. Gourishankar. An optimal automatic car-following system. *Vehicular Technology, IEEE Transactions on*, 21(2):67–73, May 1972. ISSN 0018-9545. doi: 10.1109/T-VT.1972.23503.

A. A. Peters, R. H. Middleton, and O. Mason. Leader tracking in homogeneous vehicle platoons with broadcast delays. *Automatica*, 50(1):64 – 74, 2014. ISSN 0005-1098. doi: http://dx.doi.org/10.1016/j.automatica.2013.09.034. URL http://www.sciencedirect.com/science/article/pii/S0005109813004676.

D. Roberson and D. Stilwell. Decentralized control and estimation for a platoon of autonomous vehicles with a circulant communication network. In *American Control Conference, 2006*, pages 6 pp.–, 2006. doi: 10.1109/ACC.2006.1655445.

J. Rogge and D. Aeyels. Vehicle platoons through ring coupling. *Automatic Control, IEEE Transactions on*, 53(6):1370–1377, 2008. ISSN 0018-9286. doi: 10.1109/TAC.2008.925812.

W. Rudin. *Real and complex analysis*. Tata McGraw-Hill Education, 1987.

M. Šebek and Z. Hurák. 2-d polynomial approach to control of leader following vehicular platoons. In *18th World Congress of the International Federation of Automatic Control (IFAC),(Milano, Italy), IFAC*, 2011.

P. Seiler, A. Pant, and K. Hedrick. Disturbance propagaton in vehicle strings. *IEEE Transactions on Automatic Control*, 49(10):1835–1841, 2004.

M. M. Seron, J. H. Braslavsky, and G. C. Goodwin. *Fundamental Limitations in Filtering and Control*. Springer Publishing Company, Incorporated, 1st edition, 1997. ISBN 144711244X, 9781447112440.

E. Shaw and J. Hedrick. String stability analysis for heterogeneous vehicle strings. In *American Control Conference, 2007. ACC '07*, pages 3118 –3125, july 2007. doi: 10.1109/ACC.2007.4282789.

S. Sheikholeslam and C. A. Desoer. Longitudinal control of a platoon of vehicles. In *American Control Conference, 1990*, pages 291–296. IEEE, 1990.

S. Sheikholeslam and C. A. Desoer. Control of interconnected nonlinear dynamical systems: the platoon problem. *Automatic Control, IEEE Transactions on*, 37(6):806–810, Jun 1992. ISSN 0018-9286. doi: 10.1109/9.256337.

S. Sheikholeslam and C. A. Desoer. Longitudinal control of a platoon of vehicles with no communication of lead vehicle information: a system level study. *Vehicular Technology, IEEE Transactions on*, 42(4): 546–554, 1993.

S. Stankovic, M. Stanojevic, and D. Siljak. Decentralized overlapping control of a platoon of vehicles. *Control Systems Technology, IEEE Transactions on*, 8(5):816–832, Sep 2000. ISSN 1063-6536. doi: 10.1109/87.865854.

D. Swaroop. *String stability of interconnected systems: An application to platooning in automated highway systems*. PhD thesis, California PATH Program, Inst. Transport. Studies, Univ. California, Berkeley, 1997.

D. Swaroop and J. Hedrick. String stability of interconnected systems. *Automatic Control, IEEE Transactions on*, 41(3):349 –357, mar 1996. ISSN 0018-9286. doi: 10.1109/9.486636.

D. Swaroop and J. Hedrick. Constant spacing strategies for platooning in automated highway systems. *Journal of dynamic systems, measurement, and control*, 121(3):462–470, 1999.

D. Swaroop, J. Hedrick, C. C. Chien, and P. Ioannou. A comparision of spacing and headway control laws for automatically controlled vehicles1. *Vehicle System Dynamics*, 23(1):597–625, 1994. doi: 10.1080/00423119408969077.

T. L. Willke, P. Tientrakool, and N. F. Maxemchuk. A survey of inter-vehicle communication protocols and their applications. *Communications Surveys & Tutorials, IEEE*, 11(2):3–20, 2009.

L. Xiao, F. Gao, and J. Wang. On scalability of platoon of automated vehicles for leader-predecessor information framework. In *Intelligent Vehicles Symposium, 2009 IEEE*, pages 1103 –1108, june 2009. doi: 10.1109/IVS.2009.5164436.

J. Yan and R. Bitmead. Coordinated control and information architecture. In *Decision and Control, 2003. Proceedings. 42nd IEEE Conference on*, volume 4, pages 3919–3923 vol.4, Dec 2003. doi: 10.1109/CDC.2003.1271762.

D. Yanakiev and I. Kanellakopoulos. Nonlinear spacing policies for automated heavy-duty vehicles. *Vehicular Technology, IEEE Transactions on*, 47(4):1365–1377, Nov 1998. ISSN 0018-9545. doi: 10.1109/25.728529.

B. Yu, J. S. Freudenberg, and R. B. Gillespie. String instability analysis of heterogeneous coupled oscillator systems. In *American Control Conference (ACC), 2012*, pages 6638–6643. IEEE, 2012.

D. Zwillinger. *CRC standard mathematical tables and formulae*. CRC press, 2002.

COLOPHON

This document was typeset using the typographical look-and-feel `classicthesis` developed by André Miede. The style was inspired by Robert Bringhurst's seminal book on typography "*The Elements of Typographic Style*". `classicthesis` is available for both LaTeX and LyX:

http://code.google.com/p/classicthesis/

Final Version as of October 2, 2015 (`classicthesis`).

DECLARATION

I, Andrés Alejandro Peters Rivas, certify that the Thesis is my own work and I have not obtained a Degree in this University or elsewhere on the basis of this Doctoral Thesis.

Maynooth, October 2015

Andrés Alejandro Peters Rivas
October 2, 2015